

Study of Alpha Decay of Exotic Nuclei

A Thesis Submitted
to the

University of Allahabad
for the Degree of

**Doctor of Philosophy
in Science**

by

Arati Devi



Under the Supervision of

Prof. (Mrs.) Indira Mehrotra

Head, Physics Department
University of Allahabad
Allahabad-211002
INDIA

Year 2010



इलाहाबाद विश्वविद्यालय
UNIVERSITY OF ALLAHABAD

इलाहाबाद – 211002(भारत)
Allahabad –211002(INDIA)

Physics Department
Phone : (0532) 2460993

Certificate

Certified that the candidate Mrs. Arati Devi has fulfilled all the requirements for the degree of Doctor of Philosophy in Science of the University of Allahabad, Allahabad, India.

Prof.(Mrs.) Indira Mehrotra

Thesis Supervisor
Department of Physics,
University of Allahabad
Allahabad-211002, India

Prof.(Mrs.) Indira Mehrotra

Head, Department of Physics
University of Allahabad,
Allahabad-211002, India

Prof. S.D. Dixit

Dean Faculty of Science
University of Allahabad,
Allahabad-211002, India

Acknowledgment

I would like to thank to my supervisor Prof. (Mrs.) Indira Mehrotra for her elite guidance, support and great encouragement throughout my research work. Her deep knowledge regarding the subject and her motivating advice helped me in carrying out the research work in an interesting and thoughtful manner. Also I would like to thank Prof. Basudeb Sahu who has given me time for discussion and helped me in understanding the problem during my research work. I am very grateful to the North Orissa University, where I got stay during the discussion with Prof. Sahu.

I am thankful to my seniors and fellow research scholars Dr. Shweta Prakash, Dr. P.C. Srivastava, Dr. T. Trivedi, P. Gupta and Kamalesh Maurya for their help and encouragement during my PhD. I would also thank to Shuchi, Rupali, Namrata, Dharmendra, Uma Shankar, Vineet, Jagriti, Anurag and so many countless friends who have supported me in all respects. I express my gratitude to my whole family members specially my parents (Sri Bansh Bahadur Singh and Smt Raj Kumari Devi), parents in laws (Sri Raja Ram Singh and Smt Urmila Devi) and my brothers Sri Anand Singh and Sri Shailendra Singh for their moral support, blessings and encouragement. My particular thank go to my husband Dr. Sunil Kumar Singh for his invaluable support throughout my PhD.

Arati Devi

October, 2010

Dedicated

to

My Parents

And

My Son (Aarush)

Contents

1 Introduction	1
1.1 Exotic nuclei	1
1.2 Investigating the stability of exotic nuclei	1
1.3 The limit of stability (drip line)	2
1.4 Special structural feature of exotic nuclei	4
(i) Halo	4
(ii) Skin	4
(iii) Vanishing of shell closure	4
(iv) Nuclei with N=Z	5
(v) Super deformation and hyper deformation	5
1.5 Experimental technique to produce exotic nuclei	5
1.5.1 Target fragmentation process	6
1.5.2 Projectile fragmentation process	6
1.5.3 Heavy ion fusion evaporation reaction	6
1.6 Isotope Separation Online Method (ISOL).	7
1.7 In-flight separation method	7
1.8 Decay modes	8
1.8.1 Gamma decay	8
1.8.2 Beta decay	9
(i) β^- emission	9
(ii) β^+ emission	9
(iii) Electron capture (EC)	9
1.8.3 Nucleon emission	9
(i) Proton radioactivity	10
(ii) β -delayed particle emission	10
(iii) Cluster radioactivity	10

(iv) Alpha decay	10
1.9 Branching ratio	11
1.10 Problem for the present work	11
2 Existing theories of alpha decay	15
2.1 Alpha radioactivity	15
2.2 Quantum tunneling approach	17
2.2.1 Cluster like approach	19
2.2.2 A case of asymmetric fission	21
2.3 Scattering theory approach	23
2.3.1 S-matrix method	23
2.3.2 Imaginary test potential (ITP) method	24
2.3.3 Imaginary phase shift method	24
2.3.4 Wave function method	24
2.4 Phenomenological approach	25
2.5 Present work	26
3 Models for the present work	27
3.1 Model parameter	30
4 Alpha decay study of proton rich Pb and Bi Chain	40
4.1 Introduction	40
4.2 Motivation	41
4.3 Literature survey	41
4.4 Alpha decay half life	44
4.5 Details of calculation for Pb isotopes	45
4.5.1 Model parameter	45
4.5.2 Barrier height calculation of Pb isotopes	45
4.5.3 Nuclear radii	46
4.6 WKB approximation method and Exact method	47
4.7 Result and discussion	52
4.8 Details of calculation for Bi isotopes	53

4.8.1	Model parameter	53
4.8.2	Barrier height calculation of Bi Isotopes	53
4.9	Result and discussion	58
4.10	Summary and conclusion	61
5	Alpha decay study of super heavy element in the mass region	62
	A=258-320	
5.1	Existence of Super heavy Nuclei	62
5.2	Experimental Status	63
5.3	Experimental methods for the production of Super Heavy Nuclei	64
(i)	Cold fusion reaction	65
(ii)	Hot fusion reaction with ^{48}Ca ions	65
5.4	Theoretical status	66
5.5	Model parameter	69
5.6	Result and discussion	69
5.7	Summary and conclusion	89
6	Alpha decay study using wave-function approach	91
6.1	Introduction	91
6.2	Schrodinger equation for the alpha-nucleus system	92
6.3	Life time and decay width	95
6.4	Resonance energy	97
6.5	Relative Probability Density (RPD) Method	98
6.6	Details of calculation	102
6.7	Result and discussion	103
6.8	Summary and conclusion	109
7	Summary and Conclusion	111
	Bibliography	114
	List of publications	

List of tables

4.1	Calculated and experimental half lives of proton rich even Pb isotopes. The corresponding values of parameter v_2 which gives best fit with the experimental data are also given.....	48
4.2	Predicted alpha decay half lives of five experimentally unknown proton rich even Pb isotopes.....	48
4.3	Comparison of WKB and exact transmission coefficients for different ranges with $v_0=13.3$ MeV and $Q_\alpha=7.066$ MeV.....	49
4.4	Calculated and experimental alpha decay half lives are presented. Corresponding best fit value of range parameter v_2 which gives best fit to the experimental data, assault frequency, radial position and barrier heights for each nucleus are also given.....	55
4.5	Alpha decay half life calculated by present model for the range parameter $v_2=28.094$, obtained corresponding to minimum deviation $\sigma=0.93$	55
4.6	Predicted alpha decay half life of unknown Bi isotopes, calculated by taking the range parameter v_2 , obtained corresponding to minimum deviation. Corresponding assault frequency, radial position, and barrier heights are also given. Half lives of the present work are compared with ref. [Tav 05].....	56
4.7	Calculated pre formation probability through the overlapping region has been given, and has been compared with the results of ref. [Tav 05].....	57
5.1	Calculated and experimental alpha decay half lives of known even-even SHE for ground state to ground state transition with mutual angular momentum $\ell=0$. Corresponding best fit values of the range parameter v_2 , barrier height, radial position and assault frequency are also given. Experimental data for $^{256}\text{Rf}_{104}$, $^{260}\text{Sg}_{106}$, $^{266}\text{Sg}_{106}$ and $^{264}\text{Hs}_{108}$ has been taken from ref. [Roy 00] and for other nuclei from ref. [Oga 04, 05, 06].....	73
5.2	Comparison of the calculated alpha decay half lives $T_{1/2}(\text{ms})$ with	

experimental data and other work. The value of range parameter ν_2' calculated by semiempirical relation is also given.....	74
6.1 Variation of b_1 and λ_1 to obtain experimental half life for $\alpha + {}^{286}_{113}$ system, having $Q_\alpha(\text{exp.}) = 9.95$ and $t_{1/2}(\text{exp.}) = 0.016$ Sec. Potential parameters are $r_0 = 1.1 \text{ fm}$, $a = 1.6 \text{ fm}$ and $B_0 = -78.75$	105
6.2 Calculated alpha decay half life for the decay chain of ${}^{294}_{117}$. Potential parameters are fixed at $r_0 = 0.97 \text{ fm}$, $b_1 = 0.82$ $a = 1.6 \text{ fm}$ and $B_0 = -78.75$	106
6.3 Calculated alpha decay half life for the decay chain of ${}^{293}_{117}$. Potential parameters are fixed at $r_0 = 0.97 \text{ fm}$, $b_1 = 0.82$ $a = 1.6 \text{ fm}$ and $B_0 = -78.75$	106
6.4 Predicted alpha decay half life and Q values for the isotopic chain of $Z=102$. Potential parameters are $r_0 = 0.97 \text{ fm}$, $b_1 = 0.82$ $a = 1.6 \text{ fm}$ and $B_0 = -78.75$. Parameters of the global formula are $\lambda_0 = 1.543$, $N_{i_0} = 144$, and $N_{i_1} = 157$	107
6.5 Prediction of alpha decay half life and Q values for the isotopic chain of $Z=74$. Potential parameters are fixed at $r_0 = 0.97 \text{ fm}$, $b_1 = 0.82$ $a = 1.6 \text{ fm}$ and $B_0 = -78.75$. Parameters of the global formula are $\lambda_0 = 1.245$, $N_{i_0} = 82$, and $N_{i_1} = 87$	108
6.6 Prediction of alpha decay half life and Q values for the isotopic chain of $Z=113$. Potential parameters are fixed at $r_0 = 0.97 \text{ fm}$, $b_1 = 0.82$ $a = 1.6 \text{ fm}$ and $B_0 = -78.75$. Parameters of the global formula are $\lambda_0 = 1.662$, $N_{i_0} = 167$, and $N_{i_1} = 173$	109

List of figures

1.1	Figure of the nuclear chart, the valley of β -stability is indicated by the black squares. The $N=Z$ line and neutron drip line and proton drip line are shown. The horizontal and vertical lines correspond to the magic nucleon numbers.....	3
2.1	Naturally occurring radioactive isotopes on Segre chart.....	16
2.2	Yellow region on the chart of nuclides shows the region of possible alpha emitters.....	17
2.3	Energetic of alpha particle decay. The solid curve shows the variation of potential energy with distance. The horizontal line represents the total energy of the alpha particle. If the energy is less than zero the particle will never get out. If it is greater than zero and less than the height of the barrier then, the alpha particle will tunnel through the barrier to get out.....	18
3.1	Plot of the potential (3.1) as a function of distance for $\lambda/\nu > 1.4$. Height of the barrier is equated to 20 MeV at the origin.....	31
3.2	Same as figure 3.1 for $\lambda/\nu < 1.4$	32
3.3	Same as figure 3.1 for $\lambda/\nu = 1.4$	32
3.4	Plot of potential (3.1) for $\lambda=2$, $\nu=2.2$ and different barrier height $V_B=13, 15$ and 17 MeV respectively.....	33
3.5	Plot of potential (3.1) for $V_B=15\text{MeV}$, $\nu=2.2$ and $\lambda=1,2,3$ respectively.....	33
3.6	Plot of potential for $V_B=15\text{MeV}$, $\lambda=1$ and $\nu=2.2, 3.2$ and 4.2 respectively....	34
3.7	Plot of the potential $V(r)$ as a function of radial distance for $\alpha + {}^{289}_{115}$ system. Solid line represents the form of analytical potential given by eq.(3.13), dotted line represents Wood-Saxon plus Coulomb potential given by eq. (3.18). Potential parameters of analytical potential are $B_0=-78.75$, $B_1=21.2$, $\lambda_1 = 1.63539$, $\lambda_2 = 1$, $B_2=150$, $r_0 = 0.9\text{ fm}$ and $a = 1.6\text{ fm}$. Potential parameter of eq. (3.18) are $V_{N_0} = -78.75\text{ MeV}$, $a_N = 0.84\text{ fm}$,	37

	$R_N = 7.649 \text{ fm}$, and $R_C = 9.688 \text{ fm}$	
3.8	Plot of the potential $V(r)$ presented by eq. (3.13) as a function of radial distance for $\alpha + {}^{289}_{115}$ system for different values of flatness λ_1	38
3.9	Same as figure 3.8 for different values of range parameter.....	38
3.10	Same as figure 3.8 for different values of, r_0 and λ_1 for $\alpha + {}^{278}_{109}$ system.....	39
4.1	Plot of alpha decay barrier for three limiting value of range parameter v_2 , obtained from the best fit to the experimental data corresponding to three Pb isotopes ${}^{182}\text{Pb}$, ${}^{190}\text{Pb}$ and ${}^{210}\text{Pb}$ respectively.....	44
4.2	Variation of (a) logarithm of half life time and (b) Q_α values for alpha emission with neutron number of parent isotopes of Pb chain.....	50
4.3	Variation of $\log_{10}(t_{1/2})$ for alpha emission with $E_\alpha^{-1/2} (\text{MeV})^{-1/2}$	51
4.4	Variation of transmission probability with incident energies of the alpha particle of Pb chain.....	51
4.5	Plot of the potential for three limiting value of range parameter v_2 obtained corresponding to best fit to the experimental data for ${}^{191}\text{Bi}$, ${}^{209}\text{Bi}$ and ${}^{214}\text{Bi}$	54
4.6	(a), Q_α value (b), logarithm of alpha decay half life and (c), preformation probability, S_α have been plotted against neutron number of the thallium isotope (daughter nucleus).....	59
4.7	Plot of partial alpha decay half life corresponding inverse square root of alpha decay energy Q_α for Bi isotopes.....	60
5.1	Shape of the potential barrier for two nuclei ${}^{256}\text{Rf}$ and ${}^{288}_{114}$	75
5.2	Plot of the calculated spontaneous fission (SF) half life and alpha decay half life with respect to mass numbers of the isotopic chain of parent nucleus $Z=124$. Full square on the inverted parabola shows the SF half life of the respective nucleus and black circles on line crossing the inverted parabola shows the alpha decay half life of the respective nucleus.....	75
5.3	Same as figure 5.2 for $Z=126$	76
5.4	Same as figure 5.2 for $Z=128$	76

5.5	Plot of Q value of decay and logarithm of alpha decay half life versus mass number of parent nuclei for $Z=106$	77
5.6	Same as figure 5.5 for $Z=108$	78
5.7	Same as figure 5.5 for $Z=110$	79
5.8	Same as figure 5.5 for $Z=112$	80
5.9	Same as figure 5.5 for $Z=114$	81
5.10	Same as figure 5.5 for $Z=116$	82
5.11	Same as figure 5.5 for $Z=118$	83
5.12	Same as figure 5.5 for $Z=120$	84
5.13	Same as figure 5.5 for $Z=122$	85
5.14	Same as figure 5.5 for $Z=124$	86
5.15	Same as figure 5.5 for $Z=126$	87
5.16	Same as figure 5.5 for $Z=128$	88
5.17	The plot connecting the ratio of spontaneous fission to alpha decay half-lives against the fissility parameter for $Z = 124-128$	89
6.1	Plot of the ratio of two probability densities I_1 and I_2 as a function of λ_1 for $\alpha + {}^{289}_{115}$ system $E_{c.m.}=11.03\text{MeV}$. The peak position corresponding to $I_1/I_2 \cong 1$ gives the value of λ_1	99
6.2	Plot of the ratio of two probability densities I_1 and I_2 as a function of energy for $\alpha + {}^{282}_{111}$ system for $\lambda_1=1.623825$. The peak position ($E_{c.m.}=10.22$ MeV) represents the Q value of the decay.....	100
6.3	Plot of the square modules of the wave function as a function of radial distance r for the $\alpha + {}^{286}_{113}$ system at the energy 0.005 MeV less than the exact resonance energy.....	100
6.4	Same as fig. 6.3 exactly at resonance energy $Q=9.95$ MeV.....	101
6.5	Same as fig.6.3 at energy 0.01MeV larger than the exact resonance energy...	101
6.6	Plot of λ_1 versus neutron number of target nuclei. The dots indicate the values of λ_1 , which explain the respective experimental Q values. The solid	

curve represents the global formula given by equation (6.23), for λ_1 as a function of neutron number N , with $N_{i_0} = 96$, $N_{i_1} = 105$ and $\lambda_0 = 1.313 \dots\dots$ 103

Chapter I

Introduction

1.1 Exotic Nuclei

The state of the matter on our earth is not same as of the rest of the universe. In the interior of the stars and supernovae explosions very-very high temperature and pressure predominates creating particle and nuclei which do not naturally exist on the earth. Exotic nuclei can be produced in a modern accelerator and there investigation is of great interest because of two reasons:

First theoretical models of the properties of the nuclei can be refined only by looking beyond the range of isotopes available on earth and by taking into account the widest possible spectrum of the nuclei present in the universe. Second, as it is known today that the synthesis of elements in the stars takes place via exotic nuclei. These nuclei decay principally through the emission of beta particles i.e. high speed electrons until the stable nuclei known to us on earth are left. Thus the formation of chemical elements and their abundance are essentially determined by the properties of these exotic nuclei. In laboratory exotic nuclei can be produced by different methods.

1.2 Investigating the stability of exotic nuclei

There are wide spectrums of nuclei which can be investigated experimentally. The main fact about the stability of an atomic nucleus is provided by its life span or half-life. As nuclei approach the limits of stability, they become increasingly short lived and exist for only a small fraction of a second.

The interaction of neutron and proton produces an incredible variety of nuclei, all the elements which constitute our universe from hydrogen, the lightest to uranium the heaviest of the natural elements. The stable nuclei are in equilibrium; their cohesion is such that no radioactive transmutation is possible. For a given mass the proportion of neutrons and protons corresponds to structures strongly bound by the combined action of the various interactions; strong interaction, the pairing, the spin-orbit and the coulomb

repulsion. Nature in the process of nucleosynthesis and man with particle accelerators, know how to produce nuclei outside this equilibrium. This is the field of exotic nuclei. Basically exotic nuclei are defined as extraordinary ratio of proton and neutron, either much larger or much smaller than those found in nature. Studies of nuclear matter under extreme conditions in which the nuclei are quite different in some way from those found in nature are at the forefront of nuclear research these days. Such extreme conditions include nuclei at high temperature and at high density (several times of normal nuclear density) as well as those with larger or smaller N/Z ratios. The N/Z ratio depends on the nature of the attractive nuclear force that binds the proton and neutron in the nucleus and its competition and complex interplay with the disruptive coulomb or electrostatic force that pushes the positively charged protons.

1.3 The limit of stability (Drip line)

The most fundamental thing for the understanding of our universe is the question concerning the limits within which matter can exist if even only for a very short time. Proton and neutrons are the basic building -blocks of a nucleus. In stable nuclei they have a particular ratio to one another. Chart of nuclides is shown in figure 1.1 the line of stability, neutron drip line and proton drip line is marked on the chart.

Nuclear stability is limited by the drip lines. As one moves away from the valley of beta stability e.g. by increasing the proton excess the proton separation energy starts decreasing until it becomes zero at the proton drip line. Beyond this line the proton separation energy is negative and the system cannot hold the excess proton together, rendering itself unstable. Similar is the situation with neutron excess. Proton drip line defines the limit at which nuclei become unbound to the emission of a proton from their ground states. Low Z nuclei lying beyond this limit only exist as short lived resonances and can not be detected directly. In higher Z regions of the drip line the potential energy barrier resulting from the mutual electrostatic interaction between the unbound proton and core can cause nuclei to survive long enough to be detected. The drip line is the demarcation line between the last bound isotope and its unbound neighbor and each chemical element has a lightest (proton drip line) and a heaviest (neutron drip line) nucleus.

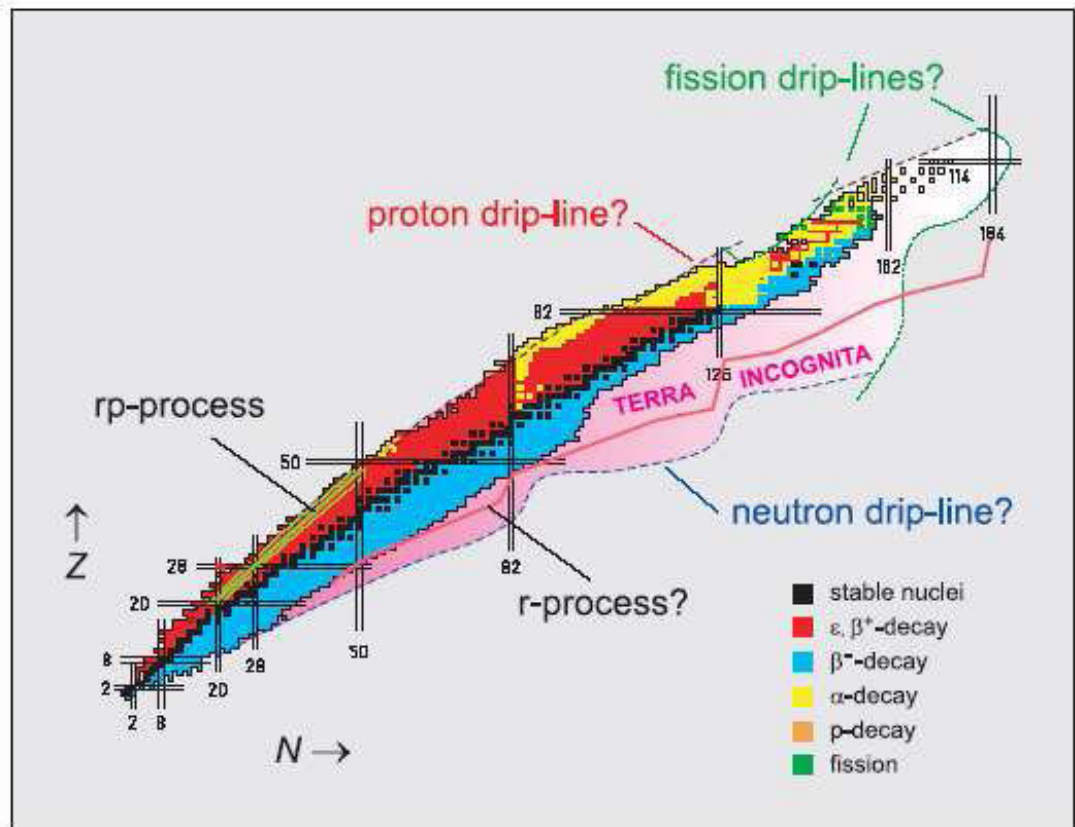


Figure 1.1: Figure of the nuclear chart, the valley of β -stability is indicated by the black squares. The $N=Z$ line and neutron drip line and proton drip line are shown. The horizontal and vertical lines correspond to the magic nucleon numbers.

The basic difference between proton drip line and neutron drip line is observed from the perspective of the semi empirical mass formula, neutron emission from neutron rich nuclei occurs when the gain in binding energy from a decrease in symmetry energy is more than the loss of volume binding energy, however proton emission from proton rich nuclei takes place when decrease of electrostatic potential take place. Consequently proton drip line lies much closer to the line of stability than the neutron drip line. The proton drip line is relatively well established for most of the elements because the Coulomb repulsion among the protons has a dramatic destabilizing effect on nuclei with

significantly fewer neutrons than protons. Finally, for proton rich nuclei at and even beyond the proton drip line, it is still possible to study the nuclei that should not exist.

1.4 Special structural features of exotic nuclei

(i) **Halo:** Halo nuclei are weakly bound exotic state of nuclear matter in which the outer one or two valence nucleons are spatially decoupled from a tightly bound core. As the binding energy becomes smaller in the vicinity of the drip lines, the valence nucleon tunnel out of the central potential, and enhance the diffuseness of the nuclear surface. This leads to extended wave function tail and hence overall large matter radii. This new phenomenon occurs in certain neutron-rich nuclei near the neutron drip line such as Be and Li with mass numbers 11. [tan 96]. In the limit of vanishing binding, extremely large neutron halos occur. No clear examples of proton halo nuclei have yet been discovered. However it has been suggested that because of the attenuating effect of the Coulomb barrier on the spatial extent of the proton wave function, the proton halo may only exist for loosely bound nuclei with $Z \leq 10$ in either an s or a p state. Initially ${}^8\text{B}$ [Shw 95, Min 92] was selected as a prime candidate for a one proton halo. The other candidate in this region is the nucleus ${}^{17}\text{Ne}$ [oza 94] which is expected to produce a two proton halo. Recently ${}^{28}\text{P}$ and ${}^{27}\text{S}$ have been suggested as possible proton halo candidate [Ren 96].

(ii) **Skin:** For a large neutron excess, the bulk of the neutron density is predicted to extend beyond the proton density creating a sort of “neutron skin”. Similar effects may appear for nuclei having large number of protons. The density of ‘halo’ state is more diffused than that of a skin. Such properties of exotic nuclei provide opportunity to study the behavior of abnormal nuclear matter with very large isospin [Kor 97]. Example of neutron skin is ${}^8\text{He}$.

(iii) **Vanishing of shell closure:** The study of nuclear structure has been advanced on the basis of the shell structure associated with the magic numbers which appear ($N = 14, 16, 34, \dots$) and some other disappear ($N = 8, 20, 40, \dots$) in moving from stable to exotic nuclei in a rather novel manner due to a particular part of the nucleon-nucleon interaction. For example: the nucleus ${}^{30}\text{Si}$ has six valence protons in the sd shell and is a

stable nucleus, while ^{24}O has no valence proton and is a neutron rich exotic nucleus. Since such changes occur as results of nuclear force, there is isospin symmetry. Similar changes can occur for the same Z values in mirror nuclei. The $N = 20$ magic structure is evident for ^{30}Si , whereas the $N = 16$ magic number arises in ^{24}O . For ^{24}O , the $0d_{3/2}$ lies close to pf shell giving rise to large gap (≈ 6 MeV) between $0d_{3/2}$ and $1s_{1/2}$. On the other hand, for stable nucleus ^{30}Si a considerable gap (4 MeV) is created between the $0d_{3/2}$ and the pf shell.

(iv) **Nuclei with $N = Z$:** When protons and neutron occupy the same orbital, mutual reinforcement of the shell gaps may lead to a stabilization of exotic shapes in the ground state. Here also the proton-neutron pairing interaction is exposed to view at its maximum. Some examples of $N = Z$ nuclei are ^{56}Ni and ^{100}Sn .

(v) **Super-deformation and hyper-deformation:** Far from the line of β -stability, medium nuclei may exhibit large deformations, even at low excitation energies. These states have a shape like a rugby ball with the ratio between the major and minor axis of 2:1 as was observed in high spin states. The super-deformed states are formed only when both of largely deformed proton and neutron orbital have large energy gap between the next orbital. It has been shown that ^{76}Sr , ^{80}Zr and ^{100}Zr are amongst the most deformed nuclei known in their ground states. It is predicted that hyper-deformed states should exist, in these regions as well. In a hyper-deformed nucleus the ratio between the major and minor axes is 3:1.

1.5 Experimental techniques to produce exotic nuclei

Nuclear phenomenon which takes place far from the line of stability is different from those close to line of stability. These nuclei which lie in this region are on the forefront of nuclear experimental research. Exotic nuclei can be produced with the use of different nuclear reactions over a wide range of energy from Coulomb barrier to relativistic energies. For the production of exotic nuclei there are basically three methods available.

1.5.1 Proton or neutron induced target fragmentation (spallation) or fission.

1.5.2 Projectile fragmentation or fission

1.5.3 Heavy ion fusion

1.5.1 Target fragmentation process:

Target fragmentation process is used to produce Neutron rich nuclei having medium mass where fragmentation reactions can be induced by neutron, energetic proton or heavy ions.

1.5.2 Projectile fragmentation process:

With the use of projectile fragmentation method a variety of ion species with unusual proton to neutron ratio, can be produced. This method is used to predominantly populate the area between the stable isotopes and proton drip line from the atomic number of projectile down to the atomic number of the lightest element [Sch 99]. At the energies above the Fermi level this method is used to produce exotic nuclei over entire range of periodic table up to the heaviest projectile beam.

1.5.3 Heavy ion fusion evaporation reaction:

Heavy ion fusion reaction takes place when the projectile energy is close to the Coulomb barrier, which is of the order of 5MeV/u. In this process a projectile beam is incident on the target and leaves a compound nucleus in stable and highly excited state with very high angular momentum. The compound nucleus losses some of its excess energy by the emission of alpha particle, proton or neutron depending on the amount of energy it contains. If contained energy is very less then gamma emission will take place. The complete fusion reaction is thus preferably used for the production of heavy elements and neutron-deficient isotopes. Examples of such reaction are $^{96}\text{Ru} (^{16}\text{O}, 4n) ^{108}\text{Te}$ and $^{96}\text{Ru} (^{16}\text{O}, 5n) ^{107}\text{Te}$ [Mac 65].

Besides a large production methods an efficient separation tools with high sensitivity down to single ions is needed. Mainly two separation principles are successfully employed in modern exotic beam facilities, the ISOL and the in-flight method [Ben 00, Gei 95].

1.6 Isotope Separation Online Method (ISOL)

The first Radioactive Ion Beam was produced about 50 years ago with the help of Isotope Separation Online Method (ISOL). This is an instrument in which a target, ion source and an electromagnetic mass analyzer are coupled in a series [Rav 89]. The apparatus is said to be on-line when the material which has to be analyzed has been put directly as the target of a nuclear bombardment, where reaction products of interest formed during the irradiation are slowed down and stopped in the system. In the ISOL technique radioactive ions are produced by charged particle or neutron which bombard on a thick targets, in which the reaction products are stopped and neutralized. Later they are diffused out to an ion source (surface ionization, plasma, laser etc.) to be ionized. These ions are electrostatically accelerated to some 40-60 keV and injected into a mass separator. Electromagnetic field separates these ions according to their charge to mass ratio. In this way, low energy (few tens to few hundred of keV) beam of one particular mass can be obtained with a rather good beam quality.

Also other methods have been developed to produce RIB are in-flight separators and ion-guide ISOL (IGISOL) systems, a variant in which the reaction products are not stopped in a solid catcher, but in a gas cell. Thus the ion beam with good ion-optical quality and energy resolution with energies 1-5 MeV/u, can be obtained by reaccelerating the radioactive beams obtained from the ISOL facility.

1.7 In-flight separation method

In-flight separation technique can be applied in a wide energy region from Coulomb barrier to (approx. 5 MeV/u) using inverse fusion reaction to very large energies (50-500 MeV/u) using projectile fragmentation reaction. In this technique sufficiently high energy beam or a projectile having mass larger than the mass of the target nuclei is made to bombard onto a relatively thin production target. The emergent exotic ions are separated by In-flight technique before they come to rest in a matter. Therefore an advantage of In-flight separation technique is that beams can be produced and delivered at high energy without reaccelerating them. The process is extremely efficient and the production target only needs to dissipate some fraction of incident beam energy. Exotic nuclei having half life of the order of 100ns to 100 ms are studied in this method. In the energy range 5-10

MeV/u mainly exotic nuclei on the neutron deficient side are produced using this technique. At high beam energy larger than 100 MeV/u the peripheral interaction between a heavy projectile and a target nucleus induces the breakup of the fast projectile into a variety of secondary ions lighter than the beam. This secondary beam is purified using an achromatic or doubly achromatic high resolution mass separator. Extremely pure beam of exotic radioactive nuclei can be obtained at rather high intensities, especially if purification is performed with a velocity filter. One substantial property of the In-flight separation process is that it is not sensitive to the chemical properties or, in general to the half life of the isotopes of the interest. Half lives are only limited by the flight times of the ions through the device, which is almost always less than 1 micro second. Thus if the suitable ion optics is given, the efficiency of the In-flight separation technique can reach 100%.

1.8 Decay Modes

Radioactivity refers to the particles which are emitted from nuclei as a result of nuclear instability. The concept of radioactivity was first discovered in 1896 by the French physicist Henry Becquerel, who was experimenting with phosphorescence. Thus nuclear decay or radioactivity is a process of unstable nucleus transforming into another by ejecting high energy particles, referred as nuclear radiation. Within the incredibly small nuclear size, the two strongest forces in nature are pitted against each other. When the balance is broken the resultant radioactivity yields particles of enormous energy. Exotic nuclei exhibit decay modes not seen near stability, such as proton radioactivity, beta-delayed particle emission. In the years that followed, yet more types were discovered triton, two neutron and three neutron decay that are beta delayed as well as electron capture, cluster decay and spontaneous fission. Alpha, beta, gamma are three basic type of radioactive decay modes.

1.8.1 Gamma decay:

In the process of electromagnetic transition or gamma decay a nucleon in a higher energy state jumps to an unfilled lower energy state with the emission of electromagnetic radiation. In the gamma decay process (electromagnetic process) number of neutron or proton do not change in the nucleus; however they make

transition from higher energy state to lower energy state of the same nucleus until eventually the ground state is reached. This process occurs in a very small fraction of second.

1.8.2 Beta Decay:

There are following three types of beta decay processes which are responsible to convert neutron in to proton and vice versa.

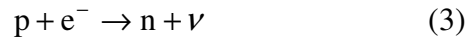
(i) β^- **emission**: the process of β^- emission is given as



(ii) β^+ **emission**: the process of β^+ emission is given as



(iii) **Electron capture (EC)**: the process of electron capture is given as



There are few more decay modes.

1.8.3 Nucleon emission

In the nucleon emission, a neutron or a proton simply comes out of a nucleus if it has enough energy. Typical times required for nucleon emission, electromagnetic processes and beta decay are 10^{-18} , 10^{-12} and 10^2 seconds respectively. They indicate that the nuclear force causing the nucleon emission is the strongest of the three and the beta decay interaction is weakest. The binding energy per nucleon represents the overall binding of nuclei. However, the question of stability in terms of neutron and proton numbers is not determined by this average quantity, but the energy required to bind the last or least bound nucleon. This energy is called the separation energy required to remove a single nucleon from a nucleus. This energy is generally about 8 MeV, so emission of a single nucleon is usually energetically possible only when the nucleus is excited about 8 MeV or more. The exotic nuclei closer to the line of stability are therefore stable as far as nucleon emission is concerned. Their decay occurs with weak interactions such as β^-

decay. As we move away from stability, the separation energy decreases thereby increasing the Q -value of decay. Various other decay modes are described below.

(i) Proton radioactivity: Beyond the region of stability partial half-lives for nucleon emission drop far more quickly than those for alpha and beta decay and this decay mode quickly dominates over them. The process in which a nucleus emits a single proton is called proton radioactivity. Unlike alpha decay proton requires no pre formation of a cluster of nucleons within the nuclear surface. A proton is emitted from the nucleus and proton number and mass number of the daughter nucleus is reduced by one. Proton radioactivity has been observed in the nuclei of odd atomic number.

(ii) β -delayed particle emission: In this process the initial β -decay populates an excited state in the daughter nucleus which is unstable to the emission of one or more nucleons. β -delayed neutron emission or β -delayed proton emissions are common near the drip lines. These decays can be observed in ^{31}Ar [Van 94], ^{65}Se , ^{73}Si , ^{69}Kr [Xu 97]. These decays have been widely studied but the analysis is often complicated by a high density of excited state.

(iii) Cluster radioactivity: Unstable neutron rich and proton rich nuclei far from the stability are out of balanced states in several meanings. The binding energy of the last nucleon is sometimes as low as 1/10 or less than that of normal stable nuclei. Such a weak binding state may also present the possibility of developing cluster structures inside a nucleus, ^6He and ^8He clusters. The spontaneous decay of radioactive nuclei with the emission of fragments heavier than alpha particle is termed as cluster radioactivity. The common feature of this emission is that the nuclei emit fragments in such a way that the daughter nuclei are always doubly magic nuclei or close to them. The experimental evidence for cluster radioactivity was first observed by Rose and Jones in 1984 in the ^{14}C emission from ^{223}Ra [Ros 84].

(iv) Alpha decay: In addition to the emission of a single nucleon, it is also possible for group of nucleons to come off. It has been observed that when large amount of excitation

energy are available, light nuclei are emitted such as ${}^4\text{He}$ nucleus or alpha particle. The energy available for decay of alpha particle is referred as Q_α -value. A necessary condition for alpha radioactivity is a positive Q_α -value.

$$Q_\alpha = [{}_Z M^A - {}_{Z-2} M^{A-4} - M({}_2\text{He}^4)]C^2 > 0$$

Where ${}_Z M^A$ and ${}_{Z-2} M^{A-4}$ are the atomic masses of parent and product nucleus respectively and $M({}_2\text{He}^4)$ is mass of the alpha particle. The effect of coulomb repulsion becomes increasingly important as the potential energy increases at a faster rate (as Z^2) than the nuclear binding energy (approximately as the mass number). This results in spontaneous alpha emission which competes with beta decay. Alpha emission shows a much greater sensitivity to the available energy than β -emission and the former dominates on moving further from stability.

1.9 Branching ratio

The branching fraction for any decay mode is defined as the fraction of particles which decay by individual decay mode with respect to the total number of particles which decay. It is equal to the ratio of the partial decay constant to the overall decay constant. If

t is life time then decay constant $\lambda = 1/t$ and branching ratio is given by $\frac{\lambda_i}{\sum_i \lambda_i}$ or $\frac{\sum_i t_i}{t_i}$.

1.10 Problem for the present work

It has been possible to discover many radioactive elements due to progress in theory, experiments and accelerator based technologies. Now a day several alpha decaying system including light, heavy and super heavy nuclei are available for study. Experimentally alpha decay of radioactive nuclei has been a powerful tool to probe the nuclear structure for the nuclei which approach line of beta stability or proton drip line [Tot 84, Wau 94, And 00]. In the experiments on super heavy nuclei alpha decay has been used as a reliable way to identify new synthesized super heavy element. Many alpha decaying systems have been observed experimentally in the region $Z=52$; $A=105$ to $Z=118$; $A=294$. A large number of lighter proton rich isotopes of Te, Xe, I and Cs have

been produced at GSI Darmstadt using fusion evaporation reaction and online mass separation [Roe 78, Sch 79, Hof 81, Kle 82]. Andreyev et al [And 99] have reported improved characteristic of $^{190,192}\text{Po}$ in complete fusion reaction and also they have experimentally observed the alpha branching ratio of 38% and 9.3% for ^{186}Pb and ^{188}Pb respectively. Discovery of heavier element started in 1940's with the synthesis of Neptunium ($Z=93$) and Plutonium ($Z=94$). Many heavier system have been discovered up to $Z=116$ and $Z=118$. There was a gap between the element $Z=116$ and $Z=118$ for a long time. Recently the scientists of Dubna [Oga 10] have synthesized the new element $Z=117$ with two isotopes $A=293, 294$. These recent experimental results have motivated us to perform theoretical study in the above mass region. In the light and heavy mass region alpha decay has been observed as the competing decay mode with the positron emission and electron capture. However in the super heavy region only alpha decay and spontaneous fission have been found as two main decay modes. When one goes to the heavy mass region alpha decay becomes dominant decay mode. Experimentally it is possible to obtain decay energy and decay half life of alpha decaying system. Experimentally alpha emitters are found to have wide range of half life ranging from 10^{26} sec for ^{209}Bi to few microseconds in super heavy region. These experimental data are used as an important tool to give nuclear structure and spectroscopic information of the alpha decaying systems. One needs theoretical base to perform such type of experiments. For theoretical description of alpha decay process several theoretical approaches have been developed, which need an appropriate alpha-daughter potential to study the phenomenon of alpha decay. In the present work alpha decay study has been performed by using two approaches (i) Quantum tunneling in unified fission model and (ii) Scattering theory as applied to decay of resonance states.

In the Gamow's theory of alpha decay the process of alpha decay is considered as quantum tunneling through a alpha nucleus barrier described by attractive square well plus Coulomb potential. The transmission coefficient is calculated by using WKB method. Later studies have shown that alpha nucleus potential gets modified due to several renormalization processes from its simple Coulomb plus nuclear form. This has led to the development of several modified forms of alpha nucleus potential in the literature. However in all the earlier studies transmission coefficient has been calculated

using WKB approximation method in which the potential between the two turning points is taken into account. Thus the tail region of the potential is neglected in the WKB approximation method. As outer potential has a Coulombic form having long tail, it should be properly taken into account. In the first approach we have used an analytically solvable form of potential developed by Sahu et al [Sah 02] to represent the alpha nucleus potential barrier. The potential is highly versatile in nature and admit exact expression for the transmission coefficient which has been used in place of commonly used WKB approximation method. Using this potential the alpha decay of the following systems have been studied

- (i) Proton rich Pb isotopes in the mass region $A=182-210$.
- (ii) Proton rich Bi isotopes in the mass region $A=189-214$.
- (iii) Super heavy nuclei with $A=258-320$

Although the potential has six parameters only one parameter ν_2 representing the range of the outer barrier has been adjusted to reproduce the experimental data. Alpha decay half lives have been predicted for experimentally unknown systems in the region $A=182-214$ by using the value of range parameter ν_2 which corresponds to minimum rms deviation of calculated values from experimental data. Also a semiempirical formula has been suggested to calculate the parameter ν_2 for unknown alpha emitters. Using this value of ν_2 half lives of alpha emitters have been predicted in the mass region $A=258-320$. Details of calculations are given in chapter IV and V.

In the second approach alpha emission has been considered as scattering phenomenon involving daughter as target and alpha as projectile. In this approach we have used the analytical potential developed by Sahu [Sah08]. The form of the potential has been developed to simulate the nuclear Wood-Saxon part in the inner region and Coulomb part in the outer region. This form of potential generates quasibound states with discrete positive energies called as resonance energy. One of these energies can be identified as decay energy or Q -value of decay with some life time. By using this potential alpha decay half has been calculated for the newly discovered decay chain of $Z=117$; $A=293, 294$. The potential has five parameters, only the parameter λ_1 representing the flatness of the barrier in the inner region has been adjusted to

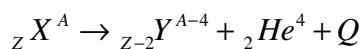
reproduce the experimental Q -value. A global formula has been developed to calculate λ_1 for unknown systems. Using this value of λ_1 , alpha decay energy and alpha decay half lives have been predicted for the isotopic chain of $Z=74, 102$ and 113 , for which experimental data are not known. For the calculation of decay energy we have used the relative probability density (RPD) method and for the calculation of half life we have used the exact expression of half life obtained by matching the two wave function, one obtained from the s-wave solution of Schrödinger equation in the interior region with the pure Coulomb wave function in the outer region. The details of calculation and results are given in chapter VI.

The present thesis has been organized in the following chapters:

Chapter I: Introduction; **Chapter II:** Existing theories of Alpha Decay; **Chapter III:** Models for the present work; **Chapter IV:** Alpha decay study of Pb and Bi Isotopes; **Chapter V:** Alpha decay study of super heavy nuclei in the mass region $A=250-328$; **Chapter VI:** Alpha decay study using wave function approach; **Chapter VII:** Summary and conclusion

2.1 Alpha Radioactivity

The ratio of neutron to proton is largely determinant of the stability of the nucleus and the tendency of radioactive decay to occur. From nuclear structure theory it is known that nucleons tend to group themselves into subunits of ${}^4\text{He}$ nuclei, and in alpha decay, a nucleus emits a helium nucleus with the release of kinetic energy.



The energy released (kinetic energy) is determined by the difference between the rest mass of the original nucleus and that of the two products. Alpha particle is a very tightly bound system with binding energy of 28 MeV. However in heavy nuclei energy required to pull out the last nucleon is about 8 MeV, energy required for alpha emission is $(4 \times 8 - 28) = 4$ MeV only. Thus for alpha cluster it is more easy to come out from the nucleus than single nucleon or other complex nuclei. Thus alpha decay is more probable decay mode in heavy nuclei than other decay modes.

Radioactivity is a natural phenomenon of our environment. There exists almost all the stable chemical element from the lowest hydrogen to highest Bi on the earth. Every element above atomic number $Z=83$ is radioactive. Naturally occurring radioactive isotopes on the Segre chart of nuclides are shown in figure 2.1. Alpha radioactivity has been observed in all nuclei above $Z > 82$. There are some naturally occurring short lived and long lived isotopes in the nature. Short lived isotopes above $Z > 82$ are ${}^{222}\text{Rn}$, ${}^{224}\text{Rn}$, ${}^{224}\text{Ra}$ and ${}^{225}\text{Ac}$, which have half life of 1-10 days. Three very heavy nuclei, ${}^{232}\text{Th}$ having half life of 14.1 billion year, ${}^{235}\text{U}$ having half life of 700 million year and ${}^{238}\text{U}$ having half life of 4.5 billion year decays through complex chain of alpha and beta and ends at the stable nuclei ${}^{208}\text{Pb}$, ${}^{207}\text{Pb}$ and ${}^{206}\text{Pb}$ respectively.

On the nuclear landscape alpha emitters have been identified by the proton drip line above $A=100$. For proton rich heavy nuclei, a possible mode of decay to a more stable state is by alpha particle emission. Short lived alpha emitters found near doubly magic ^{100}Sn are ^{107}Te , ^{108}Te and ^{111}Xe . Alpha decay always appears in decay chains of nuclides with an atomic number greater than 82. The possible alpha emitters on the chart of nuclides are shown in figure 2.2. All nuclei with mass number greater than 150 are thermodynamically unstable against alpha emission. Alpha decay is dominant decay mode only for heaviest nuclei $A \geq 210$. Alpha decay is a change from the ground state of an original nucleus to an excited or ground state of a daughter nucleus with expulsion of an alpha particle.

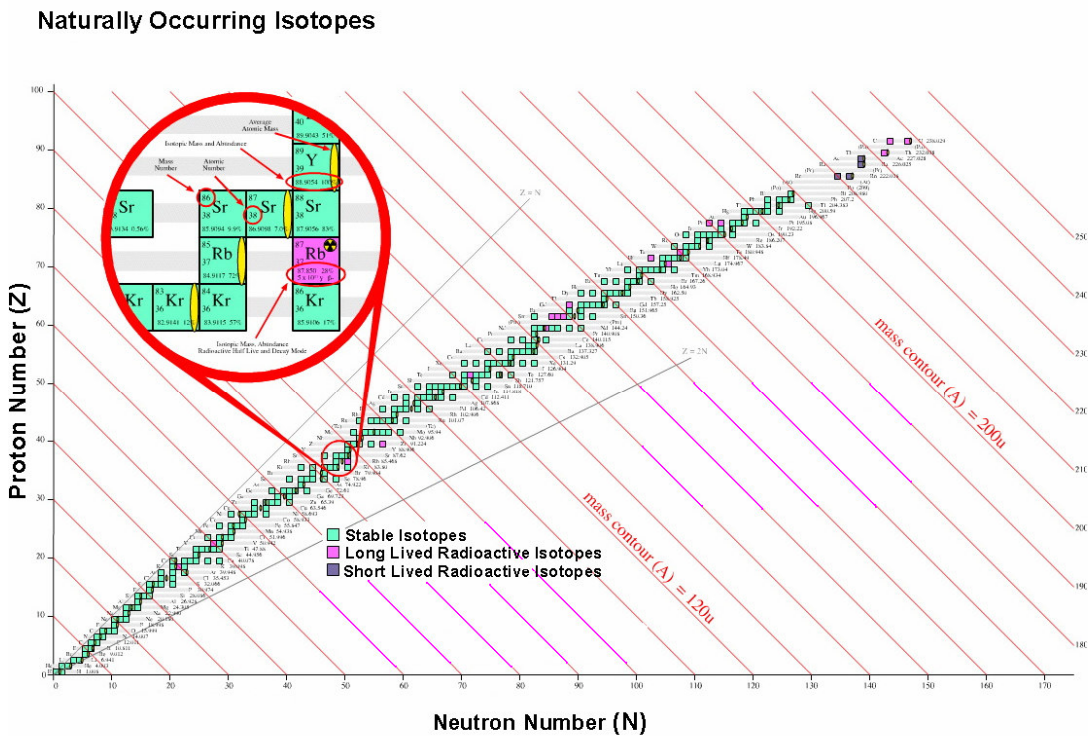


Figure 2.1: Naturally occurring radioactive isotopes on Segre chart.

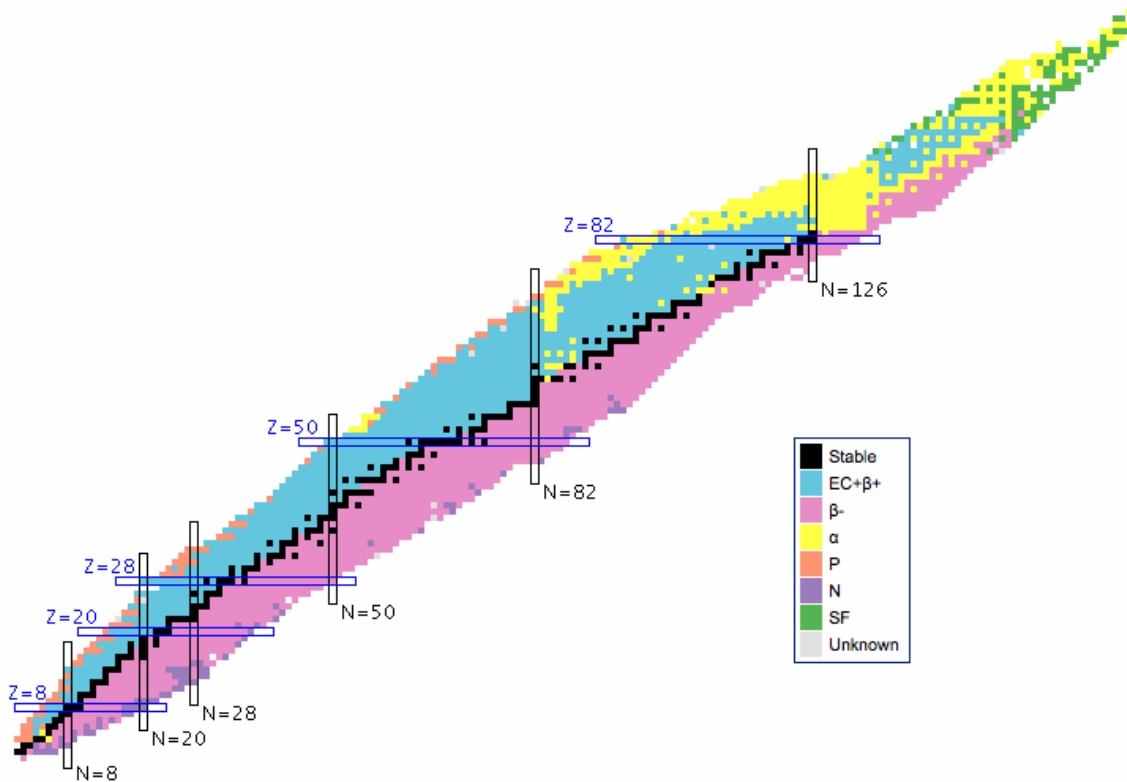


Figure 2.2: Yellow region on the chart of nuclides shows the region of possible alpha emitters.

Existing theories of alpha decay have been classified into three approaches (i) Quantum Tunneling Approach (ii) Scattering theory approach and (iii) Phenomenological approach.

2.2 Quantum Tunneling Approach

To understand the energetic of alpha particle decay, it can be understood that the alpha particle is trapped inside the product nucleus and trying to get out. Figure 2.3 shows the energetic of alpha particle decay. For an uncharged particle like a neutron in the vicinity

of a nucleus, the potential energy distribution is shaped like a well. However, an alpha particle, being positively charged also experiences an electrostatic or Coulomb repulsion which is the dominant interaction at larger separations. There is a Coulomb barrier outside the nucleus. The strong nuclear force dominates inside the nucleus. Alpha particle total energy is also shown in figure 2.3. It is partly kinetic and partly potential. The total energy should remain constant as the alpha particle leaves the nucleus. It seems impossible for the alpha particle to leave, in the region between A and B, it has a potential energy greater than its total energy. If the alpha particle is treated as a wave, this wave proceeds out from the nucleus and most of it is reflected back, a little passes through the Coulomb barrier with small probability by a quantum-mechanical process called tunneling. Using tunneling, Gammow was able to calculate dependence for the half-life as a function of alpha particle energy which was in agreement with experimental observations.

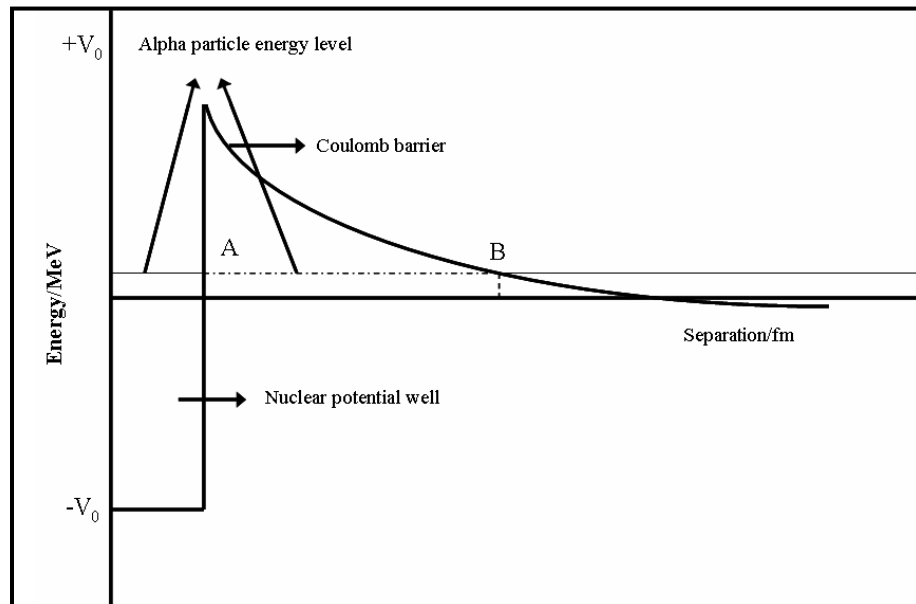


Figure 2.3: Energetic of alpha particle decay. The solid curve shows the variation of potential energy with distance. The horizontal line represents the total energy of the alpha particle. If the energy is less than zero the particle will never get out. If it is greater than zero and less than the height of the barrier then, the alpha particle will tunnel through the barrier to get out.

The quantum tunneling theory of alpha decay has been classified into two approaches

(2.2.1) Cluster like approach and (2.2.2) a case of asymmetric fission

In the first approach the decay process takes place in two steps first is the formation of alpha particle and second is the tunneling through the potential barrier. The decay constant can be calculated as the product of assault frequency, pre formation probability and transmission probability through the barrier. However in case of asymmetric fission there is an asymmetric fragmentation of parent nuclei into daughter and alpha nucleus. There is no pre formation of alpha particle inside the nucleus. The decay constant in this case is the product of only two terms assault frequency and transmission probability through the barrier.

2.2.1 Cluster like approach:

The process of alpha decay is known from the early years of the 19th century [Rut 08, 09], but the calculation of decay width was the subject of theoretical controversy. Theory of alpha decay was given by Gammow in 1928 [Gam 28] and Condon and Gurney [Con 28] independently. It was one of the first problem to which quantum mechanics was applied. For the calculations of transmission probability through the barrier it is assumed that the alpha particle is pre-formed in the nucleus before emission in the decay process. Once the alpha particle is emitted, the particle gains its final kinetic energy by electrostatic repulsion as it moves from residual nucleus.

After the theory of Gammow up to the long time the potential barrier taken for alpha decay process was of the form of square well plus Coulomb potential. Square well has been taken as attractive part of nuclear potential and Coulomb as repulsive part of the barrier. For this type of potential barrier it was difficult to reproduce the experimental data. Later to improve the results the potential barrier has been modified from its simple Coulomb form to better explain the experimental data. Many different theoretical estimates have been developed to explain the experimental results. In these models different nature and forms of the potential have been used. By adjusting the model parameters results have led to reasonable agreement with the experimental data.

Initially Buck et al [Buc 91] have used their simple cluster model having only three adjustable parameter, in which interacting barrier has been developed by taking square well as nuclear part and surface charge (Coulomb part) as repulsive part. Later Buck et al [Buc 89] have modified their model and have used Double folding cluster model for the nuclear part of the potential. Double folding model was originally developed in 1975 by Buck-Dover- Vary [Buc 75]. The model was developed using the microscopic approach, in which two body interactions has been taken into account in the formation of nuclear part of potential barrier. The model has been developed for the simplest case of spinless cluster and core which are not internally excited. The interaction potential between cluster and core has been obtained by double folding integral including cluster and core densities $\rho_1(r_1)$ and $\rho_2(r_2)$ and an effective nucleon- nucleon potential $U(|r_1 - r_2|)$. Later [Cho 08b, Sam 07] the interaction potential $U(|r_1 - r_2|)$ between the two nucleons has been given by the factorized DDM3Y effective interaction [Sat 79]. Thus for the calculation of alpha decay half life, the more realistic form of the alpha core nuclear potential has been combined with realistic Coulomb potential and centrifugal barrier to form the interacting potential barrier. Gupta and Malik [Mal 89] have developed a preformed cluster model by treating the cluster formation as quantum mechanical fragmentation process. Authors have developed the model in the coordinates of mass asymmetry, $\eta = A_1 - A_2 / A_1 + A_2$, where $A = A_1 + A_2$ and relative coordinate R. The collective potential is given by

$$V(\eta, \eta_z, R_t) = -\sum_{i=1}^2 B_i(A_i, Z_i) + \frac{Z_1 Z_2 e^2}{R_t} + V_p$$

where $R_t(\eta) = C_1 + C_2$ is central sussman radii. The charges Z_i are fixed by minimizing the sum of two binding energies B_i and the Coulomb interaction energy, V_p is the proximity potential for the touching configuration. Tavers et al [Tav 05] have proposed a model where the potential is composition of overlapping inner barrier region and external separation region. External separation region is superposition of both Coulomb and centrifugal effect. Tunneling process takes place through the resulting potential barrier which accounts for both the effects. For the overlapping region the two descriptions,

effective reduced mass and potential energy have been given by Duarte and Goncalves [Dua 96] and Poenaru et al [Poe 85].

2.2.2 A case of asymmetric fission:

For a very long time alpha decay have been studied as traditional Gamow's theory [Gam 28] but after the new theory given by Poenaru et al [Poe 79] alpha decay was successfully explained as fission like process i.e an asymmetric fission of nuclei. The main difference between the asymmetric fission like approach and cluster like approach is the behavior of the system before the formation of the nascent fragments and the correspondent potential energy surface. However in both approaches the potential barriers are identical outside of the touching configuration of the separating fragments.

Nuclear fission was discovered in 1930s. However, high mass asymmetry in fission was observed much later during 1970s. The work of Poenaru has encouraged the researchers to study alpha and exotic decay in the framework of unified fission model. In the unified fission model there is no pre formation of the cluster inside the parent nucleus. This model treat alpha and exotic decay along with cold fission as equivalent process, differing only in mass asymmetry exhibited. Thus in the unified fission model approach nucleus becomes strongly deformed and decays through a complicated shape barrier.

In 1985 Shi and Swiatecki [Shi 85] have constructed a deformation energy barrier for the process of alpha and cluster emission by modifying Coulomb repulsion between the fragments by the nuclear proximity potential up to the contact of the fragments and continue beyond the contact by an interpolation to the configuration of the parent nucleus. The proximity potential is a short range attractive force between the fragments. The inclusion of nuclear proximity attraction reduces the height and width of the barrier and hence the transmission probability by several order of magnitude through the barrier. The proximity potential is more pronounced for alpha decay than heavier clusters because proximity attraction is proportional to the reduced radius $R_1 R_2 / R_1 + R_2$ which scales as $A^{1/3}$ of smaller fragment. And Coulomb repulsion is approximately proportional to A . Thus the ratio of the nuclear potential to the Coulomb potential is proportional to $A^{-2/3}$ which increases with decreasing mass of the lighter fragment. Shanmugam et al [Sha 88] have developed a potential model, in which they have included the finite range effect by

Yukawa plus exponential potential in the post scission region. According to Nix [Nix 67] at low energies the shape of the barrier departs from a parabola. The overlapping region of the barrier which connects ground state to the touching configuration has been considered in the form of cubic barrier, which was approximated by third order polynomial given by [Nix 67]. However there is no evidence that form of the barrier in overlapping region is cubic but this assumption is intrinsically more reasonable than the assumption that it is parabolic [Sha 86]. Thus the potential for the post scission region is given as sum of nuclear Yukawa plus exponential potential and Coulomb potential. Later authors have started taking deformation effect of the parent and daughter nuclei in developing the potential model. Pik-Pichak [Pik 86] has included the deformation effect in their model by considering parent and daughter as spheroid in their ground state. Emitted particle has been considered as spherical nuclei. However they have taken only Coulomb potential in the post scission region. Shanmugam et al [Sha 90a] have modified their earlier model [Sha 88] by including the deformation effect in the potential in the post scission region. Later Shanmugam et al [Sha 90b] have modified the model [Sha 90a] in the post scission region by including charge redistribution of both the fragments. Goncalves et al [Gon 93] have developed a model by considering alpha and exotic decay process as molecular phase of the fragments. The model has been developed in the framework of effective liquid drop model. In their model authors have compensated the proximity effect by an appropriate intensity of surface term, which is controlled by radius parameter r_0 . r_0 is the only controlled parameter of the model. Later in 2000 G Royer [Roy 00] have developed a model by considering that the alpha decay process can take place in the quasi molecular shape path where the nucleon-nucleon forces act very strongly during the formation of neck between the nascent fragments and after the separation of the fragments. Thus the potential model has been developed within the framework of liquid drop model including proximity effect. This model is called as Generalized Liquid Drop Model (GLDM). Santhosh et al [San 02, San 00] have proposed a model by taking Coulomb plus proximity potential in post scission region for touching and separated fragments. The interacting potential barrier for the parent nuclei is given as sum of Coulomb plus proximity plus centrifugal part. Garcia et al [Gar 00] have used a traditional Gamow like model in which the product nucleus has been considered of

deformed ellipsoidal shape. They have assumed that before tunneling through a pure Coulomb barrier the two particle system oscillates isotropically, thus giving rise to an average frequency of oscillation $\overline{\lambda_0}(d)$, which is equivalent to average polar direction θ_0 of alpha emission. Thus Coulomb potential energy is given as $V(d, \theta_0, s) = Z_1 Z_2 e^2 g(d, \theta_0, s) / s$, where $g(d, \theta_0, s)$ is the contribution to the coulomb potential energy due to interaction energy between alpha particle and deformed product nucleus (prolate or oblate).

2.3 Scattering theory approach

In an alternative approach the process of alpha decay has been considered as the scattering phenomenon considering alpha nucleus as projectile and daughter nucleus as target. These approaches are based on quantum scattering theory, in which the decaying state can be considered as the resonant state of the alpha-daughter nucleus system. Following are the methods to calculate resonance energy and half life of the decaying system.

2.3.1 S-Matrix method:

The resonant state can be considered as the state of positive energy with finite and relatively long life time or narrow width. Partial wave S-matrix for complex momentum plane can be obtained by solving Schrödinger equation. In S-matrix approach, if for a particular partial wave S-matrix the resonance pole position is obtained at $k_p = k_r - ik_i$, then corresponding resonance energy and width are

$$E_R = \frac{\hbar^2}{2m} (k_r^2 - k_i^2)$$

$$\Gamma_R = \frac{\hbar^2}{2m} (4k_r k_i)$$

This method has been followed to study the resonances in several applications [Mah 06, Sah 02a, Sah 03, Sah 91, Pre 08]. However this approach of calculating resonance energy and related half life is quite difficult in the cases when the width of the decaying system is quite narrow.

2.3.2 Imaginary test potential (ITP) method:

In order to obtain resonances in scattering theory a small imaginary attractive potential called as test imaginary potential has to be added to the real potential of the alpha-daughter system. The variation of partial wave reaction cross section with energy gives maxima at certain energies. Then the position of the maxima of the reaction cross section is identified as the resonance energies [Sah 02a].

2.3.3 Imaginary phase shift (IPS) method:

This method has been developed by using the concept of time delay to calculate resonance energy. The quantity $\tau_\ell = \frac{1}{k} \frac{d\delta_\ell}{dk}$ is defined as time delay of the wave packet due to the trapping of the incident wave in the resonance configuration [Sah 02a]. The variation of τ_ℓ with k gives peak and peak position can be identified as resonances. These results are further analyzed by using the test imaginary potential of strength W . In this case of the S-matrix $S = e^{2i\delta}$ near the resonances depends on the strength of the potential. In this case the complex phase shift $\delta = \delta_r + i\delta_i$ gives corresponding complex time delay. At the resonance, the peak position in the reaction cross section is clearly related to the zero crossing point with a negative slope of the variation of τ_i with k [Sah 02a]. This fact has been used to locate the resonance position. Further, the variation of the derivative $\frac{d\delta_i}{dW}$ with W can be used to estimate the width of the resonance for the real potential with $W = 0$.

2.3.4 Wave function method:

To overcome the difficulties of (i) S-matrix method, which have numerical difficulties in searching the pole position in the complex energy plane [Mah 06, Sah 02a], (ii) variation of reaction cross section using test imaginary potential [Sah 02a], (iii) variation of phase shift time as a function of energy in the phase shift method [Sah 02a] and (iv) WKB approximation method [Mah 06]. Sahu [Sah 08] have developed another quantal method (wave function method) for alpha-nucleus problem. The wave function method depends critically on the behavior of the wave function, so specific estimate of the wave function

is necessary in these calculations. In this method the behavior of the quasibound state wave function has been used to calculate the narrow widths. For a given potential the s-wave Schrödinger equation is solved for the wave function. This exact wave function within the nuclear interaction region is properly matched with outside Coulomb wave function, which is found appropriate in the outer region at radial position within the barrier region. These two wave functions have been used to develop an analytical method to calculate the decay width or half life of the decaying system. Using the confinement property that exactly at resonance energy the probability density in the interior region is very large compared to outer region, and bound state like behavior of the wave function, decay energy or resonance energy of the decaying state has been calculated.

2.4 Phenomenological approach

Till now large number of phenomenological formulae have been given to obtain alpha decay half life from the beginning of the knowledge of the alpha decay process [Taa 61, Vio 66, Kel 72, Hor 74, Poe 83, Hat 90, Dec 94, Roy 00, Gei 11]. However these formulae are not able to give deep microscopic description of the mechanism of the alpha decay process. Nevertheless they have been used in the prediction of half life of unknown nuclei or to see the systematic of decay half life in the wide range of nuclides. The first formula for the alpha decay half life was given by Geiger-nuttall rule [Gei 11].

$$\log_{10}(T_{1/2}) = A + BE_{\alpha}^{-1/2} \quad (1)$$

Where A and B are the constants depending on the isotopic chain. Half lives calculated by using eq.(1) shows the discrepancy from the experimental data for the set of e-o, o-e or o-o nuclei. Eq.1 shows the dependence of half life on the alpha particle energy, this fact has been taken into account in all the phenomenological formulae developed yet. Later some more accurate phenomenological formulae have been developed for alpha decay half life by taking into account the effect of atomic number, mass number, and shell effect. Also the effect of e-e, o-o, e-o and o-e nuclei have been considered [Gei 11, Vio 66]. Brown et al [Bro 92] have developed a semiempirical formula for even-even alpha emitter by using universal scaling law. Parkhomenko et al [Par 05] have given a semiempirical relation by taking in to account the excitation energy of e-o, o-o and o-e nuclei by adjustable parameters, as the excitation energy of these states are not known.

Poenaru et al [Poe 06] have developed a semiempirical formula based on the fission theory of alpha decay. Mediros et al [Med 06] have developed a semiempirical formula which is based on quantum mechanical tunneling mechanism of the decay process. In developing the formulae overlapping and centrifugal effects have been taken into account. Many other [Poe 06b, Poe 80, Bas 04, Sam 07, Cho 06, Hor 04] semiempirical relationships for the alpha decay half life of heavy and super heavy nuclei have also been developed.

2.5 Present work

In the present work we have studied alpha radioactivity in the framework of Quantum tunneling using unified fission model approach. For the calculation of transmission probability through the barrier we have used exact expression of transmission probability given by Sahu [Sah 02]. Also we have studied the phenomenon of alpha decay in the scattering theory approach using the wave function method for the calculation of decay energy and half lives [Sah 08].

Chapter III

Models for the Present Work

A large number of studies indicate that the effective barrier for the emission of alpha particle gets modified from its simple Coulomb plus centrifugal form due to various physical processes like nuclear forces, proximity force effect, deformation of fragments, shell effects etc. This notion of modification of the barrier due to various renormalization processes can be incorporated by developing a versatile potential barrier. In the present work we have used two different forms of analytical potential as described below. One for the Quantum tunneling approach and the other for the Scattering theory approach.

For the Quantum tunneling approach we have used an analytically solvable potential barrier developed by Sahu *et al.* [Sah 02] to describe the phenomenon of alpha radioactivity. The potential barrier is asymmetric in nature and the biggest advantage of this potential is that it is highly versatile and admits exact expression of transmission probability across the barrier.

The symmetric form of the potential has been constructed by modifying the attractive one dimensional potential of Ginnochio [Gin 84]. The Potential $V(x)$ is expressed as

$$V(x) = V_0 v(r) \quad (3.1)$$

where V_0 is the strength of the potential in units of energy. $v(r)$, the functional form of the potential is given as

$$v(r) = \lambda^2 \nu(\nu + 1)(1 - y^2) + \frac{1 - \lambda^2}{4} [5(1 - \lambda^2)y^4 - (7 - \lambda^2)y^2 + 2](1 - y^2) \quad (3.2)$$

Here λ and ν are two dimensionless parameters. The parameter λ accounts for the shape of the barrier and ν measures the height of the barrier. The function $y(r)$ is related to the radial variable r by the relation

$$r = \frac{1}{\lambda^2} [\tanh^{-1} y - (1 - \lambda^2)^{1/2} \tanh^{-1}(1 - \lambda^2)y] \quad (3.3)$$

The range of r is $-\infty \leq r \leq \infty$, hence y is defined in the range $-1 \leq y \leq 1$. The parameter λ can have any positive value $0 < \lambda < \infty$. The height of the potential is maximum at the origin $x = 0$ and is given as

$$V_B = V_0 \left[\lambda^2 \left(\nu^2 + \nu - \frac{1}{2} \right) + \frac{1}{2} \right] \quad (3.4)$$

For a fixed value of V_B , the variation of ν will show the change in range of the barrier instead of height. Varying the different value of the parameter λ , ν and V_B a variety of symmetric potential can be generated. The symmetric potentials of different height, range and shape obtained by varying these parameters are shown in fig.3.1 to 3.6. A composite barrier can be generated by placing two symmetric potentials of the form (3.2) side by side. The potential is expressed as

$$V(x) = V_{01}v_1(r)\Theta(-r) + V_{02}v_2(r)\Theta(r) \quad (3.5)$$

where the two step functions have the property $\Theta(r \leq 0) = 0$ and $\Theta(r > 0) = 1$. The potential $v_i(r)$, where $i = 1, 2$ is given by (3.2). Hence $V(x) = V_{01}v_1(r)$ is the potential in the region $r \leq 0$ and $V(x) = V_{02}v_2(r)$ is in the region $r > 0$. The composite form of the barrier has six parameters λ_1, ν_1, V_{01} and λ_2, ν_2, V_{02} . By equating the heights of the two side of the barrier in the above expression (3.5) a single barrier is generated specified by different sets of parameters on either side. This composite barrier can become symmetric, asymmetric, flatter or less flat on either side depending on the values of the parameters. Thus the potential is highly versatile in nature and is suitable for the alpha decay study.

In the present work the asymmetric fission barrier for alpha decay study has been used. The fission barrier potential $V(x)$ has two components, inner barrier in overlapping region and outer barrier in non overlapping region. The potential is given as

$$V(x) = V_{01} \left[\lambda_1^2 \nu_1 (\nu_1 + 1) (1 - y_1^2) + \frac{1 - \lambda_1^2}{4} [5(1 - \lambda_1^2) y_1^2 + 2] (1 - y_1^2) \right], \quad (3.6)$$

For $0 \leq x \leq C_t$

$$V(x) = V_{02} \left[\lambda_2^2 \nu_2 (\nu_2 + 1) (1 - y_2^2) + \frac{1 - \lambda_2^2}{4} [5(1 - \lambda_2^2) y_2^2 + 2] (1 - y_2^2) \right] \quad (3.7)$$

For $x > C_t$

where V_{01} and V_{02} are the strength of the potential in MeV. The parameters ν_1 and λ_1 specify the range and flatness at the top of the potential in the interior region. ν_2 , λ_2 specify the range and flatness at the top of the potential in the outer region. C_t is the touching radius of the daughter nucleus and emitted alpha particle. A new dimensionless variable ρ_n is defined as

$$\rho_n = (x - C_t) b_n \quad \text{with } b_n = \sqrt{\frac{2\mu V_0}{\hbar^2}}, \quad n=1,2.$$

b_n has the dimension of [length]⁻¹

$$\rho_n = \frac{1}{\lambda_n^2} [\tanh^{-1} y_n - (1 - \lambda_n^2)^{1/2} \tanh^{-1} (1 - \lambda_n^2) y_n] \quad (3.8)$$

In the internal region x varies from 0 to C_t , ρ_1 varies from a large negative value ($-C_t b_1$) to zero while in the outer region x ranges from C_t to ∞ and y_2 varies from 0 to 1. The value of the potential is maximum at $y=0$ and is expressed as the height of the barrier. In the inner region, the height of the barrier at $x=C_t$ ($y_1=0$) is

$$V_{B1} = V_{01} \left[\lambda_1^2 \left(\nu_1^2 + \nu_1 - \frac{1}{2} \right) + \frac{1}{2} \right] \quad (3.9)$$

In the outer region the height of the barrier at $x=C_t$ ($y_2=0$) is

$$V_{B2} = V_{02} \left[\lambda_2^2 \left(\nu_2^2 + \nu_2 - \frac{1}{2} \right) + \frac{1}{2} \right] \quad (3.10)$$

A single barrier of certain height V_B in MeV at $x=C_t$ is set by taking

$$V_{01} = \frac{V_B}{\left[\lambda_1^2 \left(\nu_1^2 + \nu_1 - \frac{1}{2} \right) + \frac{1}{2} \right]} \quad \text{and} \quad V_{02} = \frac{V_B}{\left[\lambda_2^2 \left(\nu_2^2 + \nu_2 - \frac{1}{2} \right) + \frac{1}{2} \right]}$$

So that $V_{B1}=V_{B2}$.

The above expressions are applicable for $\ell = 0$ angular momentum state of the emitted particle. The asymmetric potential barrier $V(x)$ is analytically solvable and exact expression for the transmission coefficient across the barrier is given as [Sah 02]

$$T = \frac{16\pi^4 \lambda_1 \lambda_2 h_1 h_2}{[(\lambda_2^2 |L_1|^2 + \lambda_1^2 |L_2|^2)(s_1^2 + h_1^2)(s_2^2 + h_2^2) + 8\pi^4 \lambda_1 \lambda_2 (s_1 s_2 + h_1 h_2)]} \quad (3.11)$$

$$s_1 = \sin(\pi \bar{v}_1), s_2 = \sin(\pi \bar{v}_2), h_1 = \sinh\left(\frac{\pi k_1}{\lambda_1^2}\right), h_2 = \sinh\left(\frac{\pi k_2}{\lambda_2^2}\right), k_1 = \sqrt{\frac{Q}{V_{01}}}, k_2 = \sqrt{\frac{Q}{V_{02}}}$$

Where

$$\bar{v}_1 = \left[\frac{1}{4} - v_1(v_1 + 1) + \frac{\lambda_1^2 - 1}{\lambda_1^4} k_1^2 \right]^{1/2} - \frac{1}{2}$$

$$\bar{v}_2 = \left[\frac{1}{4} - v_2(v_2 + 1) + \frac{\lambda_2^2 - 1}{\lambda_2^4} k_2^2 \right]^{1/2} - \frac{1}{2}$$

3.1 Model parameter

The potential form (3.6, 3.7) used in the present work has six parameter λ_1, v_1, V_{01} and λ_2, v_2, V_{02} , describing the potential on either side of the merger. These parameters are connected to each other through the expressions obtained by equating the two side of the barrier at $x = C_t (\rho = 0)$

$$V_B = V_{01} \left[\lambda_1^2 (v_1^2 + v_1 - \frac{1}{2}) + \frac{1}{2} \right] = V_{02} \left[\lambda_2^2 (v_2^2 + v_2 - \frac{1}{2}) + \frac{1}{2} \right] \quad (3.12)$$

By choosing different values of these parameters a variety of potential can be generated with different shape and range. The shape of the barrier is very sensitive to the values of v and λ . If $\lambda/v < 1.4$ there is a single barrier but for $\lambda/v > 1.4$ then there is double barrier with pocket in the middle. $\lambda/v = 1.4$ is the limiting value. Typical forms of the potential for three ratios are shown in figure 3.1 to 3.3. Variation in shape of the potential with other parameters is shown in figure 3.4 to 3.6. As λ increases potential falls off more sharply, whereas the range of the potential increases with v for fixed height. Earlier studies have shown that the inner barrier is very narrow and sharply falling. Shanmugam [Sha 88] and Duarte [Dua 97] have also shown in independent studies that the width of the inner barrier decreases with decrease in mass of the emitted particle. Thus for the alpha decay study the potential parameters λ_1, v_1 and λ_2 has been chosen so as to simulate narrow sharply falling inner region, parabolic at the top and long ranged Coulombic tail in the outer region. The potential generated is asymmetric in nature and exact expression

given by eq. (3.11) is used for the calculation of transmission coefficient across the barrier.

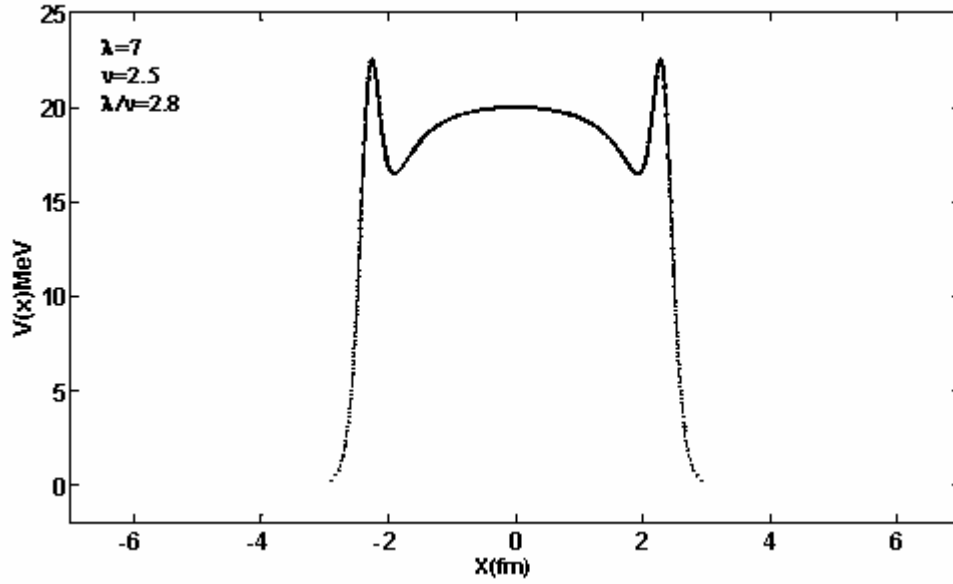


Figure 3.1: Plot of the potential (3.1) as a function of distance for $\lambda/\nu > 1.4$. Height of the barrier is equated to 20 MeV at the origin.

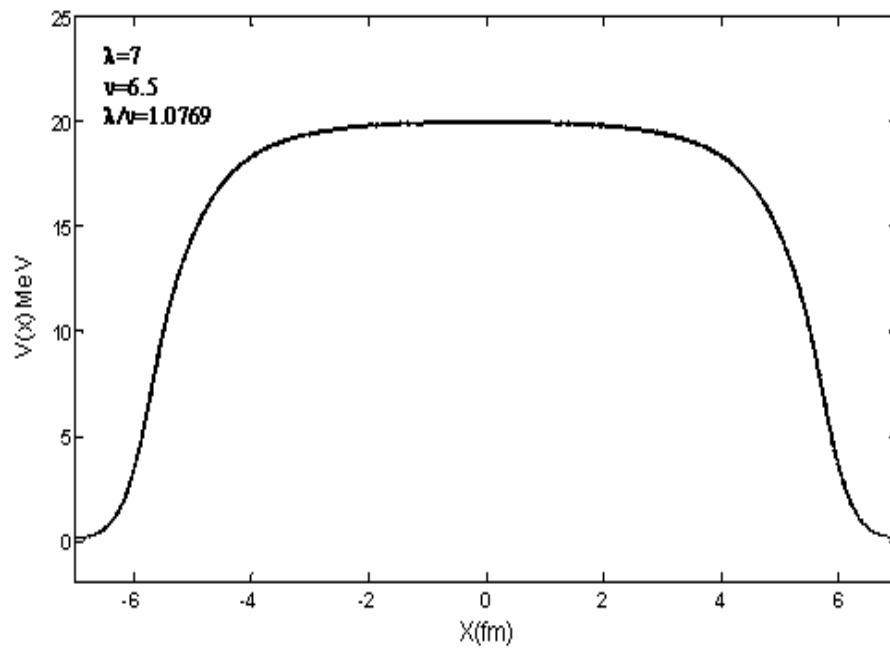


Figure 3.2: Same as figure 3.1 for $\lambda/\nu < 1.4$.

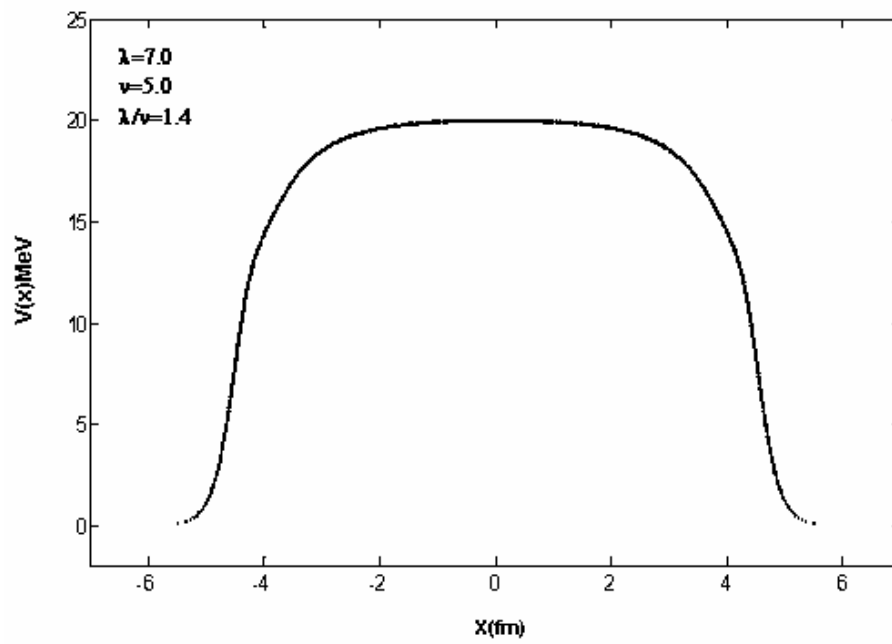


Figure 3.3: Same as figure 3.1 for $\lambda/\nu = 1.4$.

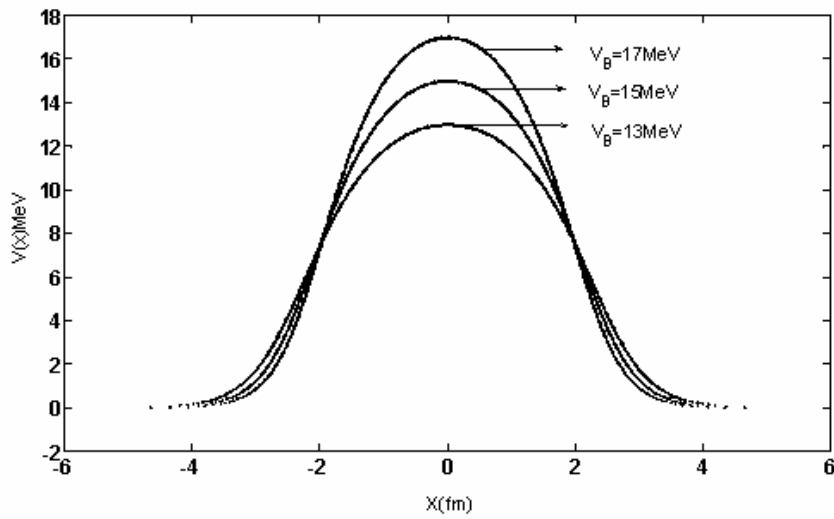


Figure 3.4: Plot of potential (3.1) for $\lambda=2$, $\nu=2.2$ and barrier heights $V_B=13, 15$ and 17 MeV respectively.

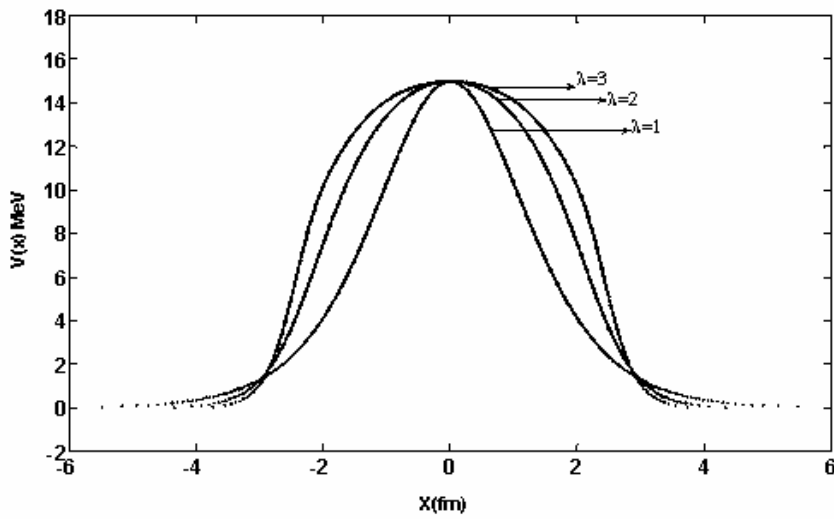


Figure 3.5: Plot of potential (3.1) for $V_B=15$ MeV, $\nu=2.2$ and $\lambda=1,2,3$ respectively.

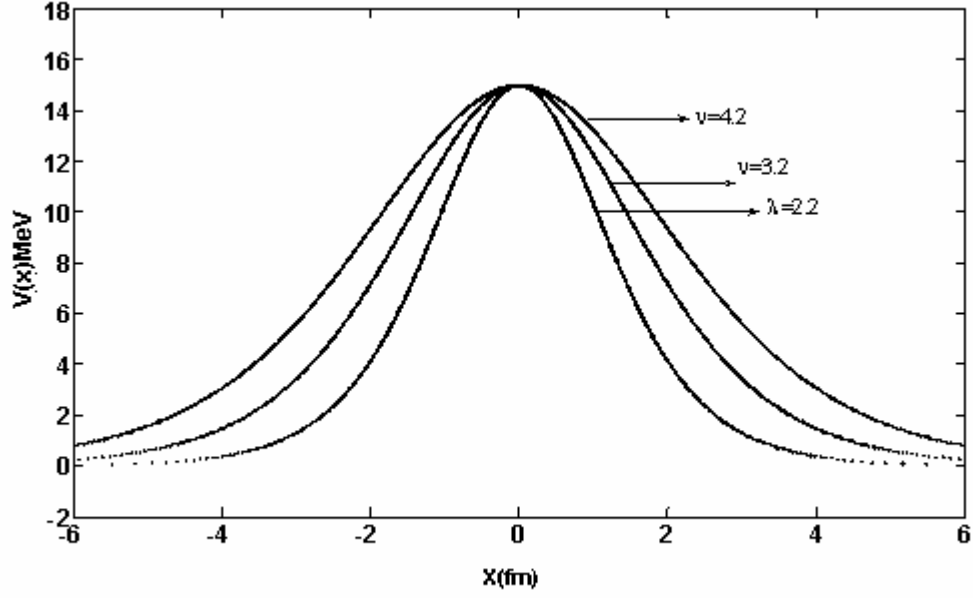


Figure 3.6: Plot of potential (3.1) for $V_B=15$ MeV, $\lambda=1$ and $\nu=2.2, 3.2$ and 4.2 respectively.

In the scattering theory approach alpha emission has been considered as the quantum collision phenomenon involving daughter as target and alpha as projectile. The potential generated in the nucleus-nucleus scattering is characterized by a pocket followed by barrier. Such a potential can also be represented by an analytically solvable form of potential of Sahu [Sah 08] and can be expressed as

$$V(r) = \begin{cases} V_{01}\{\lambda_1^2 B_0 + (B_1 - B_0)(1 - y_1^2)\} + \xi_1 & \text{if } 0 < r < R_1 \\ V_{02}\{\lambda_2^2 B_2(1 - y_2^2) + \xi_2\} & \text{if } r \geq R_1 \end{cases} \quad (3.13)$$

$$\xi_1 = \left(\frac{1 - \lambda_1^2}{4} \right) [5(1 - \lambda_1^2)y_1^4 - (7 - \lambda_1^2)y_1^2 + 2](1 - y_1^2)$$

$$\xi_2 = \left(\frac{1 - \lambda_2^2}{4} \right) [5(1 - \lambda_2^2)y_2^4 - (7 - \lambda_2^2)y_2^2 + 2](1 - y_2^2)$$

V_{01} and V_{02} are the strength of the potential in MeV, m is the mass of the particle moving under the influence of the potential. A dimensionless variable ρ_n has been defined as $\rho_n = (r - R_1)b_n$ with $b_n = [(2m/\hbar^2)V_{0n}]^{1/2}$, $n=1, 2$. ρ_n is related to new variable y_n as

$$\rho_n = \frac{1}{\lambda_n^2} [\tanh^{-1} y_n - (1 - \lambda_n^2)^{1/2} \tanh^{-1} (1 - \lambda_n^2)^{1/2} y_n] \quad (3.14)$$

The ranges of variation of r , ρ_n , and y_n are as follows. In the inner region r varies from 0 to R_1 , ρ_1 varies from $-R_1 b_1$ to 0 while y_1 starts with a value close to -1 and ends up with zero at $r = R_1$. In the outer barrier region while r varies from R_1 to ∞ , ρ_2 varies from 0 to ∞ and hence y_2 varies from 0 to 1. The parameters λ_1 , B_0 and B_1 specify the potential in the interior region $r < R_1$ and parameters λ_2 and B_2 specify the potential in the outer barrier region $r > R_1$. The height of the potential barrier has been defined at $r = R_1$ or $y_1 = y_2 = 0$ as

$$V_B = V_{01} \left[\lambda_1^2 B_1 + \frac{1 - \lambda_1^2}{2} \right] = V_{02} \left[\lambda_2^2 B_2 + \frac{1 - \lambda_2^2}{2} \right] \quad (3.15)$$

or $V_{01} = \frac{V_B}{[\lambda_1^2 B_1 + (1 - \lambda_1^2)/2]}$ and $V_{02} = \frac{V_B}{[\lambda_2^2 B_2 + (1 - \lambda_2^2)/2]}$

The parameter λ_1 and B_1 control the flatness and range in the inner region $r < R_1$ and λ_2 and B_2 control the flatness and range in outer region $r \geq R_1$. Near the origin the value of the potential is $V_{01} \lambda_1^2 B_0$ MeV. B_0 is the magnitude of the potential near the origin, which can be positive or negative, and thus the potential pocket of different depth can be generated in the region $0 < r \leq R_1$. Radial position corresponding to top of the barrier is given by

$$R_1 = r_0 (A_p^{1/3} + A_t^{1/3}) + 2.72 \quad (3.16)$$

and barrier height is given by

$$V_B = \frac{Z_t Z_p e^2}{R_1} \left(1 - \frac{a}{R_1} \right) \quad (3.17)$$

Where A_t and A_p are the mass number of target and projectile respectively and Z_t and Z_p are the corresponding atomic numbers, r_0 and a are distance parameter in fm and $e^2 = 1.4398 \text{ MeV fm}$. The potential presented by eq. (3.13) altogether has seven parameters, namely $\lambda_1, B_0, B_1, \lambda_2, B_2, r_0$ and a to describe the total effective potential. Considering some values for these parameters $\lambda_1 = 1.63539$, $B_0 = -78.75$, $B_1 = 21.2$, $\lambda_2 = 1$, $B_2 = 150$, $r_0 = 0.9 \text{ fm}$ and $a = 1.6 \text{ fm}$ for $\alpha + {}^{289}_{115}$ system we have plotted the potential expressed by eq. (3.13) shown by solid curve in the fig. 3.7. Different form of pocket and barrier can be generated by the variation of these parameters so as to closely reproduce the alpha plus nucleus potential.

In the earlier studies the phenomenological alpha-daughter potential is taken to be of the form

$$V_T(r) = V_N(r) + V_C(r) \quad (3.18)$$

where $V_N(r)$ is nuclear part and $V_C(r)$ is the repulsive Coulomb part of the barrier. Sahu has simulated the analytical alpha-daughter potential (3.13) with the phenomenological Wood-Saxon potential developed in double folding model in the framework of relativistic mean field theory [Mah 06] in the inner region and Coulomb plus centrifugal part in the outer region. The analytical potential (3.13) in the short range region $0 < r < R_1$ simulates the form given below

$$V_N(r) = -V_{N0} / \{1 + \exp[(r - R_N)/a_N]\} \quad (3.19)$$

$$V_C(r) = \begin{cases} (Z_t Z_p e^2)(3R_C^2 - r^2)/(2R_C^3) & \text{if } 0 < r < R_C \\ (Z_t Z_p e^2)/r & \text{if } r > R_C \end{cases} \quad (3.20)$$

The parameters of the potential described by eq. (3.19) and (3.20) are $V_{N0} = -78.75 \text{ MeV}$, $a_N = 0.84 \text{ fm}$, $R_N = 7.649 \text{ fm}$, and $R_C = 9.688 \text{ fm}$. Plot of the potential (3.18) is shown by dotted curve in the fig. 3.7. Also the variations in the shapes of the potential with potential parameters have been shown from fig. 3.8 to 3.10.

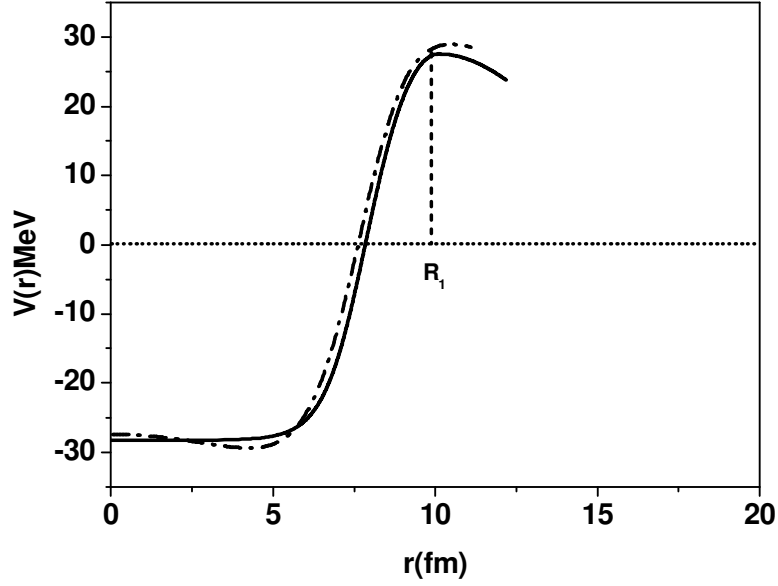


Figure 3.7: Plot of the potential $V(r)$ as a function of radial distance for $\alpha + {}^{289}\text{115}$ system. Solid line represents the form of analytical potential given by eq.(3.13), dotted line represents Wood-Saxon plus Coulomb potential given by eq. (3.18). Potential parameters of analytical potential are $B_0=-78.75$, $B_1=21.2$, $\lambda_1 = 1.63539$, $\lambda_2 = 1$, $B_2=150$, $r_0 = 0.9 \text{ fm}$ and $a = 1.6 \text{ fm}$. Potential parameter of eq. (3.18) are $V_{N0} = -78.75 \text{ MeV}$, $a_N = 0.84 \text{ fm}$, $R_N = 7.649 \text{ fm}$, and $R_C = 9.688 \text{ fm}$.

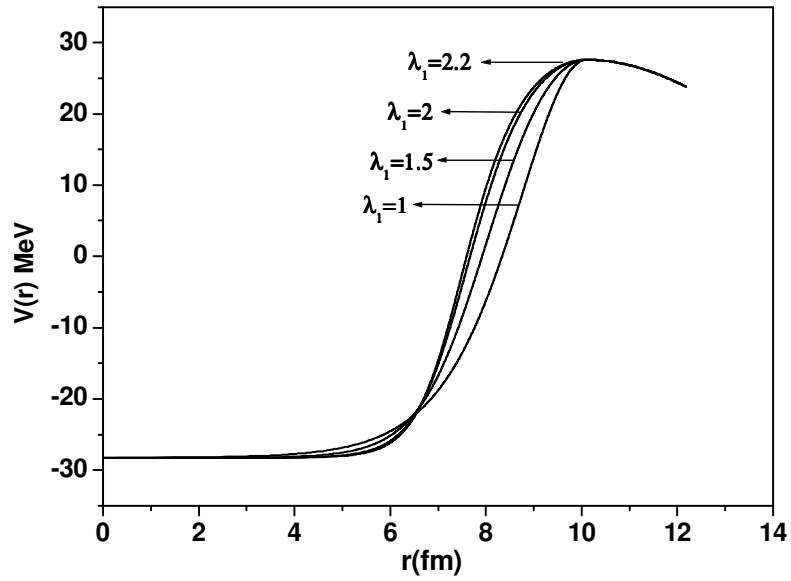


Figure 3.8: Plot of the potential $V(r)$ presented by eq. (3.13) as a function of radial distance for $\alpha + {}^{289}_{115}$ system for different values of flatness λ_1 .

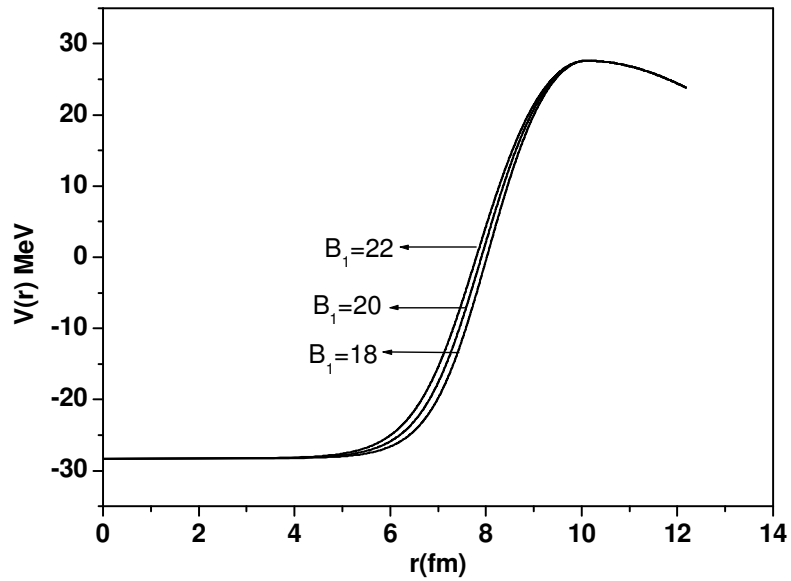


Figure 3.9: Same as figure 3.8 for different values of range parameter B_1 .

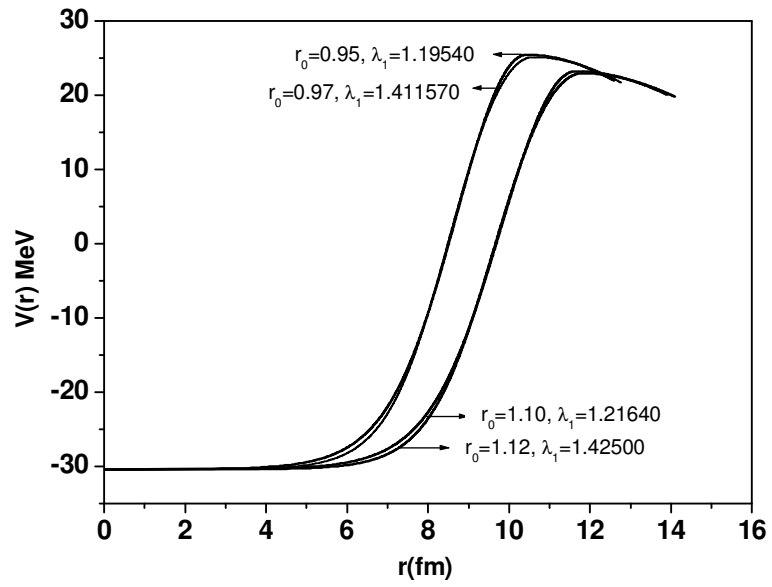


Figure3.10: Same as figure 3.8 for different values of, r_0 and λ_1 for $\alpha + 109^{278}$ system.

Chapter IV

Alpha decay study of proton rich Pb and Bi Chain

4.1 Introduction

In the chart of nuclides, nuclei lying above ^{100}Sn are of special interest for nuclear research since it includes the heaviest $Z=N$ known nuclei stable to proton emission. This region of nuclides exhibit diversity in the nuclear structure and also exhibit diversity in new decay modes. In this region of nuclides alpha decay is the dominant decay mode. When the alpha decay branches become very small positron and proton decay may be competing modes. Beta delayed two proton radioactivity, the direct emission of a proton pair from ground state and cluster radioactivity are other possible decay mode but these have not yet been observed in this region of nuclides.

Alpha decay process provides peculiar information about the spectroscopy of very neutron deficient nuclei in the region $Z < 82$ and $N > 82$ [Pag 96]. It is considered that from the decay data of ground and isomeric states detailed structure information on energy levels can be determined. Main aim of the experiments has been to focus on improvement of the measurements on the alpha decay energies and half life of the nuclei. In the study of alpha decay characteristics of ^{190}Po , ^{189}Bi and ^{186}Pb isotopes Andreyev et al [And 97] have reported improved values on alpha energies and half lives, which give clear characterization of the behavior of such exotic systems. Alpha decay studies of neutron deficient isotopes provide information on the nuclear mass surface close to the proton drip line. It has been observed that alpha decay favors the population of states in the daughter nucleus with similar spin and parity as the parent nucleus [Tav 98]. Many important and remarkable observations have been made from the experimental data of alpha emission in odd A alpha emitters by Hanauer et al [Han 61], Navarro et al [Nav 62], Soinski et al [Soi 70], Dilmanian et al [Dil 82] and more recently by Soinski and Shiley [Soi 74]. Wouters et al [Wou 86] and Schuurmans et al [Sch 96] have shown for the first time that anisotropic alpha emission in favored decays is mainly determined by the structure shell effect of the decaying nucleus, not being necessarily related to

deformation. From the detailed analysis of the proton, alpha and cluster radioactivity it is possible to get information on structure and nuclear mass of some exotic nuclei which are not yet experimentally observed. There are two types of difficulties in description of the decay properties of the nuclei which exist far from the line of stability. First is the lack of data as well as accurate estimation on nuclear masses, nuclear sizes and electromagnetic moments. And second is the lack of models to describe the structure of loosely bound nuclei.

4.2 Motivation

On the experimental front, with the advent of accelerator based research, it has been possible to synthesize and measure alpha energies and half lives for exotic nuclei. From the experimental data it has been observed that for proton rich isotopes in the region $Z \geq 82$ alpha emission and electron capture are two competing mode of decay [nndc]. It has been observed that in the chain of neutron deficient Pb isotopes the alpha branching ratio changes from small value of $< 1\%$ for ^{202}Pb to $\leq 100\%$ in ^{182}Pb [nndc]. The corresponding half lives of various isotopes exhibit large variation from 1.7×10^{14} sec to 5.5×10^{-2} sec as the neutron number changes from $N = 120$ to $N = 100$. Similarly in the chain of proton rich Bi isotopes alpha branching ratio changes from $1.0 \times 10^{-4}\%$ for ^{197}Bi to 100% for ^{187}Bi and corresponding half life changes from 9.33min to 32ms. The proton rich Pb and Bi isotopes thus offer an interesting region to test the validity of existing theories of alpha decay as one move from the region of naturally occurring stable isotopes with $Z / N \cong 0.65$ to the region close to proton drip line with $Z / N \cong 0.82$ for ^{182}Pb and $Z / N \cong 0.79$ for ^{187}Bi .

4.3 Literature Survey

The existing theoretical studies on alpha decay have been performed using the approaches discussed in chapter II. Using unified fission model approach Shi and Swiatecki [Shi 85] have studied alpha and cluster radioactivity by taking the interacting barrier as Coulomb plus proximity potential with no adjustable parameter. Authors have calculated penetrability factor for alpha and ^{14}C emission for $Z=88$ and $A=222, 223$ and 224 and also have calculated penetrability factor for the emission of some heavier cluster

in the region $Z=88, 89$ and $A=221-225$. Shanmugam *et al.* [Sha 95, Sha 90a] have used their model, which determines the height of the barrier correctly and has been used to calculate branching ratios for the spontaneous emission of ^{14}C and ^{24}Ne from certain actinide nuclei (^{221}Fr , $^{221-224,226}\text{Ra}$, ^{225}Ac , $^{232-233}\text{U}$). Later Shanmugam *et al.* [Sha 90b] have used the modified model to study alpha radioactivity in the region $Z=64-94$ and $A=152-242$ and found good agreement with the experimental data. Goncalves *et al.* [Gon 93], Duarte *et al.* [Dua 04] and Tavares *et al.* [Tav 98] have used their model to study alpha and cluster radioactivity. Goncalves *et al.* [Gon 93] have calculated half lives of parent nuclei for ^{14}C , ^{20}O , ^{23}F , ^{24}Ne , ^{28}Mg and ^{32}Si emission in the region $Z=87-96$ and $A=221-242$. Tavares *et al.* [Tav 98] have used this model for alpha radioactivity in the region $Z=52-111$ and $A=106-272$. Calculations have been performed for the set of e-e, e-o, o-e and o-o nuclei. In all the case good agreement has been found with the experimental data, however better agreement has been observed for the set of e-e nuclei. G.Royer [Roy 00] have calculated alpha decay half life for the set of e-e and e-o nuclei in the region $Z=52-110$; $A=107-269$ and for o-e and o-o in the region $Z=53-111$; $A=111-272$. In all the cases they have found good agreement with experimental data. Garcia et al [Gar 00] have calculated alpha decay half life for the even-even nuclei in the region $Z=52-108$ and $A=106-264$ for their ground state to ground state transition with mutual angular momentum $\ell = 0$.

In the cluster model approach Buck and Merchant [Buc 89] have used their folding model to calculate alpha decay half life in the region $^{106}\text{Te}-^{266}\text{109}$. Tavares *et al.* [Tav 05] have used a potential barrier which includes the centrifugal and overlapping effects. They have calculated half life values and have studied the effect of pairing and shell closure of neighboring nuclei on the half life for alpha decay in the vicinity of the 126 neutron shell closure of the parent and daughter nuclei. Tavares *et al.* [Tav 05] have used this model for alpha decay half life calculation for ground state to ground state transitions ($\ell = 5$) for twenty one Bi isotopes with A ranging between 189 and 214.

Mediros *et al.* [Med 06] have calculated alpha decay half life by using semiempirical model. Calculations have been performed for the alpha decay half life of 336 nuclides corresponding to their ground state to ground state transitions with mutual angular momentum ($\ell = 0$). They have also predicted the alpha decay half life for some

new alpha emitters namely ^{180}W , ^{184}Os and ^{228}Ra . Santosh et al [San 08] have used a semiempirical formula to calculate the alpha decay half life in the region $Z=85-102$ and $A=215-259$. Authors have compared the result with one calculated by VSS [Vio 66] formula and by Horoi [Hor 04]. Calculations have been performed in the region $Z=52-108$ and $A=106-264$. Parkhomenko et al [Par 05] have applied their phenomenological formula to calculate alpha decay half life of e-e nuclei in the region $Z=84-116$; $N=130-180$, for o-e nuclei in the region $Z=85-107$; $N=130-160$, for e-o nuclei in the region $Z=84-114$; $N=130-175$ and for o-o in the region $Z=85-111$; $N=125-160$.

Silestanu et al [Sil 01] have studied alpha, cluster and proton decay in the trans tin region $52 \leq Z \leq 56$; $54 \leq N \leq 60$ and in trans lead region $84 \leq Z \leq 88$; $130 \leq N \leq 136$. Good agreement has been found with experimental data.

In the present work we have studied the systematic for alpha emission from Pb and Bi isotopes using the asymmetric form of analytically solvable potential presented by equation (3.5) along with (3.6) and (3.7) described in detail in chapter III in the framework of unified fission like approach. The potential model has been successfully used in the study of above barrier resonances by Sahu et al [Sah 02] and in the study of proton radioactivity by Mehrotra et al [Meh 08]. We have used exact expression of transmission coefficient in place of commonly used WKB method.

In the chain of Pb isotopes alpha decay half life has been calculated for experimentally known proton rich even-even Pb isotopes in the region $A=182-196$, 202 and 210 for their ground state to ground state transition with mutual angular momentum $\ell = 0$. We have predicted the alpha decay half life for unknown even – even Pb isotopes in the mass region $A=198-208$. In the chain of Pb isotopes there are four stable isotopes of Pb at mass number $A=204$, 206, 207 and 208. Along with these stable isotopes half lives of $A=198$ and 200 are not measured yet. We see from the energetic of decay that these isotopes are energetically possible for the emission of alpha particle. Therefore we have predicted the half lives of unknown even-even Pb isotopes by using the present model. In the chain of Bi isotopes we have studied in the mass region $A=189-214$. Alpha decay half life has been calculated for experimentally known Bi isotopes in the mass region $A=191-195$, 209,211-214 and predicted for those which are experimentally unknown in the region $A=189$, 197-208. The calculations for the Bi isotopes have been

performed for the ground state to ground state transition with their mutual angular momentum $\ell = 5$. Good agreement has been found with the experimental data.

4.4 Alpha decay half life

The decay rate in the unified fission model approach is given by the relationship

$$P = P_0 T \quad (4.1)$$

where the assault frequency P_0 is calculated from the zero point vibration energy of ref.[Poe 86] given as

$$E_v = 1/2 h P_0 \quad (4.2)$$

Transmission probability T has been calculated by using exact expression given by eq.(3.11). The half life time t is calculated as $t = \log_e 2/P$.

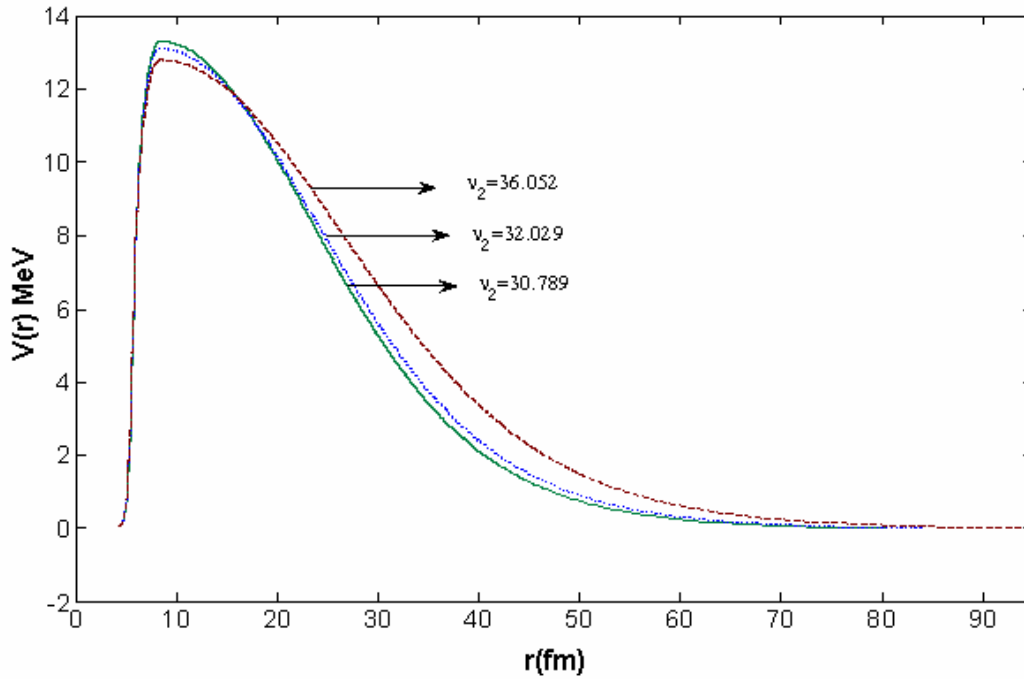


Figure 4.1 Plot of alpha decay barrier for three limiting value of range parameter v_2 , obtained from the best fit to the experimental data corresponding to three Pb isotopes ^{182}Pb , ^{190}Pb and ^{210}Pb respectively. Respective v_2 value for each Pb isotope is given in table 4.1.

4.5 Details of calculation for Pb isotopes

4.5.1 Model parameters

Potential parameters for the problem of Pb isotopes have been fixed at $\lambda_1 = 3.2$ and $\nu_1 = 2.3$ indicative of narrow sharply falling inner region of the potential. The contribution of the inner barrier to the half life values is small. As the outer potential barrier simulates the slowly falling long ranged coulomb barrier for $l = 0$, we have fixed $\lambda_2 = 1.1$ and varied ν_2 starting from a large base value 30 to 37 to reproduce the experimental half life. In the calculations decay energy Q_α of the known Pb isotopes has been taken from the ref. [nndc] and for unknown isotopes we have used theoretical Q_α values given by Audi and Wapstra [Aud03]. Assault frequency calculated by using eq.(4.2) is of the order of 10^{20} s^{-1} in the case of even-even Pb isotopes. Results are shown in table 4.1.

4.5.2 Barrier height calculation of Pb isotopes

In the decay problems barrier height of the decaying system should correspond to Coulomb plus centrifugal potentials. Shanmugam *et al.* [Sha90b] have chosen the barrier height approximately 14MeV for ^{152}Gd and 17MeV for ^{238}U respectively for $\ell = 0$ alpha transition. Tavares *et al.* [Tav05] have taken barrier height nearly 28MeV and 30MeV for ^{209}Bi and ^{187}Bi respectively. But the earlier studies show that inclusion of nuclear potential and various renormalization processes tends to reduce the barrier height substantially. Royer [Roy00] have modified the alpha decay barrier height by including proximity force effect which lowers the Coulomb barrier to a height between 10 MeV and 17.5 MeV in the region of nuclides $Z=52-110$ and $A=108-269$. For the barrier height of the Pb isotopes we have taken barrier height V_B of ^{182}Pb to be 13.3 MeV for $\ell = 0$ from the work of Royer [Roy00]. Treating this as reference the barrier heights of other Pb isotopes are calculated as $V_B' = (R_i/R_i')V_B$ where R_i and R_i' are the touching radii. These values lie between 10.8 MeV to 13.4 MeV.

4.5.3 Nuclear radii

R_t is the touching radius of the two nuclei *i.e.* $R_t = R_d + R_\alpha$, where R_d is the daughter radius have been calculated from the droplet model of atomic nuclei [Mye77, Mol95].

Radii have been thus evaluated as

$$R_i = \frac{Z_i}{A_i} R_{pi} + \left(1 - \frac{Z_i}{A_i}\right) R_{ni}, \quad i = p, d \quad (4.3)$$

Where R are given by

$$R_{ji} = r_{ji} \left[1 + \frac{5}{2} \left(\frac{\omega}{r_{ji}} \right)^2 \right], \quad j = p, n; \quad i = p, d \quad (4.4)$$

where $\omega = 1 \text{ fm}$ is the diffuseness of the nuclear surface, and r is the equivalent sharp radius of neutron ($j = n$) or proton ($j = p$) density distribution following the finite – range droplet model description of nuclei by moller et al [Mol95], thus giving

$$r_{pi} = r_0 (1 + \bar{\epsilon}_i) \left[1 - \frac{2}{3} \left(1 - \frac{Z_i}{A_i} \right) \left(1 - \frac{2Z_i}{A_i} - \bar{\delta}_i \right) \right] A_i^{1/3},$$

$$r_{ni} = r_0 (1 + \bar{\epsilon}_i) \left[1 + \frac{2}{3} \frac{Z_i}{A_i} \left(1 - \frac{2Z_i}{A_i} - \bar{\delta}_i \right) \right] A_i^{1/3},$$

Where
$$\bar{\epsilon}_i = \frac{1}{4e^{0.831A_i^{1/3}}} - \frac{0.191}{A_i^{1/3}} + \frac{0.0031Z_i^2}{A_i^{4/3}},$$

$$\bar{\delta}_i = \left(1 - \frac{2Z_i}{A_i} + 0.004781 \frac{Z_i}{A_i^{2/3}} \right) \left/ \left(1 + \frac{2.52114}{A_i^{1/3}} \right) \right.,$$

$r_0 = 1.16 \text{ fm}$, and nuclear radius parameter $r_{0i} = R_i / A_i^{1/3}$ ($i = p, d$)

The value of alpha particle radius has been fixed at $R_\alpha = (1.62 \pm 0.01) \text{ fm}$. This value comes from the charge density distribution resulting from data on elastic electron scattering from ^4He as measured by Sick *et al.* [Sic76].

4.6 WKB approximation method and Exact method

In order to test the accuracy of exact method over WKB method we have calculated T_{Exact} and T_{WKB} for Eckart barrier of different ranges using eq. (4.5) and (4.6) given below. Results are shown in table 4.3. We have fixed $\lambda = 1$ in the potential described by eq. (3.2), which reduces to the symmetric Eckart barrier of the form $V(r) = V_0 \operatorname{sech}^2(x/2a)$, where $a = 1/2b$ for $\lambda = 1$. Exact expression of the transmission probability through the Eckart barrier is given as [Zaf 93]

$$T_{\text{exact}}^{\text{Eckart}}(E) = \frac{\sinh^2(\pi f')}{[\sinh^2(\pi f') + \cosh^2(\pi g')]} \quad (4.5)$$

$$\text{where } f' = \left[\frac{E}{\Delta'} \right]^{1/2}$$

$$g' = \left[\left(\frac{V_0}{\Delta'} \right) - \frac{1}{4} \right]^{1/2}$$

$$\text{and } \Delta' = \frac{\hbar^2}{8ma^2}$$

Expression of transmission probability in the WKB approximation method is given as [Zaf 93]

$$T_{\text{WKB}}^{\text{Exact}}(E) = [1 + \exp\{2\pi(q' - f')\}]^{-1} \quad (4.6)$$

$$\text{where } q' = \left(\frac{V_0}{\Delta'} \right)^{1/2}$$

Table 4.1: Calculated and experimental half lives of proton rich even Pb isotopes. The corresponding values of parameter v_2 which gives best fit with the experimental data are also given.

Parent Nucleus	Assault freq.(P_0) $\times 10^{20} \text{ sec}^{-1}$	Q_α (MeV) Exp.	v_2	$\log_{10}[t_{1/2}](\text{sec.})$ Cal.	$\log_{10}[t_{1/2}](\text{sec.})$ Exp.
^{182}Pb	3.58	7.06	30.78	-1.26	-1.26
^{184}Pb	3.43	6.77	30.07	-0.25	-0.26
^{186}Pb	3.28	6.47	31.24	1.00	1.00
^{188}Pb	3.09	6.11	31.47	2.04	2.04
^{190}Pb	2.89	5.69	32.02	3.90	3.90
^{192}Pb	2.64	5.22	32.83	6.56	6.56
^{194}Pb	2.40	4.73	33.99	9.99	9.99
^{196}Pb	2.14	4.23	32.98	9.86	9.86
^{202}Pb	1.31	2.59	31.98	14.23	14.23
$^{210}\text{Pb}^*$	1.92	3.79	36.05	16.56	16.57

* ^{210}Pb is neutron rich

Table 4.2: Predicted alpha decay half lives of five experimentally unknown proton rich even Pb isotopes.

Parent Nucleus	Assault freq. (Po)Sec $^{-1}$.	Q_α (theo.) (MeV)	$\log_{10}(t_{1/2})\text{Sec}$ Cal.
^{198}Pb	1.88×10^{20}	3.718	11.68
^{200}Pb	1.60×10^{20}	3.158	13.73
^{204}Pb	9.99×10^{19}	1.969	18.85
^{206}Pb	5.76×10^{19}	1.135	23.47
^{208}Pb	2.62×10^{19}	0.5169	28.23

Table4.3: Comparison of WKB and exact transmission coefficients for different ranges with $v_0 = 13.3$ MeV and $Q_\alpha = 7.066$ MeV.

$\frac{1}{a}$ (fm ⁻¹)	$\Delta = \hbar^2/2ma^2$ (Mev)	T_{WKB}	T_{Exact}	$T_{\text{WKB}} / T_{\text{Exact}}$
0.5	1.25	1.38×10^{-5}	1.57×10^{-5}	0.878
1.0	5.0	3.48×10^{-3}	4.48×10^{-3}	0.776
2.0	20	0.058	0.088	0.659
4.0	80	0.200	0.402	0.497
8.0	320.51	0.333	0.754	0.441
16.0	1300.72	0.414	0.927	0.446
32.0	5200	0.419	0.981	0.427

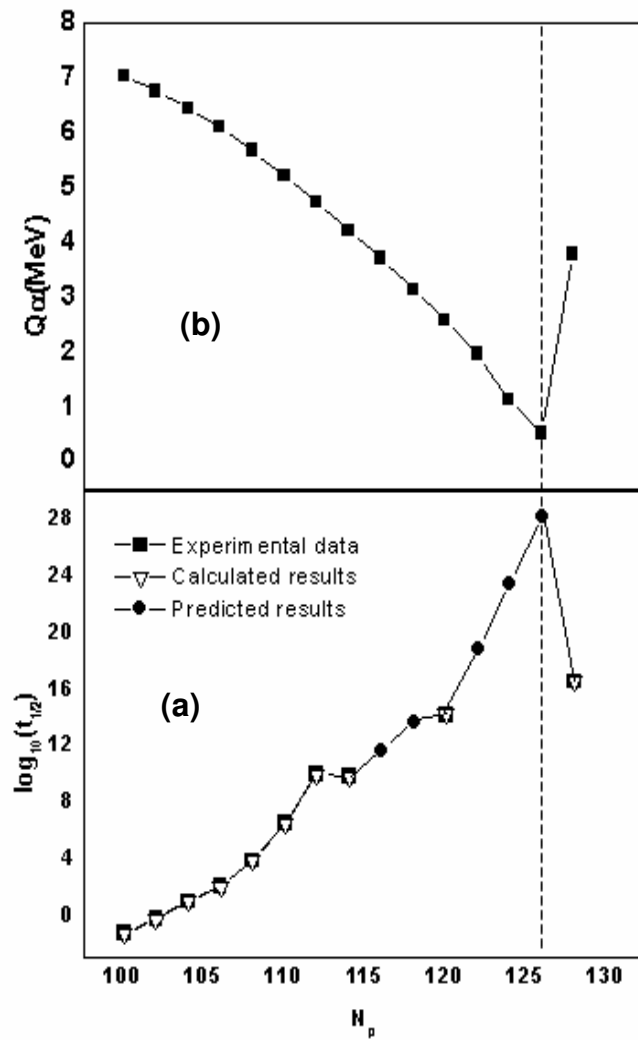


Figure 4.2: Variation of (a) logarithm of half life time and (b) Q_α values for alpha emission with neutron number of parent isotopes of Pb chain.

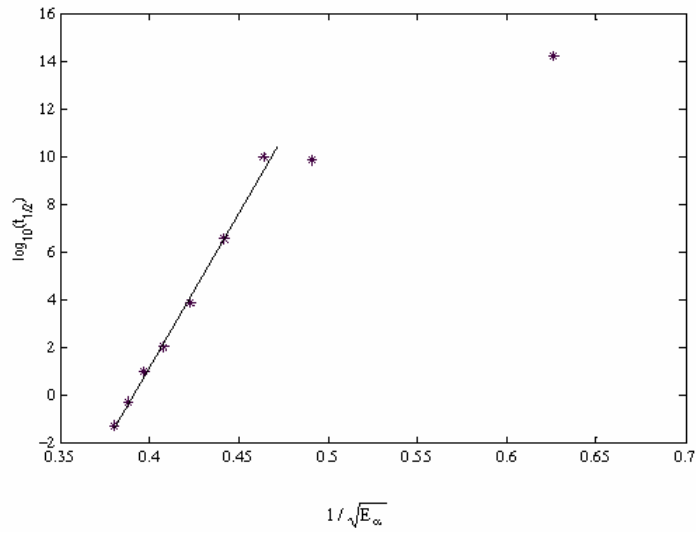


Figure 4.3: Variation of $\log_{10}(t_{1/2})$ for alpha emission with $E_{\alpha}^{-1/2} (\text{MeV})^{-1/2}$.

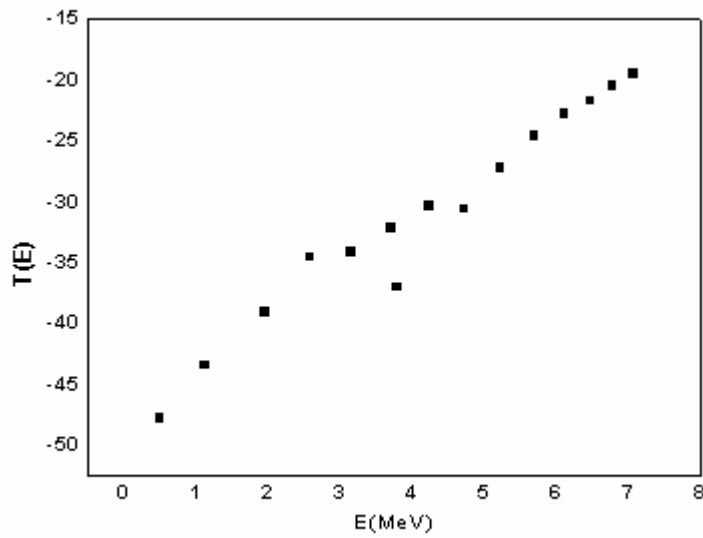


Figure 4.4: Variation of transmission probability with incident energies of the alpha particle of Pb chain.

4.7 Result and discussion

The half lives of experimentally known even Pb isotopes $^{182-196}\text{Pb}$, ^{202}Pb and ^{210}Pb have been calculated corresponding to best fit value of the range parameter v_2 . Results are shown in table 4.1. In all the cases good agreement with experimental data is obtained by varying the parameter v_2 which controls the range of the outer region of the potential barrier. The resulting barrier for the limiting and mid values of v_2 is shown in fig 4.1. We have calculated minimum rms deviation of range parameter v_2 for 10 known experimental data. The rms deviation has been calculated by using the

$$\text{relation } \sigma = \left\{ \frac{1}{N} \sum_{i=1}^N \left[\log_{10} \left(\frac{T_{1/2}^e}{T_{1/2}^c} \right) \right]^2 \right\}^{\frac{1}{2}} \quad (4.7)$$

We have obtained the minimum rms deviation of 2.78 corresponding to $v_2 = 33$. For this v_2 , half lives of five experimentally unknown even Pb isotopes $^{198,200,204,206}\text{Pb}$ and ^{208}Pb have been predicted. $^{204,206,208}\text{Pb}$ are stable isotope in the chain of lead, which are found to have very large half life of the order of several years. Results are shown in table 4.2. Partial alpha decay half life $\log_{10}(t_{1/2})$ and alpha decay energy Q_α has been plotted as a function of neutron number of parents nuclei. Plot is shown in fig.4.2. From the plot it is clear that partial alpha decay half life is perfect inverse reflection of alpha decay energy Q_α . The influence of 126 neutron shell closure which in turn is manifested in the Q_α value is clearly evidenced, particularly the doubly magic ^{208}Pb isotope shows the highest half life in the chain of Pb isotopes. Thus our model demonstrates the shell closure effect correctly. It means Q_α value is the main quantity which gives strength to the alpha activity of an isotopic sequence, which ultimately depends on pairing and shell effects. The energies of alpha particle E_α are calculated from experimental Q_α value using the expression $E_\alpha = (A - 4/A) Q_\alpha$. The variation of logarithm of half life with $1/\sqrt{E_\alpha}$ is shown in fig.4.3. The empirical Geiger Nuttal law $\log_{10} t_{1/2} = C_1 + C_2 E_\alpha^{-1/2}$ is followed upto $A=194$ with $C_1 = -5 \text{ sec}$ and $C_2 = 17.7 \text{ MeV}^{1/2} \text{ sec}$. From the comparison of WKB and exact transmission coefficients given in table 4.3 it is observed that the WKB

approximation becomes poorer with increasing range a . We observe that the parameter $\Delta = \hbar^2/2ma^2$ sets the lower limit on energy above which the WKB approximation would work well provided $V_0 > \Delta$ [Zaf 93]. The condition, $E > \Delta$ comes to the de Broglie wavelength of the incident particle being less than that of the size of the “obstacle” i.e., when $\lambda_d < 2\pi a$. When $\lambda_d > 2\pi a$ the tunneling becomes more and more quantal and hence the semiclassical approximation becomes poorer. Fig. 4.4 shows the plot of transmission probability with respect to incident energies, which shows the direct dependence of transmission probability on incident energies.

4.8 Details of calculation for Bi isotopes

4.8.1 Model parameter

For the Bi isotopes parameters in the inner region of the potential barrier has been fixed at $\lambda_1 = 3.2$, $\nu_1 = 2.2$ and in the outer region at $\lambda_2 = 1.2$ to simulate the narrow sharply falling inner region parabolic at the top and long ranged Coulombic tail in outer region. ν_2 is varied to reproduce the experimental half life. Present calculation has been performed for the Bi isotopes in the mass region $A=189-214$ for their ground state to ground state transitions with mutual angular momentum $\ell = 5$. The choice for $\ell = 5$ comes from spin and parity conservation laws ($J_p = J_d + J_\alpha + \ell$), $\pi_p = \pi_d \cdot \pi_\alpha (-1)^\ell$ and for alpha transition ($J_\alpha^{\pi_\alpha} = 0^+$) [Tav 05]. In the present calculations Q_α has been taken from the ref. [nndc]. For the Bi isotopes calculated assault frequency of the order 10^{20} sec^{-1} has been obtained calculated by using eq. (4.2). Results are listed in table 4.4 and 4.6.

4.8.2 Barrier height calculation of Bi Isotopes

Outer region of the potential barrier should correspond to Coulomb plus centrifugal form. The expression of transmission probability is applicable for $\ell = 0$ angular momentum state. For higher angular momentum states an additional centrifugal term $V_l = [\hbar^2/2\mu] \ell(\ell+1)/r^2$ should be incorporated in the Schrödinger eq. As it is not possible to solve exactly the Schrödinger equation with this potential V_l incorporated in the potential given by eq.(3.5) along with (3.6) and (3.7), we approximately incorporate the

effect of this term by making the ℓ dependence as follows. S-wave height V_B at ρ is replaced by the partial wave height. In the present calculations the barrier height has been calculated by using the expression of the reference [Sah 99]

$$V_B^\ell = V_B + \frac{\hbar^2}{2\mu} \frac{\ell(\ell+1)}{R_B^2}$$

Where radial position R_B and barrier height V_B has been calculated by using global formula [Sah 99]

$$R_B = r_0(A_1^{1/3} + A_2^{1/3}) + 2.72$$

$$V_B = \frac{Z_1 Z_2 e^2}{R_B} \left(1 - \frac{a}{R_B}\right)$$

where A_1 , A_2 and Z_1 , Z_2 are the mass numbers and atomic numbers of alpha and daughter nucleus respectively. r_0 and a are two distance parameter and $e^2 = 1.4398$ MeV fm. We have fixed $r_0 = 1.07$ fm and $a = 0.63$ fm [Sah 99] in our calculations. Barrier heights has been calculated for each Bi isotope separately for their ground state to ground state transition with mutual angular momentum $\ell = 5$. The calculated barrier height varies in the range from 21.7916 MeV for $\alpha + {}^{210}_{81}Tl$ system to 22.3399 MeV for $\alpha + {}^{185}_{81}Tl$ system.

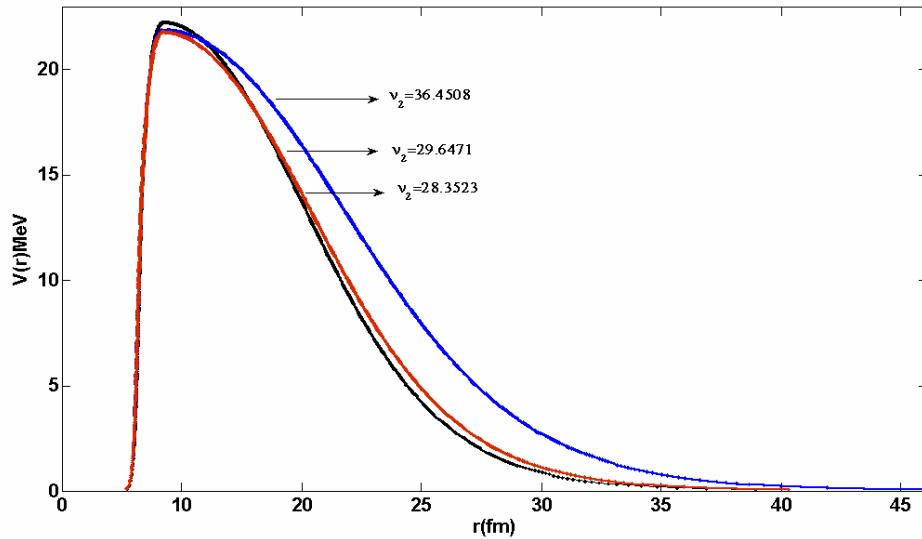


Figure 4.5: Plot of the potential for three limiting value of range parameter v_2 obtained corresponding to best fit to the experimental data for ${}^{191}\text{Bi}$, ${}^{209}\text{Bi}$ and ${}^{214}\text{Bi}$.

Table 4.4: Calculated and experimental alpha decay half lives are presented. Corresponding best fit value of range parameter ν_2 which gives best fit to the experimental data, assault frequency, radial position and barrier heights for each nucleus are also given.

Parent nucleus	Q_α (MeV)	Assault Freq. (P_0) (10^{20}s^{-1})	Radial Position R_B (fm)	Barrier Height (V_B^ℓ)MeV	Range parameter (ν_2)	Log ₁₀ ($t_{1/2}$) Exp. (Sec.)	Log ₁₀ ($t_{1/2}$) Cal. (Sec.)
¹⁹¹ Bi	6.778	3.108	10.5373	22.2705	28.3523	2.849	2.849
¹⁹³ Bi	6.304	2.891	10.5590	22.2459	28.8022	4.503	4.503
¹⁹⁵ Bi	5.832	2.674	10.5806	22.2019	29.5767	6.785	6.785
²⁰⁹ Bi	3.137	1.438	10.7277	21.8951	36.4508	26.77	26.77
²¹¹ Bi	6.750	3.095	10.7481	21.8530	28.0644	2.187	2.187
²¹² Bi	6.207	2.177	10.7583	21.8369	28.8436	4.571	4.571
²¹³ Bi	5.982	2.743	10.7684	21.8113	28.9402	5.149	5.149
²¹⁴ Bi	5.621	1.889	10.7785	21.7916	29.6471	7.161	7.161

Table 4.5: Alpha decay half lives calculated by present model for the range parameter $\nu_2=28.094$, obtained corresponding to minimum deviation $\sigma=0.93$ are given. Calculated results have been compared with ref [Tav 05].

Parent nucleus	Log ₁₀ ($t_{1/2}$) (Sec.) Exp.	Log ₁₀ ($t_{1/2}$) (Sec.) present work	Log ₁₀ ($t_{1/2}$) (Sec.) [Tav 05]
¹⁹¹ Bi	2.849	3.8516	2.6064
¹⁹³ Bi	4.503	4.7440	4.4579
¹⁹⁵ Bi	6.785	5.6536	6.5289
²⁰⁹ Bi	26.77	11.6806	26.5079
²¹¹ Bi	2.187	3.6705	2.3560
²¹² Bi	4.571	4.7398	4.5315
²¹³ Bi	5.149	5.1492	5.119
²¹⁴ Bi	7.161	5.8989	7.2201

Table 4.6: Predicted alpha decay half life of unknown Bi isotopes, calculated by taking the range parameter V_2 , obtained corresponding to minimum deviation. Corresponding assault frequency, radial position, and barrier heights are also given. Half lives of the present work are compared with ref. [Tav 05].

Parent nucleus	Q_α (MeV)	Assault frequency P_0 (10^{20}s^{-1})	Radial Position R_B (fm)	Barrier Height V_B (MeV)	$\text{Log}_{10}(t_{1/2})$ Cal.	$\text{Log}_{10}(t_{1/2})$ [Tav 05]
^{189}Bi	7.270	3.33	10.5154	22.339	2.9803	0.8751
^{197}Bi	5.210	2.389	10.6020	22.1564	6.9125	9.7627
^{199}Bi	4.932	2.261	10.6233	22.1112	7.4861	11.3010
^{200}Bi	4.700	1.648	10.6339	22.0899	8.0092	12.7443
^{201}Bi	4.500	2.063	10.6444	22.0667	8.4211	14.1004
^{202}Bi	4.340	1.522	10.6550	22.0454	8.8008	15.3010
^{203}Bi	4.090	1.875	10.6655	22.0224	9.3573	17.1335
^{204}Bi	3.960	1.389	10.6759	22.0018	9.6728	18.2672
^{205}Bi	3.695	1.694	10.6884	21.9765	10.2816	20.5999
^{206}Bi	3.530	1.238	10.6967	21.9584	10.7112	22.2014
^{207}Bi	3.281	1.504	10.7070	21.9380	11.3169	24.8451
^{208}Bi	3.051	1.070	10.7174	21.9153	11.9424	27.5922

Table 4.7: Calculated pre formation probability through the overlapping region has been given. Results of ref. [Tav 05] have been given for comparison.

Parent nucleus	Preformation probability $S_{\alpha}(10^{-3})$ Present calculation	Preformation probability $S_{\alpha}(10^{-3})$ [Tav 05]
^{189}Bi	5.5	6.66
^{191}Bi	4.8	6.35
^{193}Bi	4.2	6.07
^{195}Bi	3.6	5.80
^{197}Bi	3.0	5.46
^{199}Bi	2.7	5.34
^{200}Bi	2.5	5.22
^{201}Bi	2.4	5.13
^{202}Bi	2.3	5.05
^{203}Bi	2.1	4.94
^{204}Bi	2.0	4.89
^{205}Bi	1.8	4.77
^{206}Bi	1.7	4.70
^{207}Bi	1.6	4.60
^{208}Bi	1.6	4.50
^{209}Bi	1.5	4.56
^{211}Bi	5.0	6.81
^{212}Bi	4.2	6.43
^{213}Bi	3.9	6.29
^{214}Bi	3.5	6.06

4.9 Result and discussion

The alpha decay half life values of 8 experimentally known alpha emitting Bi isotopes have been calculated for their ground state to ground state transitions with mutual angular momentum $l = 5$. Experimental half life values have been taken from the reference [Tav 05] for $l = 5$ transitions. In all the cases good agreement with experimental results is obtained by varying just one parameter v_2 which controls the range of the barrier in the outer region. Calculated alpha decay half lives of experimentally known Bi isotopes corresponding to best fit values of range parameter v_2 are shown in table 4.4. The minimum rms deviation has been calculated by using the eq. (4.7). The calculated minimum rms deviation obtained is 5.40 corresponding to range parameter $v_2 = 28.9402$. Width of the outer barrier is exceptionally large for ^{209}Bi compared to that of other isotopes. If ^{209}Bi is excluded from the fit the rms deviation (σ) drops to a value of 0.93. Using this v_2 half life values of experimentally known Bi isotopes have been calculated in the region $A = 191-195, 209-214$ and have been predicted in the region $A = 189, 197-208$ for their ground state to ground state transition with mutual angular momentum $l = 5$. Results are shown in table 4.5 and table 4.6 respectively. In table 4.5 we have compared the result of the present calculation with the experimental result and results of ref. [Tav05]. From table 4.6 it is observed that our predicted life time values are lower than those of ref. [Tav05]. The Q_α values used in the ref. [Tav05] are slightly larger than our values. Also a constant value of assault frequency $2 \times 10^{21} \text{ s}^{-1}$ has been used in the ref. [Tav05] which is higher than our calculated values. The reason for the discrepancy can be traced to the choice of barrier height in the present work. The average barrier height in ref. [Tav05] is ~ 30 Mev. Whereas in the present work we have calculated the barrier height for each isotope separately, this comes between 21 MeV to 22 MeV. Shape of the potential barrier for the alpha decaying system for three limiting value of range parameter v_2 is shown in fig.4.5. The wide barrier for ^{209}Bi ($v_2 = 36.4508$) is reflective of the shell closure effect so that it can be excluded from the fitting calculation. In fig. 4.6 alpha decay energy, pre-formation probability and logarithm of half life values have been plotted with respect to neutron no. of daughter nuclei where influence of the 126-neutron shell closure is clearly evidenced.

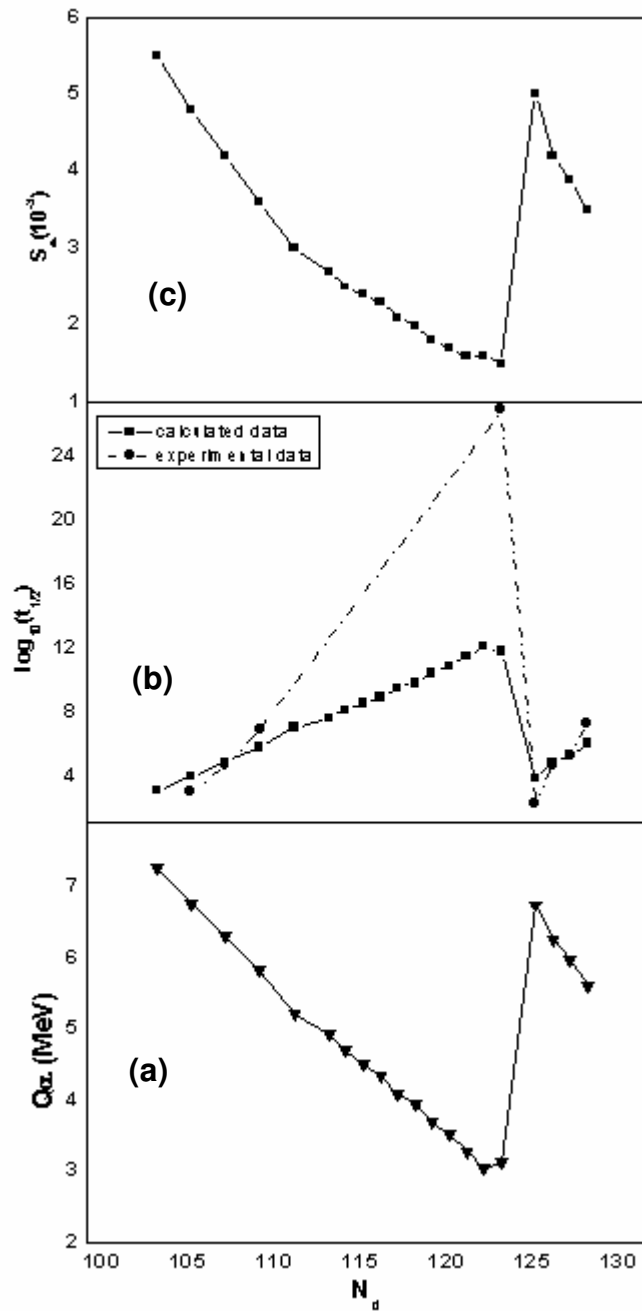


Figure 4.6 (a), Q_α value (b), logarithm of alpha decay half life and (c), preformation probability, S_α have been plotted against neutron number of the thallium isotope (daughter nucleus).

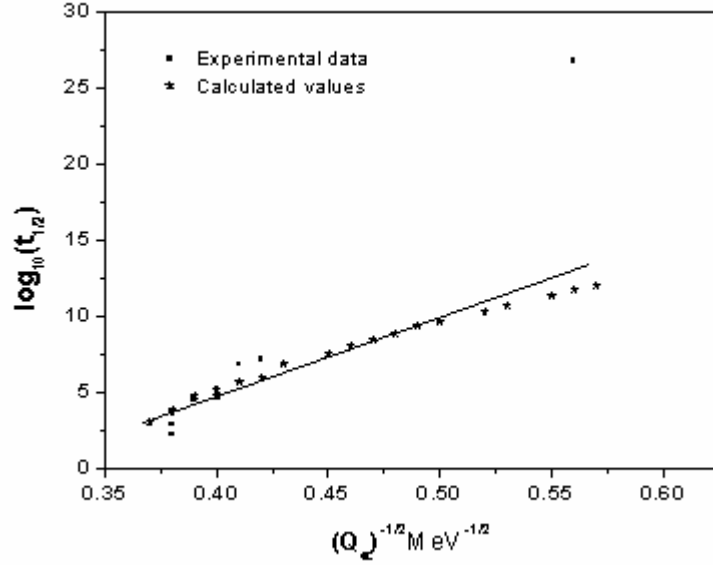


Figure 4.7: Plot of partial alpha decay half life with respect to inverse square root of alpha decay energy Q_α for Bi isotopes.

It is clear from the fig. that alpha activity of ^{211}Bi is much more than its neighboring isotope ^{209}Bi which exhibit particularly the highest half-life. Also fig.4.6 shows that the behavior of the partial alpha decay half life is a perfect inverse reflection of alpha decay energy Q_α and of the pre-formation probability S_α . S_α is the probability of formation of alpha particle through the inner region of the barrier or it correspond to the arrival of the alpha particle to the nuclear surface. In table 4.7 we have shown the pre formation probability calculated in the present work along with the pre formation probability of ref [Tav 05] for comparison. Thus it has been observed that the transmission probability through the inner region of the barrier is less than one and is of the order of 10^{-3} comparable to the results of reference [Tav05]. In fig.4.7 dependence of half life values upon $Q_\alpha^{-1/2}$ has been shown for data listed in table 4.5 and 4.6. The plot shows almost linear variation following Geiger –Nuttal law. There is a strong correlation between the half life and the energy available for decay. From the figure 4.5 it is seen that outer barrier is exceptionally large for ^{209}Bi further it is expected that the renormalization of the barrier for ^{209}Bi , with neutron shell closure at $N=126$, should be different than others due

to shell closure effect and hence an average barrier should not reproduce the ^{209}Bi half life well. For another value of potential parameters the half life can be produced closer to the experimental values, however to make the consistency we have taken same values of the parameters for each nucleus. The neutron shell closure effect in the vicinity of $N=126$ is clearly reflected in the alpha particle preformation probability factor and Q_α values.

4.10 Summary and Conclusion

In the present work a parameterized form of the potential has been used for detailed analysis of proton rich even Pb isotopes and Bi isotopes. We have calculated alpha decay half life for experimentally known Pb and Bi isotopes and have predicted for experimentally unknown in the region $Z=82$; $A=182-210$ and $Z=83$; $A=189-214$ respectively, using present model in the unified fission like approach. Good agreement has been obtained with the variation of just a single parameter v_2 . Predictions for half life of unknown nuclei have been made by using v_2 values obtained corresponding to minimum deviation. The parameters of the potential are chosen so as to simulate a narrow tail in the inner region, parabolic at the top and a long Coulombic tail in the outer region. The wide barrier obtained for ^{209}Bi is reflective of the renormalization of the potential due to shell closure effects. The present calculation has three distinct advantages over the previous works employing similar techniques. Firstly, in the present method it has been possible to parameterize the complete geometrical shape of the barrier. Secondly, we have calculated assault frequency from the zero point vibration energy data instead of using a constant value. Thirdly, exact expression for transmission coefficient through the barrier has been used to calculate the half-lives whereas in the earlier studies transmission probabilities through the barrier have been calculated using WKB approximation method. We have also made the comparative study of WKB and exact method. Our analysis shows that in WKB approximation method, commonly used in most of the earlier calculations, the tail part of the potential outside the turning point is not properly accounted in transmission probability calculations. The neutron shell closure effect in the vicinity of $N=126$ is clearly reflected in the alpha particle preformation probability factor and Q_α values.

Chapter V

Alpha Decay Study of Super heavy Nuclei in the mass region

A=258-320

5.1 Existence of Super heavy Nuclei

There are 81 stable element and about 300 stable nuclei existing on the earth. About 2,200 nuclei have been made artificially. Making heavier nuclei by artificial process is very difficult because the disruptive electrostatic force between positively charged protons increases rapidly with atomic number in comparison with the cohesive nuclear forces that hold the nucleons together. Super heavy nuclei are the heaviest element that populate beyond the boundary of the periodic table and are inhabited in upper right corner of the nuclear landscape but limit of their territory are unknown. Because of large electrostatic forces emission of alpha particle and spontaneous fission are the main decay modes in super heavy region. The interplay between strong and electrostatic forces is responsible for the structure of super heavy element. In case of super heavy nuclei coulomb interaction can not be treated as small perturbation to the dominating nuclear interaction and it influences proton and neutron distribution significantly. Each unstable isotope is characterized by its half life. Half life of the isotopes ranges from less than thousandth of a second to billions of year. Some nuclei have half life comparable to the age of the earth however some are short lived. Short lived isotopes are not found on the earth. Thousands of short lived isotopes are continually created in cosmos. Though their existence is small but they play major roll in formation of the elements in the universe. Some stable nuclei exist beyond the chart of nuclides because of closed proton and neutron shells. It is observed from the theories and later approved by the experiments that after achieving certain configuration of proton and neutron lives of nuclei will be longer. A nucleus with completely filled proton or neutron shell is called as magic nuclei because it is more stable than its neighboring nuclei. Most of the magic nuclei are spherical in shape but some can lower their energy and hence increase their stability by rearranging

proton and neutrons into deformed shells accommodating a different number of nucleons. The closing of these deformed shells lead to deformed magic number. Advanced computer program and accelerator based research are very helpful in understanding the structure and stability of super heavy nuclei. The shape of the super heavy nuclei can help in determining the stability or life of the nucleus. A typical life time of super heavy nucleus is of the order of millisecond. A super heavy nucleus may be much more stable or long lived depending on the shape of the nuclei. The specific feature of super heavy nuclei is that it does not exist in terrestrial material because of radioactive decay but they can be produced artificially in neutron capture and heavy ion induced reactions [Fle 81]. Starting from uranium and thorium the lifetimes of the nuclei of known element decreases with increase in their atomic numbers. For example isotopes of elements 106 & 107 have half lives ranging from one second to one millisecond [Oga 74, Oga 76, Ghi 74, Mun 81a]. The tendency of decreasing lifetime continues in the region of heaviest elements.

5.2 Experimental Status

Beyond actinides ($Z=89-103$) there exist a region where one can find super heavy elements with large life times. This region of super heavy elements in the region $250 \leq A \leq 320$ is called as magic island or island of instability. Because of the progress in accelerator based research, experiments and theoretical nuclear models it has been possible to discover SHE across the island of instability. By using radioactive Ion Beam (RIB) facilities one can reach to the ultimate magic island where the neutron rich SHE resides. Most of the heavy and super heavy elements have been discovered in Lawrence Berkeley Laboratory (USA), Joint Institute of Nuclear Research in Dubna, Gesellschaft für Schwerionenforschung (GSI) in Germany and RIKEN (Japan). Study of super heavy nuclei began in 1940s with the synthesis of heavy elements, neptunium ($Z=93$) and plutonium ($Z=94$) having atomic number greater than the uranium ($Z=92$). Americium ($Z=95$) and curium ($Z=96$) were synthesized in 1944, berkelium ($Z=97$) in 1949. Californium ($Z=98$), einsteinium ($Z=99$) and fermium ($Z=100$) in 1952 and mendelevium ($Z=101$) were synthesized in 1955 [Eur 02]. These entire ranges of heavy elements have been produced by neutron irradiation or by bombardment of proton, deuteron or alpha

particle in a cyclotron with the exception of the fermium nucleus in which in turn was formed through the capture of 17 neutrons by ^{238}U followed by the subsequent beta decays. In nature a similar process called as r-process takes place in supernova which is responsible for the synthesis of heavy elements in nature. First observation on super heavy nuclei has been made in early 1980's for the element with $Z=107-109$ and later alpha decay chain have been experimentally detected from $^{269}110$, $^{271}110$, $^{272}111$, $^{277}112$ and $^{283}112$ [Arm 03, 85; Hof 07, 00, 98]. It was observed that these elements have very short life time. For example $^{277}112$ have half life of the order of $300\ \mu\text{s}$. Recently the doubly magic deformed ^{270}Hs ($Z=108$, $N=162$) super heavy nucleus has been produced [Dvo 06]. The element Darmstadtium ($Z=110$) was confirmed in 2002 by independent work of Lawrence Berkley Laboratory (USA) [Gin 03] and Institute of Chemical and Physical Research (RIKEN) in Japan [Mor 04a]. $Z=111$ and $Z=112$ were also confirmed at RIKEN. Later scientists of the RIKEN have reported synthesis of $^{278}113$ [Oga 04]. It is observed that production cross section decreases with increasing atomic number. Thus it has been very difficult to discover heavier element in cold fusion reactions using lead or bismuth targets. By using hot fusion reaction with ^{48}Ca beam and actinides target several new element with $Z=113-116$ and 118 and several new isotopes of $Z=110$ and 112 have been discovered at Joint Institute of Nuclear Research Dubna (Russia). Recently new nucleus $Z=117$, $A=293,294$ have been synthesized in Dubna [Oga10]. None of these experiment have reached the $N=184$ region as yet. The most important thing observed is that half life of an isotope increases with increasing neutron number. For example in going from $^{282}112(N=170)$ to $^{285}112(N=173)$, the half life increases from 1 ms to 34 sec [Oga 04a].

5.3 Experimental methods for the production of Super Heavy Nuclei

To understand the territory of the island of stability, predicted by theoretical models scientists have been motivated to synthesize the heaviest or super heavy nuclei. Synthesis of nuclei in the island of stability is very difficult, because the nuclei available for target and projectile do not provide the necessary number of neutrons. Also the experimental problem starts with increasing atomic number, because the production cross section decreases exponentially with increase in atomic number. From the literature it is known

that heaviest nuclei have been synthesized in heavy-ion fusion reactions. In this process a compound nucleus is formed with some excitation energy. On the basis of excitation energy of compound nucleus and their survival probability in the process of neutron emission, this reaction has been classified into two classes (i) cold fusion reaction and (ii) hot fusion reaction.

(i) Cold fusion reaction:

In this class of reaction when heavy target ^{208}Pb or ^{209}Bi get fused with massive projectile nucleus ($A=50-70$) a compound nucleus is formed with excitation energy of $E_x=20-11$ MeV and evaporation product is obtained with $Z=104-112$ [Oga 88; Hof 00; Mor 04a, 04b]. Transition of this nucleus to the ground state takes place through the emission of only one neutron and gamma rays. This is the main advantage of this reaction. As the projectile ion mass increases, the cross section for the formation of the evaporation product decreases sharply owing to the appearance of limitations on fusion already in the entrance channel of the reaction. For the first time using the cold fusion reaction the elements with atomic number $Z=107-112$ were synthesized and also their radioactive decay were investigated.

(ii) Hot fusion reaction with ^{48}Ca ions:

In this class of reaction heavy actinide are used as target and ^{48}Ca as projectile. After fusion a compound nucleus is formed with excitation energy 30-40MeV, which is called hot fusion reaction. In this case the formation of the compound nucleus competes with strongly asymmetric fission. Transition of this compound nucleus to ground state takes place through the emission of three or four neutrons and gamma rays. This reaction exhibit low survival probability because of fission that interrupt the cooling process through the sequential emission of neutrons. The main reason of the choice of neutron rich isotope ^{48}Ca as projectile and ^{244}Pu and ^{248}Cm as the target is to obtain compound nuclei with $Z=114-116$ and $N=178-180$ near the closed shell $Z=114$ and $N=184$. This reaction has been used for the synthesis of heavy nuclei with $Z \geq 112$, where cold fusion reaction is at the limit of experimental possibilities.

5.4 Theoretical status

For the first time realistic theoretical calculations for the super heavy nuclei were started in 1966. These calculations were based on the shell correction (or macroscopic-microscopic) method. These calculations have been used to predict the nucleus with $Z=114$, $N=184$ ($^{298}\text{Uuq}_{114}$), which has been recognized to be doubly magic centre of an island of long lived super heavy nuclei. Later in 1990s more refined model, based on self consistent mean field theory and realistic effective nucleon-nucleon interactions, were used in the study of super heavy nuclei. By using theoretical model it has been observed that existence of nuclei with $Z > 102$ are entirely due to quantal shell effects. According to classical liquid drop model, the shape of the nucleus depends on the interplay between surface tension and Coulomb force of electrostatic repulsion. The characteristic of surface tension is to make the nucleus spherical and is proportional to $A^{2/3}$, and characteristic of Coulomb repulsion is to make nucleus deformed and is proportional to $Z^2/A^{1/3}$ [Eur 02]. At large values of Z^2/A the Coulomb force of repulsion becomes strong enough to make the liquid drop unstable to surface distortions and nuclei fissions spontaneously [Boh 39, Fre 39]. Using theoretical models for the heaviest elements excellent agreement with the experimental data have been observed, however large theoretical uncertainties can be seen in the unknown regions of nuclear chart. There is no particular opinion among the nuclear physicists regarding centre of the shell stability in the super heavy region. Since in the super heavy nuclei the single particle level density is relatively large, small shift in the position of single particle due to the Coulomb or spin-orbit interaction can be crucial for determining the shell stability of a nucleus. Most of the macroscopic-microscopic or self consistent approaches have predicted $Z=114$ to be magic after $Z=82$. Self consistent methods suggest that the centre of the proton shell stability should be shifted to higher proton numbers, $Z=120, 124$ or 126 . However for neutrons most non relativistic calculations predict $N=184$ as magic number while the relativistic mean field theory predicts magic number at $N=172$ due to slightly different spin-orbit interaction and predicts deformed proton magic number at 110 and deformed neutron magic number at 162 . According to microscopic nuclear theories there is a significant enhancement in nuclear stability when approaching the closed spherical shell with $Z=114$ or $Z=120$ and $N=184$. Myres and Swiatecki [Mye 65] observed that the shell corrections added to liquid

drop model indicates the possibility of closed shell at $Z=114$ and $N=184$ which was latter confirmed by A.Sobiczewski et al [Sob 66]. In 1969 Nilsson et al [Nil 69] predicted that the longest fission half life around the nucleon number $Z=114$, $N=184$ and the stability against spontaneous fission in this region is due to extra binding resulting from the shell effect which essentially increases the alpha decay half life for nuclei with $Z<114$, $N<184$ and decreases for those with $Z>114$, $N>184$.

Discovery of super heavy nuclei has opened a vast area of understanding of the structure of nuclei. One of the major goals of the nuclear theory is to develop a nuclear model and semiempirical formula to be able for the prediction of the life time of super heavy element. Employing more appropriate alpha –daughter potential and by using more appropriate nuclear model, half life of the super heavy nuclei can be calculated and a clue can be given to the experiments pursuing on super heavy elements. On the theoretical front several attempts have been made to calculate the alpha decay half lives of SHE using different approaches. In the microscopic approach using double folding model Samanta et al [Sam 07] have calculated alpha decay half life in the region $Z=102-116$, 118 . These authors have used Viola Seaborg formula to calculate alpha decay half life for the comparison. Chowdhary et al [Cho 07] have calculated alpha decay half life of $Z=113$ and its decay products using experimental Q values for $\ell = 0$ and $\ell = 5$, mutual angular momentum states respectively and later Chowdhary et al [Cho 08a] have also calculated alpha decay half life in the region $Z=102-120$. Later Samanta [Sam 07a, Sam 09] and Chowdhary et al [Cho 08a, Cho 08b] have predicted alpha decay half lives of isotopes in the region $100 \leq Z \leq 130$ and obtained good agreement with the experimental data of experimentally known isotopes. Z.Z. Ren et al [Ren 07] have calculated alpha decay half life, alpha decay energies and spontaneous fission half life of super heavy nuclei for the several isotopes in the region $Z=106-118$ and have obtained good agreement with the experimental data.

Generalized liquid drop model (GLDM) and Coulomb plus proximity potential model (CPPM) are two macroscopic approaches, which are commonly used to develop a potential barrier for alpha-daughter system. G.Royer et al [Roy 02] have calculated alpha decay half life in the region $Z=104-118$ and $A=250-302$ using GLDM and phenomenological formula and later they have predicted half lives in the region $Z=112-$

126 and A=270-323 [Roy 04] using same model. Q values have been calculated by using Thomas Fermi model. Zhang et al [Hon 06] have used Generalized liquid drop model (GLDM) to calculate alpha decay half lives for experimentally observed nuclei Z=112,114,116,118 and have also used their model to predict the half lives of several isotopes in the region Z=105-120 [Zha 07]. Q values have been calculated by using finite range droplet model (FRDM). Good agreement has been found with experimental data. Santhosh et al [San 09] have made comparative study of alpha decay and spontaneous fission half life in the region Z=100-122 by using CPPM model. They also have found good agreement with the experimental data. Using the effective liquid drop model approach Duarte et al [Dua 04] have predicted alpha decay half life in the region $110 \leq Z \leq 135$ and $155 \leq N \leq 220$. Dong Jian Min et al [Don 08] have calculated alpha decay half life of some isotopes of Z=113 and some of their alpha decay products using GLDM and Cluster model approach. Both the models are successful to reproduce the experimental data for the calculations corresponding to mutual angular momentum $\ell = 0$ state. They have included the nonzero mutual angular momentum state also through the centrifugal effect and show the significant effect of nonzero angular momentum on the half lives of SHN. In almost all the cases discussed above Q_α values has been taken either experimentally or by phenomenological mass formula of Myres- Swiatecki, Muntian and KUTY.

In an alternative approach Sahu [Sah 08] have used the wave function method for evaluating the alpha decay half lives of super heavy nuclei in the region Z=106 -118. In yet another approach Prema et. al. [Pre 08] have used S-matrix formulation for the calculation of alpha decay half life of super heavy nuclei Z=110, A=269 and Z=112, A=277. Gambhir et al [Gam 03] have calculated ground state properties and alpha decay half life of the decay chain of Z=112 in the framework of relativistic mean field theory.

In the present work we have studied alpha decay half life of super heavy nuclei in the region Z=106-128 and A=258-320 for their ground state to ground state transition with mutual angular momentum $\ell = 0$ in a unified fission like approach. We have used a highly versatile, asymmetric and analytically solvable form of alpha-daughter potential based on Ginocchio's potential developed by Sahu [Sah 02] which has been described in

chapter III. For the calculations exact expression of transmission probability given by eq. (3.11) has been used in place of commonly used WKB approximation method.

5.5. Model parameter

In the present work to generate a potential barrier for alpha decaying system we have fixed $\lambda_1 = 3$ and $\nu_1 = 2.2$ in the inner region and $\lambda_2 = 1.2$ in the outer region and ν_2 has been varied to obtain the experimental half lives. For the radial position and height of the potential barrier we have used a global formula given by [Sah 99]

$$R_B = r_0(A_1^{1/3} + A_2^{1/3}) + 2.72$$

$$V_B = \frac{Z_1 Z_2 e^2}{R_B} \left(1 - \frac{a}{R_B} \right)$$

Where A_1, A_2 and Z_1, Z_2 are the mass numbers and atomic numbers of the alpha and daughter nuclei respectively. r_0 and a are two distance parameter and $e^2 = 1.4398$ MeV fm. Parameters are fixed at $r_0 = 0.9$ fm and $a = 1.6$ fm for our system of interest [Sah 08]. Barrier height for each isotope has been calculated separately and ranges from 25.3450 MeV for $\alpha + {}^{262}\text{Rf}_{104}$ system to 30.0218 MeV for $\alpha + {}^{302}\text{126}$ - system. The decay rate has been calculated by $P = P_0 T$. Where P_0 is the assault frequency and T is the transmission coefficient across the barrier. The assault frequency P_0 is calculated from the zero point vibration energy $E_v = \frac{1}{2} h P_0$ [Poe86], which in turn depends directly on Q value of decay. Results are shown in table 5.1. The half life t is calculated as $t = \log_e 2/P$.

5.6 Result and discussion

In the present work we have calculated the alpha decay half lives of ${}^{256}\text{Rf}_{104}$, ${}^{260}\text{Sg}_{106}$, ${}^{266}\text{Sg}_{106}$, ${}^{264}\text{Hs}_{108}$, ${}^{286}\text{114}$, ${}^{288}\text{114}$, ${}^{290}\text{116}$, ${}^{292}\text{116}$ and ${}^{294}\text{118}$ for ground state to ground state transition with mutual angular momentum $\ell = 0$, using an analytically solvable asymmetric potential that admits exact solution for the transmission coefficients.

Calculations have been performed by varying the range parameter ν_2 so as to obtain the best fit to the experimental half life. Results are shown in table 5.1. Good agreement has been obtained with the experimental data by variation of just one parameter ν_2 . Plot of the resulting potential barrier for two nuclei ^{260}Sg and $^{292}116$ are shown in figure 5.1. In the phenomenological formula of Geiger-Nuttall and VSS [Sob 89] or in any other semiempirical relation of half life and decay energy the logarithm of half life is proportional to Z/\sqrt{Q} in the leading term. Also it is expected that logarithm of half life should be directly proportional to the width of the barrier defined by range parameter ν_2 . From table 5.1 it has been observed that $(\nu_2\sqrt{Q})/Z$ is nearly constant for most of the isotopes. Thus a semiempirical formula $\nu_2' = \frac{Z'}{Z} \sqrt{\frac{Q'}{Q}} \times \nu_2$ has been used to calculate range parameter ν_2' for the unknown super heavy nuclei. ν_2 corresponding to minimum Q value is taken as a base value for the calculation of ν_2' , and theoretical Q_α values calculated from KUTY mass estimate [Kou 05] have been used in the calculation of half lives of unknown super heavy nuclei. To test the accuracy of this formula alpha decay half lives of experimentally known nuclei have been calculated corresponding to the range parameters ν_2' , calculated by semiempirical formula. Calculated half lives are compared with the earlier studies and with the experimental data. Results shown in table 5.2 are in good agreement with the experimental data and other studies for all cases. In some of the cases, our results are in closer agreement with experimental data than those obtained with DDM3Y. This shows the reliability of the semiempirical formula.

Santhosh et al [San09] have made a comparative study of spontaneous fission (SF) and alpha decay half lives of super heavy elements for $Z=100-122$. We have extended these calculation for the chain of $Z =124; A=288-312$, $Z=126; A=292-318$ and $Z=128; A=294-324$. SF half has been calculated by using phenomenological formula of Ren [Ren05] given as

$$\log_{10}(T_{1/2})_{yr} = 21.08 + C_1 \frac{(Z-90-\nu)}{A} + C_2 \frac{(Z-90-\nu)^2}{A} + C_3 \frac{(Z-90-\nu)^3}{A} + C_4 \frac{(Z-90-\nu)(N-Z-52)^2}{A}$$

Where $C_1 = -548.825021, C_2 = -5.359139, C_3 = 0.767379$ and $C_4 = -4.282220$

The seniority term ν was introduced taking the blocking effect of unpaired nucleon on the transfer of many nucleon-pairs during the fission process and $\nu = 0$ for spontaneous fission of even–even nuclei. The results are shown in fig. 5.2-5.4. In the chain of $Z=124$ -128 predicted alpha half life is of the order of 10^{-5} sec. to 10^{-12} sec, however predicted maximum SF half life is of the order of 10^{46} sec to 10^{72} sec. SF half life versus mass number curve is in the shape of inverted parabola whereas alpha decay half lives vary as straight lines. SHE which lies within the point of intersection of the two curves would decay prominently by alpha emission. We have predicted alpha decay half life of unknown even-even super heavy nuclei in the region $Z=106$ -122; $A= 258$ -304 and $Z=124$ -128; $A= 292$ -320. As half life of a nuclei for a particular decay mode strongly depends on the Q value of the decay. In the present work for unknown Q_α values we have used Q values calculated by using KUTY mass estimates. The result of ref. [Cho08b] obtained with DDM3Y interaction are also given for comparison. Our predicted result shows very small deviation with ref [Cho08b], however in some cases they are very close to the result of ref [Cho08b]. The plot of decay energy Q_α and alpha decay half life against mass number of parent nuclei for $Z=106$ -128 are shown in fig. 5.5-5.16. From the plots we have observed that in the chain of $Z=106$; $A=258$ -272, half life ranges from 1.05×10^{-4} sec to 104.41 sec, in the chain of $Z=108$; $A=262$ -278, half life ranges from 1.74×10^{-5} sec to 733.27 sec, for $Z=110$; $A=268$ -286, half life ranges from 7.7×10^{-6} sec to 3.51×10^8 sec, for $Z=112$; $A=272$ -290, half life ranges from 2.18×10^{-6} sec to 5.99×10^7 sec for $Z=114$; $A=274$ -298 half life ranges from 2.39×10^{-7} sec to 1.10×10^9 sec and for $Z=116$; $A=278$ -302 half life ranges from 5.90×10^{-8} sec to 19.20 sec. Thus it has been observed that alpha decay half life increases with increasing neutron number but decreases with increasing proton number. The isotopes which are short lived are stable against spontaneous fission or may decay via spontaneous fission with very large of the order of several year of spontaneous fission half life. These isotopes have alpha decay as dominant decay mode and can be synthesized in the laboratory [San09]. In the region for $Z > 116$ in the isotopic chain of $Z=118$ -128; $A= 280$ -320 half life ranges from 3.46×10^{-12} sec for $^{314}_{128}$ to 0.33 sec for $^{302}_{118}$. This decreasing trend of half life values with increasing Z shows that alpha decay becomes more dominant decay mode for the higher

Z values in the super heavy region. Thus in the region Z=114-128 highest half life has been observed at Z=114 and N=184, which is recognized as doubly magic nuclei.

Relativistic mean field calculation on SHE [Rut 97, Ben 99] suggest that after Z=82 next proton and neutron magic number are at Z=114,126; N=184 and Z=120, N=172. But some recent microscopic nuclear theories [Sto 06] point out the island of stability centered around Z=114,120,124,126 and N=184. It is clear from figs. 5.12-5.15 that in the chain of Z=120; A=284-306, highest half life is observed at N=184, reflecting the shell closure effect. In the chain of Z=122; A=284-304, and Z=124; A=292-310 highest half life has been observed at N=178. Also in the chain of Z=126; A=298-314, highest half life is observed at N=178. This shows that in super heavy region magic number may change from nucleus to nucleus [Hon 05] as indicated in reference [Hon 06].

In figure 5.17 we have shown the plot for the ratio of logarithm of spontaneous fission half life and logarithm of alpha decay half life versus fissility parameter for Z=124-128 similar to one proposed by Studier et al [Stu 54] and later by Santhosh et al [San 09]. It is observed from the plot that the ratio of half lives increases with increasing fissility parameter reaches to maximum value and then start decreasing with increasing fissility parameter for a particular isotopic chain. It also has been observed that the ratio increases with increasing fissility parameter with increasing atomic number. Similar to ref. [Stu 54, San 09] we have connected the isotopes which are differ in atomic number by two and mass number by six units by a straight line. At a particular point on this line the ratio start decreasing with increasing fissility parameter. The fissility parameter has

been calculated by using the relation
$$X = \frac{Z^2/A}{50.883 \left[1 - 1.7826 \left((N - Z)/A \right)^2 \right]}$$
, where

Z^2/A is fissionability parameter [San 09].

Table 5.1: Calculated and experimental alpha decay half lives of known even-even SHE for ground state to ground state transition with mutual angular momentum $\ell = 0$. Corresponding best fit values of the range parameter ν_2 , barrier height, radial position and assault frequency are also given. Experimental data for $^{256}\text{Rf}_{104}$, $^{260}\text{Sg}_{106}$, $^{266}\text{Sg}_{106}$ and $^{264}\text{Hs}_{108}$ has been taken from ref. [Roy 00] and for other nuclei from ref. [Oga 04, 05, 06].

Parent Nucleus (A_Z)	Q^{exp} (MeV)	Barrier Height V_B (MeV)	Radial position R_B (fm)	Assault freq. (P_0) 10^{20}s^{-1}	Range parameter (ν_2)	$\text{Log}_{10}(t_{1/2})$ Sec Cal. Present work	$\text{Log}_{10}(t_{1/2})$ Sec Exp.
$^{256}\text{Rf}_{104}$	8.95	25.009	9.83	4.54	27.6964	-0.44	-0.44
$^{260}\text{Sg}_{106}$	9.93	25.438	9.86	5.03	27.4109	-2.07	-2.07
$^{266}\text{Sg}_{106}$	8.76	25.345	9.90	4.44	28.6286	1.53	1.53
$^{264}\text{Hs}_{108}$	10.58	25.865	9.89	5.36	26.7743	-3.60	-3.60
$^{286}_{114}$	10.35	26.980	10.05	5.25	28.1022	-0.79	-0.79
$^{288}_{114}$	10.09	26.949	10.06	5.11	28.3237	-0.096	-0.096
$^{290}_{116}$	11.00	27.399	10.07	5.58	27.8605	-1.82	-1.82
$^{292}_{116}$	10.80	27.371	10.09	5.48	27.7510	-1.74	-1.74
$^{294}_{118}$	11.65	27.821	10.10	5.91	27.4493	-3.05	-2.74

Table5.2: Comparison of the alpha decay half lives $T_{1/2}(\text{ms})$ calculated in the present work with the experimental data and other work. The value of range parameter ν_2' calculated by using semiempirical relation is also given.

Parent Nucleus (A_Z)	Q^{exp} (MeV)	Range parameter (ν_2')	$T_{1/2}(\text{ms})$				
			Expt.	Present work	DDM3Y [Cho08b]	GLDM [Zha 07]	VSS [Cho08b]
$^{256}\text{Rf}_{104}$	8.95	27.7870	0.36×10^3	0.50×10^3	-	0.30×10^3	-
$^{260}\text{Sg}_{106}$	9.93	26.8880	8.5	1.6	5.34	2	5.50
$^{266}\text{Sg}_{106}$	8.76	28.6286	33.88×10^3	33.88×10^3	157×10^3	4.57×10^3	263×10^3
$^{264}\text{Hs}_{108}$	10.58	26.5415	0.25	0.13	0.57	0.15	0.60
$^{286}_{114}$	10.35	28.3269	0.16×10^3	0.36×10^3	6.9	0.05×10^3	8.5
$^{288}_{114}$	10.09	28.6902	0.80×10^3	3.09×10^3	0.16×10^3	0.22×10^3	0.22×10^3
$^{290}_{116}$	11.00	27.9574	15	21.3	8.21	3.47	9.55
$^{292}_{116}$	10.80	28.2142	18	94.8	8.65	10.45	0.10
$^{294}_{118}$	11.65	27.6339	0.89	1.7	0.14	0.34	0.13

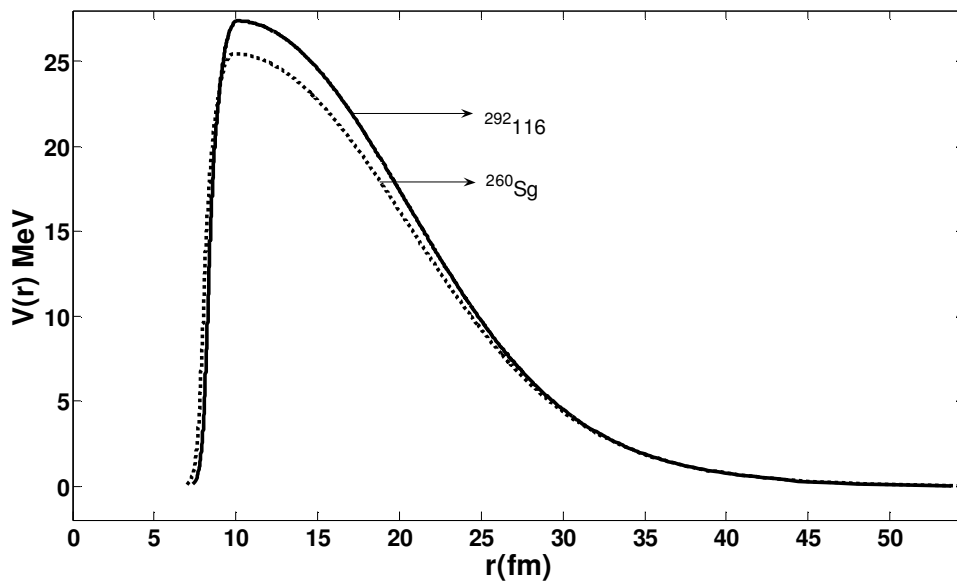


Figure 5.1: Shape of the potential barrier for two nuclei ^{260}Sg and $^{292}116$.

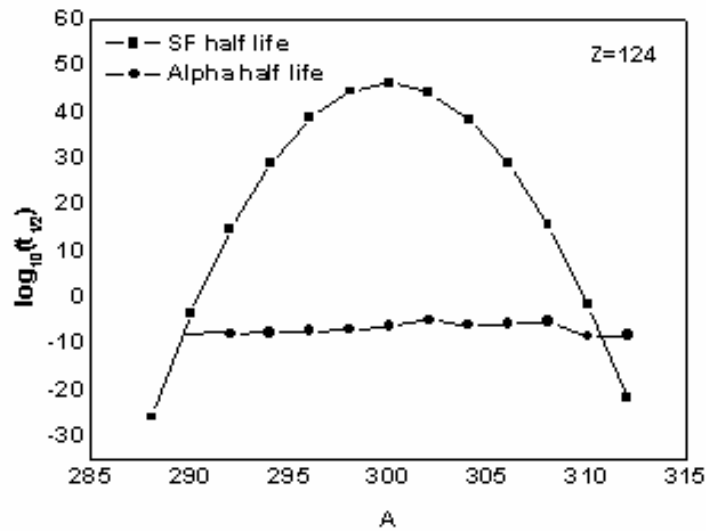


Figure 5.2: Plot of the calculated spontaneous fission (SF) half life and alpha decay half life with respect to mass numbers of the isotopic chain of parent nucleus $Z=124$. Full square on the inverted parabola shows the SF half life of the respective nucleus and black circles on line crossing the inverted parabola shows the alpha decay half life of the respective nucleus.

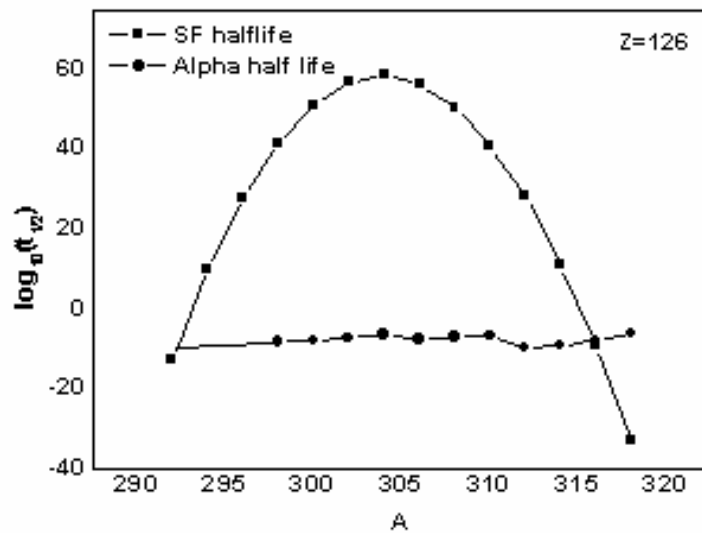


Figure 5.3: Same as figure 5.2 for $Z=126$.

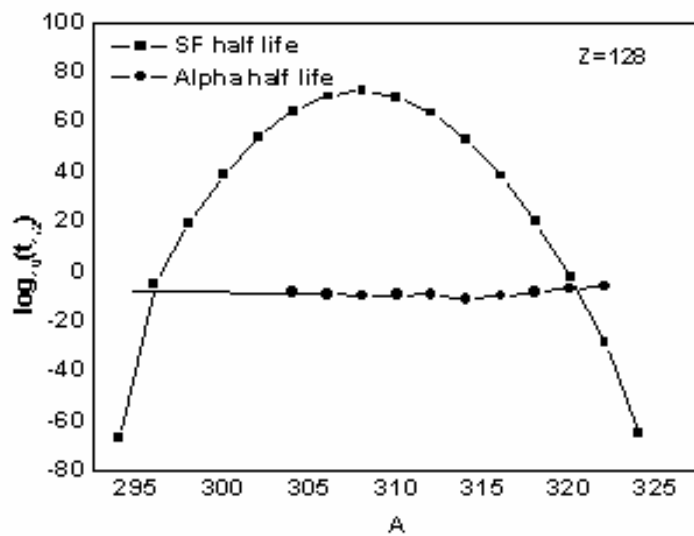


Figure 5.4: Same as figure 5.2 for $Z=128$.

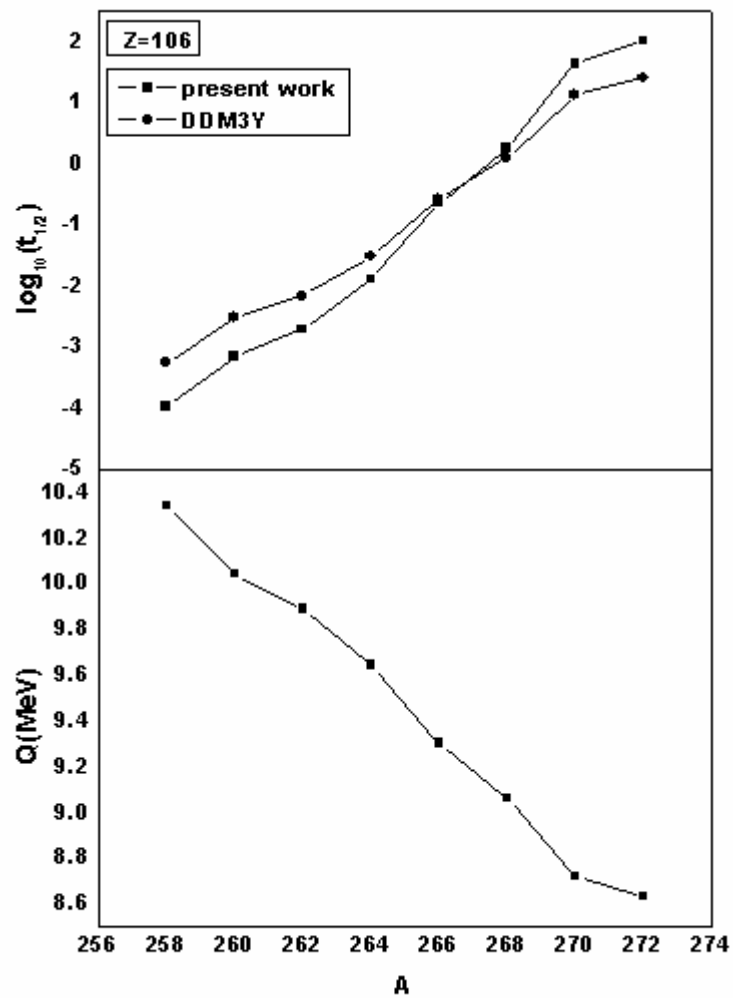


Figure 5.5: Plot of Q value of decay and logarithm of alpha decay half life versus mass number of parent nuclei for Z=106.

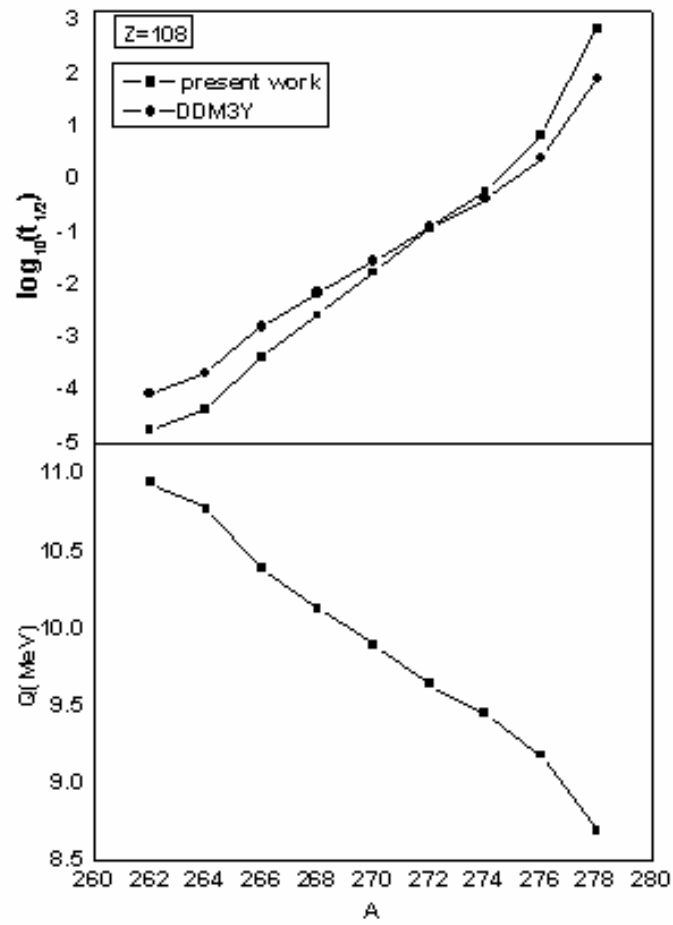


Figure 5.6: Same as fig. 5.5 for $Z=108$

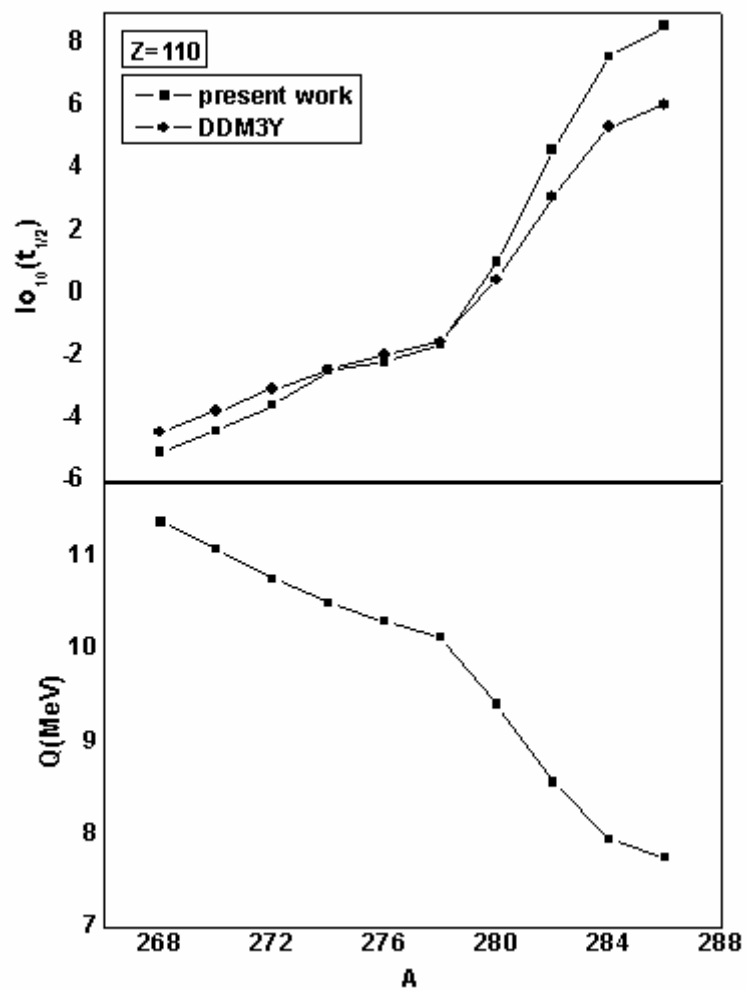


Figure 5.7: Same as figure 5.5 for Z=110.

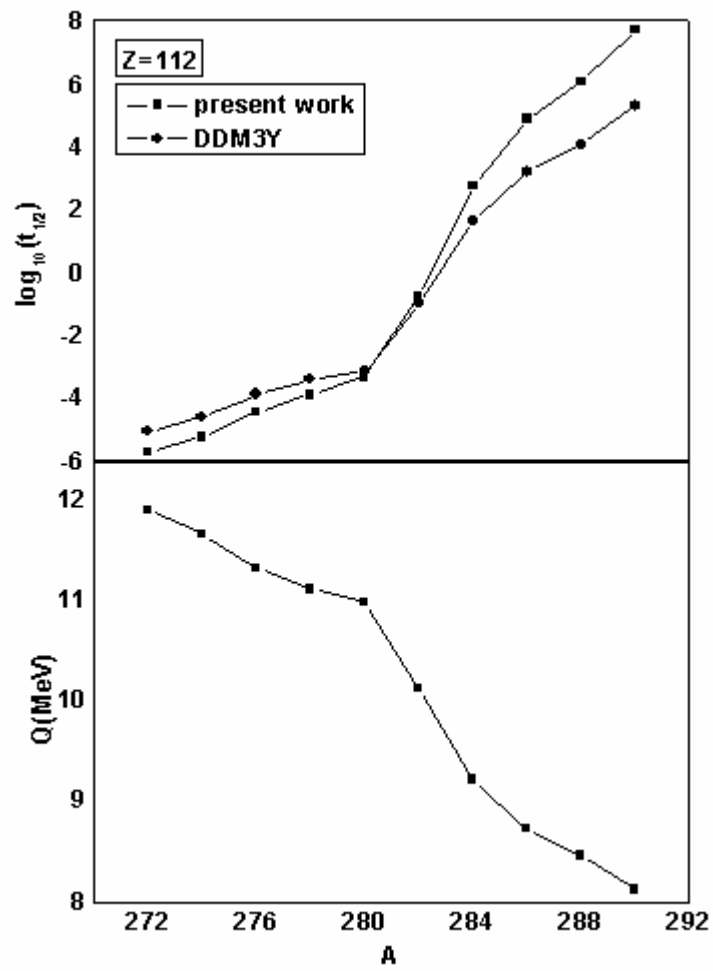


Figure 5.8: Same as figure 5.5 for Z=112.

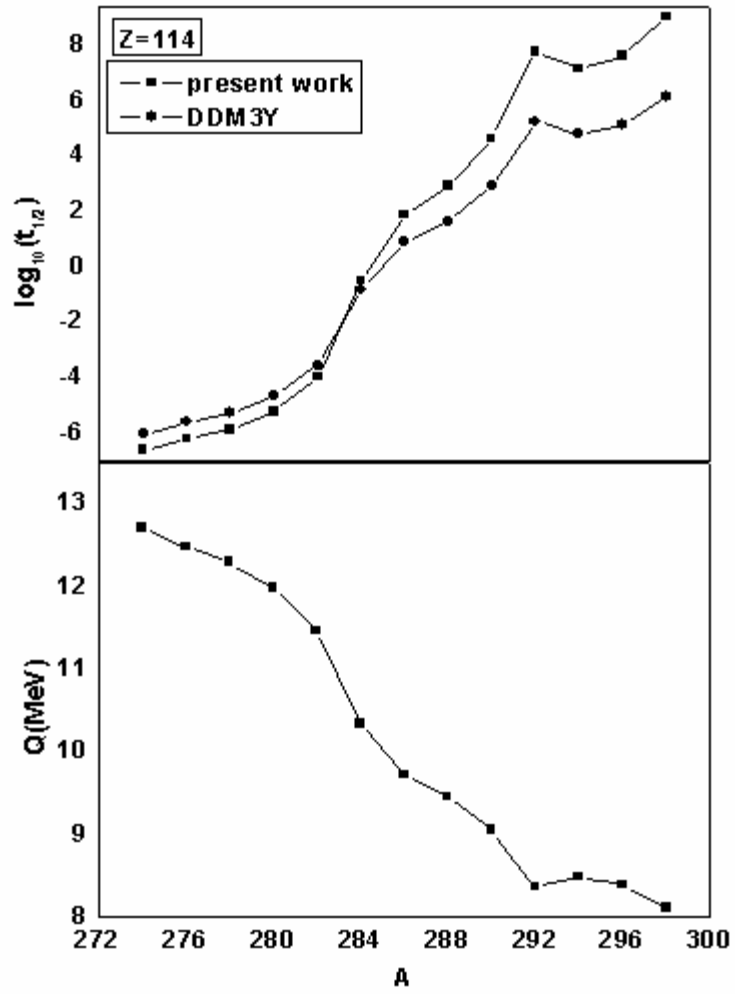


Figure 5.9: Same as figure 5.5 for Z=114.

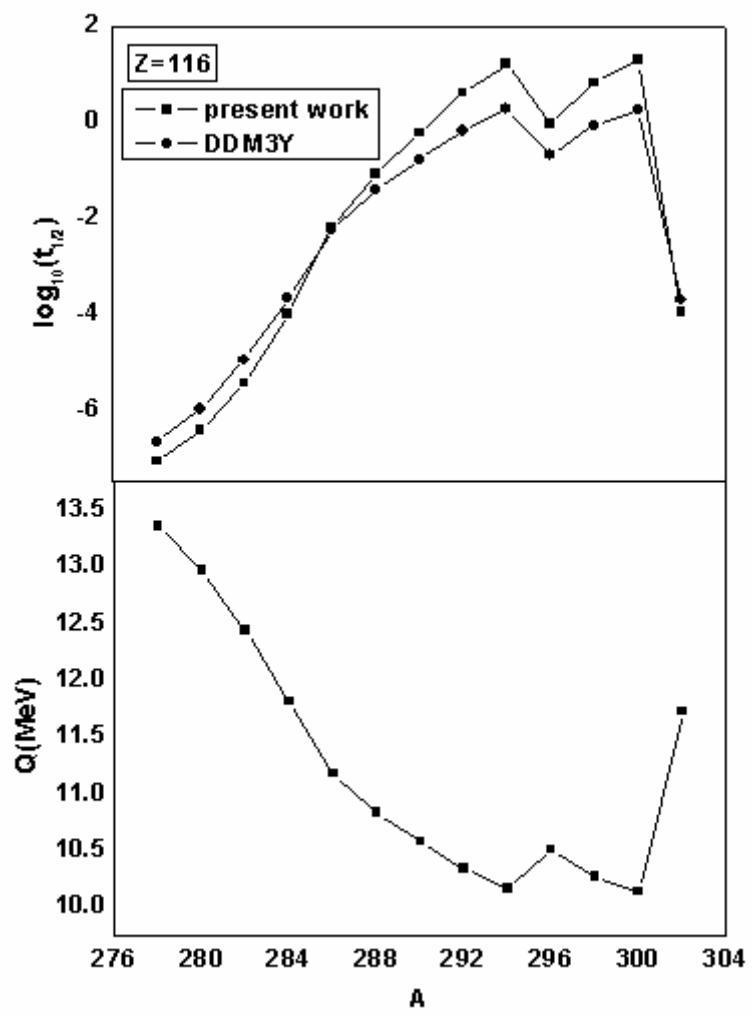


Figure 5.10: Same as figure 5.5 for Z=116.

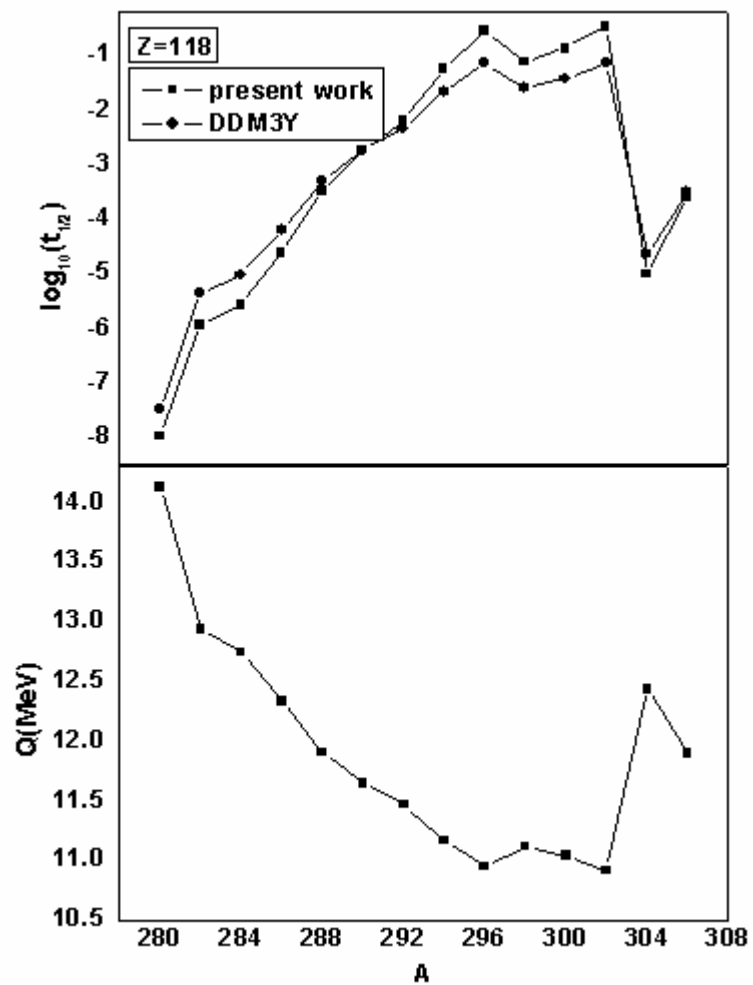


Figure 5.11: Same as figure 5.5 for Z=118.

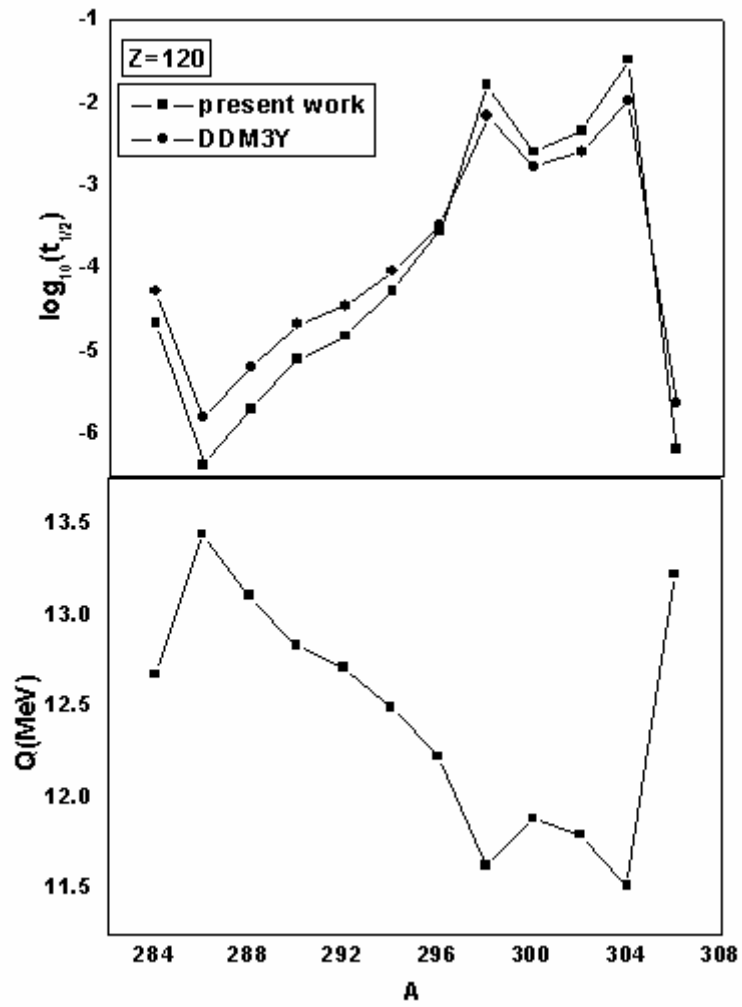


Figure 5.12: Same as fig.5.5 for $Z=120$.

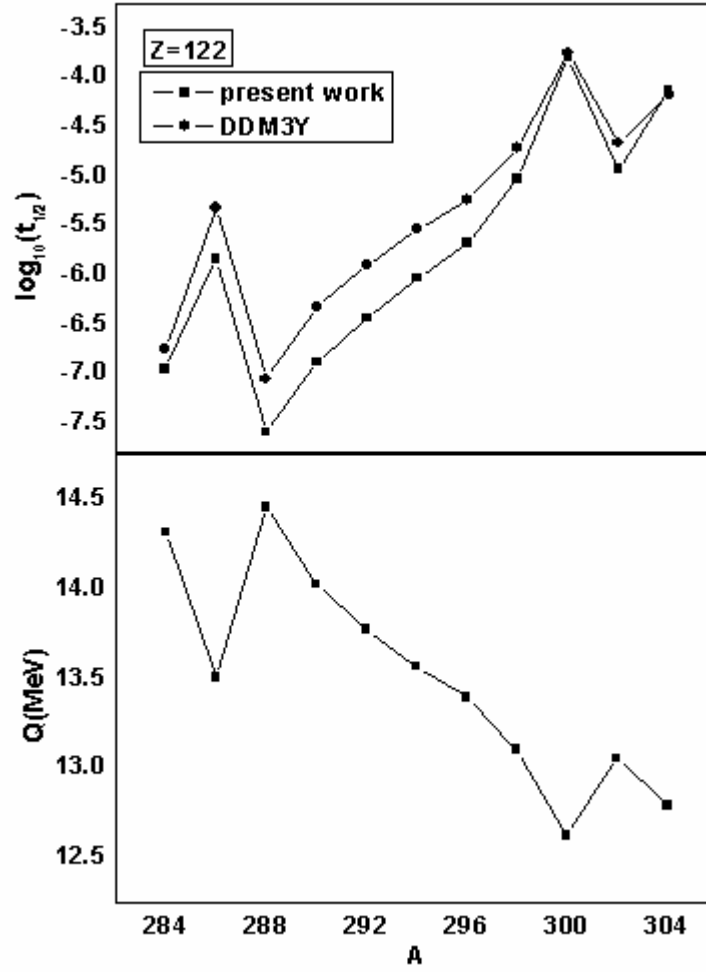


Figure 5.13: Same as fig.5.5 for Z=122.

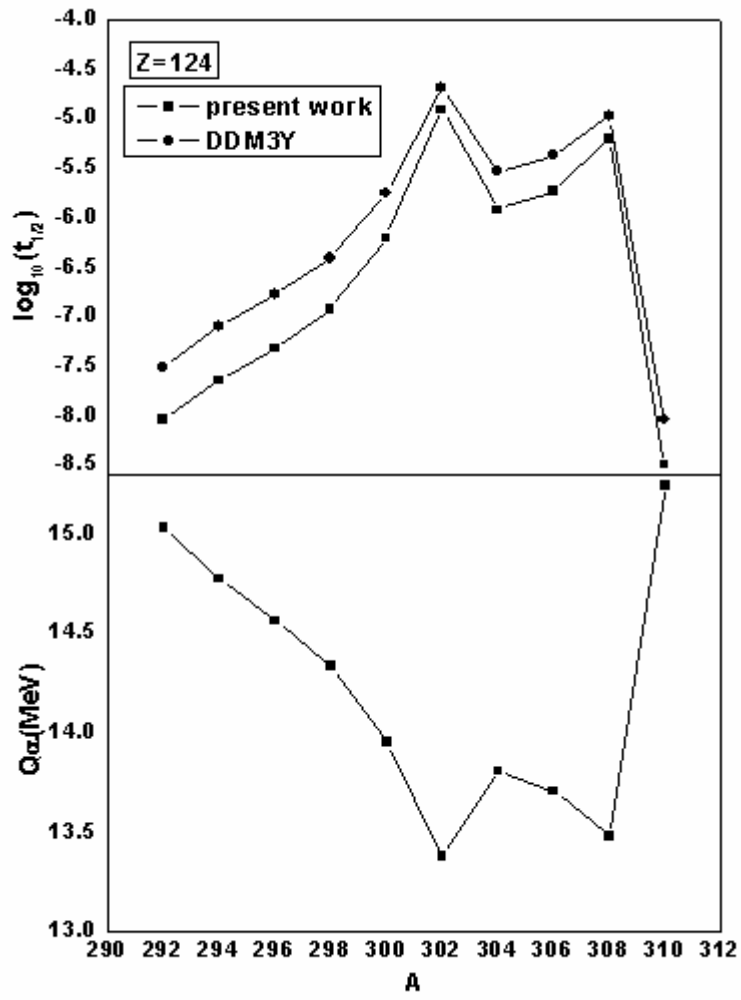


Figure 5.14: Same as fig. 5.5 for Z=124.

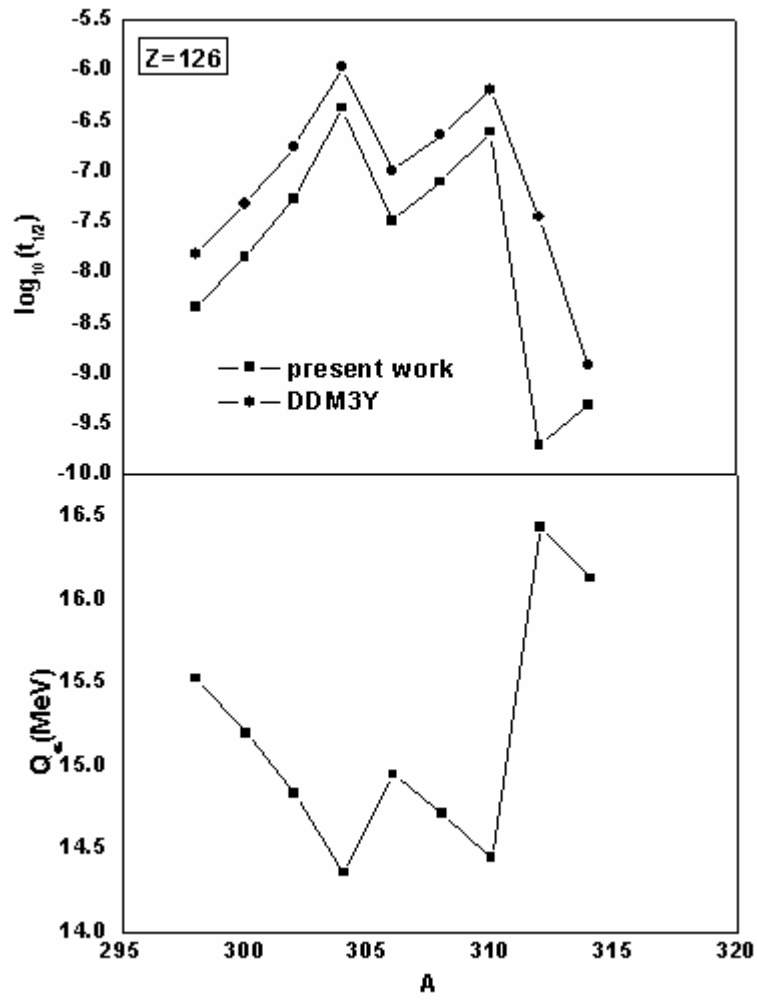


Figure 5.15: Same as fig. 5.5 for Z=126.

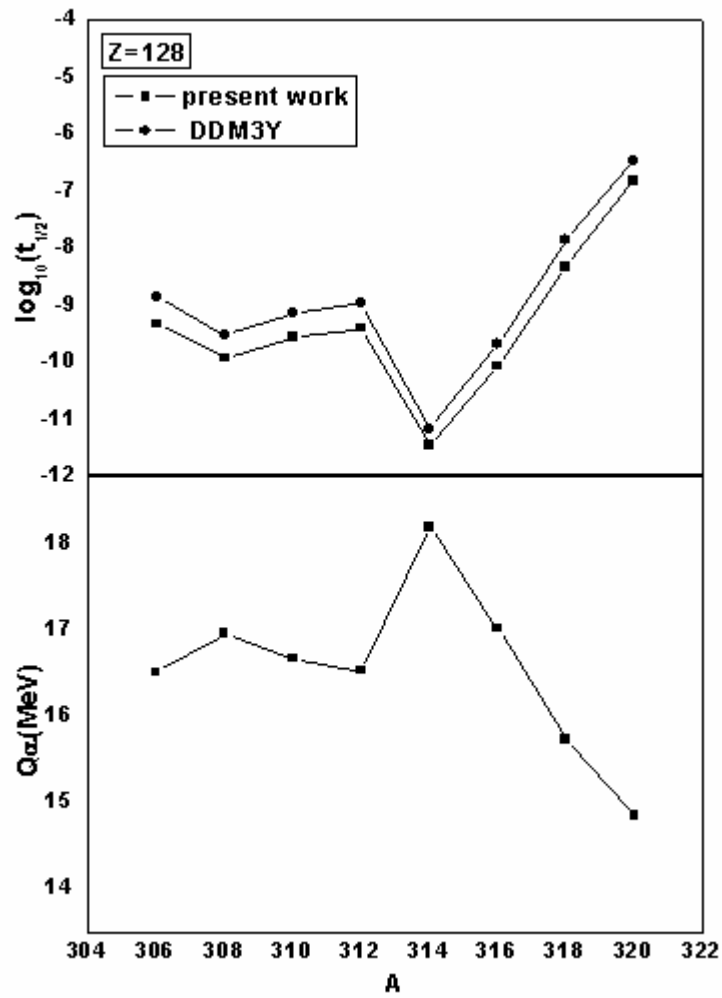


Figure 5.16: Same as fig. 5.5 for $Z=128$.

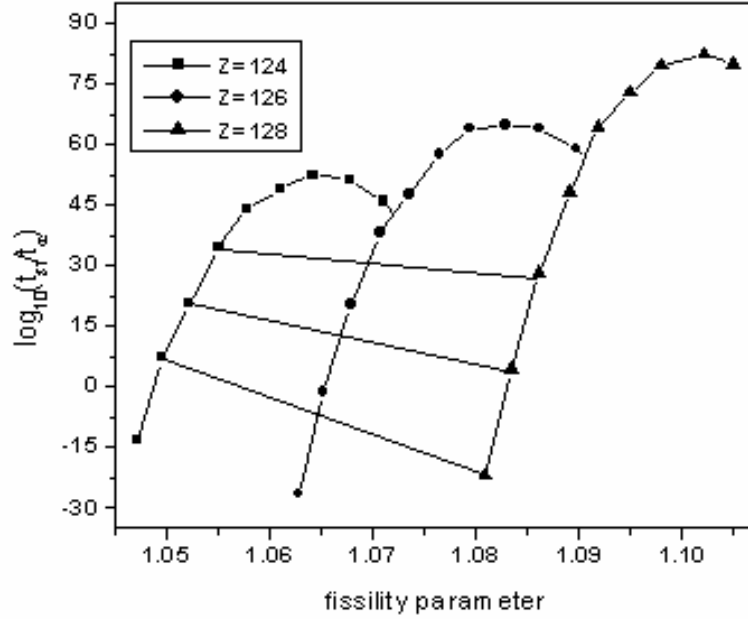


Figure 5.17: The plot connecting the ratio of spontaneous fission to alpha decay half-lives against the fissility parameter for $Z = 124$ – 128 .

5.7 Summary and conclusion

In the present work we have calculated alpha decay half life of experimentally known even-even super heavy element $^{256}\text{Rf}_{104}$, $^{260}\text{Sg}_{106}$, $^{266}\text{Sg}_{106}$, $^{264}\text{Hs}_{108}$, $^{286}\text{114}$, $^{288}\text{114}$, $^{290}\text{116}$, $^{292}\text{116}$ and $^{294}\text{118}$ with experimental Q values by using an asymmetric potential model in the unified fission like approach. Good agreement has been found with experimental data by varying just one single parameter ν_2 . To calculate the range parameter ν_2 of unknown systems a semiempirical relation has been developed between range parameter and decay energy. Alpha decay half lives for unknown even-even isotopes in the region $106 \leq Z \leq 128$ and $258 \leq A \leq 320$ have been predicted. In our calculations we have used theoretical Q values calculated by using KUTY mass estimates [Kou 05]. The predicted results of the present model differ from the work of Chowdhary et al [Cho08b], based on microscopic calculations only slightly. Our predicted results are more reliable than the work of Chowdhary et al [Cho08b], calculated by using DDM3Y interaction in the following aspects. (i) We have used exact expression to calculate transmission probability

through the potential barrier instead of commonly used WKB approximation method. The WKB method does not take into account the behavior of the potential in the tail region. (ii) Renormalization effects are incorporated in our model by appropriate choice of λ and ν . However it is not incorporated in the work of Chowdhary et al [Cho 08b] and Samanta [Sam 07, Sam 09] and so the form of their potential has sharp peak of Coulomb barrier. The predicted alpha decay half lives of unknown SHE can serve as a guideline for future experiments.

Alpha decay study using wave-function approach

6.1 Introduction

Different theoretical approaches of alpha decay have been discussed in detail in chapter II. In the present work alpha emission has been considered as quantum collision phenomenon involving daughter as target and alpha as projectile. A proper theoretical approach and appropriate alpha-daughter nucleus potential is needed to describe the process of alpha emission. After obtaining appropriate potential, the alpha decay process can be subjected to a quasi-molecular decay path, which is governed by a composite potential with a pocket in the nuclear inner region and a barrier in the outer region. The resulting composite potential is the combined effect of attractive nuclear force and repulsive Coulomb force.

In the present work we have solved the Schrödinger equation for the process of alpha decay using the analytically solvable three dimensional potential of Sahu [Sah 08]. The alpha-daughter potential comprises of an attractive nuclear potential in the inner region which usually has a Wood-Saxon form and a repulsive Coulomb potential in the outer region beyond the touching radius. This form is simulated by using the analytical expression of the potential. Standard technique described in the literature [Abe 98, Dav 00, Mag 98, Bug 85] of obtaining the decay width (half life) from the behavior of the quasibound state wave function has been used to calculate the half life. In this method the exact wave function in the nuclear region obtained from solving the Schrödinger equation is matched with the pure Coulomb wave function found appropriate in the outer region at a radial position within the barrier region. To estimate the resonance energies or the Q -value of decaying state, confinement property and the bound-state-like behavior of the wave function at the resonance state is taken into account. Relative probability density (RPD) method has been used to calculate Q value of decay [Sah 08].

We have calculated the decay energy and alpha decay half life for recently discovered [Oga 10] alpha decay chain of $^{294}117$ and $^{293}117$. We have also predicted

alpha decay energy and alpha decay half life for the isotopic chain of Z=74, 102 and 113, for which experimental data are not known.

6.2. Schrodinger equation for the alpha-nucleus system

For the potential given by eq.(3.13), the reduced Schrödinger equation for the s wave can be written in the dimensionless form as

$$\frac{-d^2 u_1(\rho_1)}{d\rho_1^2} + \{[\lambda_1^2(B_1 - B_0)(1 - y_1^2) + \xi_1] - \frac{E_{c.m.}}{V_{01}} + \lambda_1^2(B_0)\} u_1(\rho_1) = 0, \quad r \leq R_1 \quad (6.1)$$

$$\frac{-d^2 u_2(\rho_2)}{d\rho_2^2} + \{[\lambda_2^2 B_2(1 - y_2^2) + \xi_2] - \frac{E_{c.m.}}{V_{02}}\} u_2(\rho_2) = 0, \quad r > R_1 \quad (6.2)$$

$E_{c.m.}$ is the centre of mass energy. These equations can be solved analytically. The solution of the Schrödinger equation $u_1(\rho_1)$ in the region $r \leq R_1$ is given by

$$u_1(\rho_1) = A_1 [\lambda_1^2 + (1 - \lambda_1^2) z_1^2]^{1/4} (1 - z_1^2)^{-\frac{ik_1}{2\lambda_1^2}} \times F\left(a_1, b_1, c_1, \frac{1 - z_1}{2}\right) \\ + A_2 [\lambda_1^2 + (1 - \lambda_1^2) z_1^2]^{1/4} (1 - z_1^2)^{\frac{ik_1}{2\lambda_1^2}} \times F\left(a_1', b_1', c_1', \frac{1 - z_1}{2}\right) \quad (6.3)$$

where in order to determine the eigenfunction the variable r has been transformed to a new variable z via the transformation

$$z_1 = \frac{\lambda_1 y_1}{[1 + (\lambda_1^2 - 1) y_1^2]^{1/2}}$$

$F(a, b, c, z)$ is the hypergeometric function, and

$$a_1 = \bar{\nu}_1 + 1 - \frac{ik_1}{\lambda_1^2}, \quad b_1 = -\bar{\nu}_1 - \frac{ik_1}{\lambda_1^2}, \quad c_1 = 1 - \frac{ik_1}{\lambda_1^2},$$

$$a_1' = \bar{\nu}_1 + 1 + \frac{ik_1}{\lambda_1^2}, \quad b_1' = -\bar{\nu}_1 + \frac{ik_1}{\lambda_1^2}, \quad c_1' = 1 + \frac{ik_1}{\lambda_1^2},$$

$$\bar{\nu}_1 = \left[\frac{1}{4} - (B_1 - B_0) + \frac{\lambda_1^2 - 1}{\lambda_1^4} k_1^2 \right]^{1/2} - \frac{1}{2},$$

$$k_1^2 = \frac{E_{c.m.}}{V_{01}} - \lambda_1^2 B_0.$$

The solution $u_2(\rho_2)$ in the outer region $r > R_1$ is given by

$$\begin{aligned}
 u_2(\rho_2) = & A_3[\lambda_2^2 + (1 - \lambda_2^2)z_2^2]^{1/4} (1 - z_2^2)^{-\frac{ik_1}{2\lambda_2^2}} \times F\left(a_2, b_2, c_2, \frac{1 - z_2}{2}\right) \\
 & + A_4[\lambda_2^2 + (1 - \lambda_2^2)z_2^2]^{1/4} (1 - z_2^2)^{\frac{ik_2}{2\lambda_2^2}} \times F\left(a_2', b_2', c_2', \frac{1 - z_2}{2}\right)
 \end{aligned} \tag{6.4}$$

where

$$z_2 = \frac{\lambda_2 y_2}{[1 + (\lambda_2^2 - 1)y_2^2]^{1/2}}$$

and

$$a_2 = \bar{v}_2 + 1 - \frac{ik_2}{\lambda_2^2}, \quad b_2 = -\bar{v}_2 - \frac{ik_2}{\lambda_2^2}, \quad c_2 = 1 - \frac{ik_2}{\lambda_2^2},$$

$$a_2' = \bar{v}_2 + 1 + \frac{ik_2}{\lambda_2^2}, \quad b_2' = -\bar{v}_2 + \frac{ik_2}{\lambda_2^2}, \quad c_2' = 1 + \frac{ik_2}{\lambda_2^2},$$

$$\bar{v}_2 = \left[\frac{1}{4} - B_2 + \frac{\lambda_2^2 - 1}{\lambda_2^4} k_2^2 \right]^{1/2} - \frac{1}{2}$$

$$k_2^2 = \frac{E_{c.m}}{V_{02}}$$

At the origin $r = 0$, we have

$$\rho_1 = -R_1 b_1, \quad y_1 = y_{01} = -[1 - 2e^{2\lambda_1^2(\rho_{01} - |\rho_1|)}]$$

$$\text{where } \rho_{01} = \frac{(\lambda_1^2 - 1)^{1/2}}{\lambda_1^2} \tan^{-1}(\lambda_1^2 - 1)^{1/2},$$

$$z_1 = z_{01} = \frac{\lambda_1 y_{01}}{[1 + (\lambda_1^2 - 1)y_{01}^2]^{1/2}}$$

Applying the boundary condition at $r \rightarrow 0$, $u_1(\rho_1) \rightarrow 0$

$$C_1 = -\frac{A_2}{A_1} = (1 - z_{01}^2)^{\frac{ik_1}{\lambda_1^2}} \frac{F\left(a_1, b_1, c_1, \frac{1 - z_{01}}{2}\right)}{F\left(a_1', b_1', c_1', \frac{1 - z_{01}}{2}\right)} \quad (6.5)$$

$$F\left(a_1, b_1, c_1, \frac{1 - z_{01}}{2}\right) = \frac{\Gamma\left(1 - \frac{ik_1}{\lambda_1^2}\right)\Gamma\left(\frac{ik_1}{\lambda_1^2}\right)}{\Gamma(-\bar{\nu}_1)\Gamma(1 + \bar{\nu}_1)} + \left(\frac{1 + z_{01}}{2}\right)^{\frac{ik_1}{\lambda_1^2}} \quad (6.6)$$

where

$$\begin{aligned} & \times \frac{\Gamma\left(1 - \frac{ik_1}{\lambda_1^2}\right)\Gamma\left(\frac{-ik_1}{\lambda_1^2}\right)}{\Gamma\left(\bar{\nu}_1 + 1 - \frac{ik_1}{\lambda_1^2}\right)\Gamma\left(-\bar{\nu}_1 - \frac{ik_1}{\lambda_1^2}\right)} \\ F\left(a_1', b_1', c_1', \frac{1 - z_{01}}{2}\right) &= \frac{\Gamma\left(1 + \frac{ik_1}{\lambda_1^2}\right)\Gamma\left(\frac{-ik_1}{\lambda_1^2}\right)}{\Gamma(-\bar{\nu}_1)\Gamma(1 + \bar{\nu}_1)} \\ &+ \left(\frac{1 + z_{01}}{2}\right)^{\frac{ik_1}{\lambda_1^2}} \frac{\Gamma\left(1 + \frac{ik_1}{\lambda_1^2}\right)\Gamma\left(\frac{ik_1}{\lambda_1^2}\right)}{\Gamma\left(\bar{\nu}_1 + 1 + \frac{ik_1}{\lambda_1^2}\right)\Gamma\left(-\bar{\nu}_1 + \frac{ik_1}{\lambda_1^2}\right)} \end{aligned} \quad (6.7)$$

$$(1 - z_{01}^2)^{\frac{-ik_1}{\lambda_1^2}} \cong \exp\left\{-2ik_1\left(\frac{1}{\lambda_1^2}\log 2 - \frac{1}{\lambda_1^2}\log \lambda_1 + \rho_{01} - b_1 R_1\right)\right\} \quad (6.8)$$

$$\left(\frac{1 + z_{01}}{2}\right)^{\frac{ik_1}{\lambda_1^2}} \cong \exp\left\{-2ik_1\left(\frac{1}{\lambda_1^2}\log \lambda_1 - \rho_{01} + b_1 R_1\right)\right\} \quad (6.9)$$

The property of the wave function $u_2(\rho_2)$ for large $\rho_2 \rightarrow \infty$ (or $r \rightarrow \infty$) gives

$$u_2 = A_4 2^{\frac{ik_2}{\lambda_2^2}} e^{-ik_2 \rho_2} [e^{-ik_2 \rho_2} - S_m e^{ik_2 \rho_2}] \quad \text{for } \rho_2 \rightarrow \infty \quad (6.10)$$

where the scattering matrix denoted by S_m is expressed as

$$S_m = C_2 \exp\left[(-2ik_2)\left(\frac{\log 2}{\lambda_2^2} - \rho_2\right)\right], \quad (6.11)$$

with

$$C_2 = -\frac{A_3}{A_4},$$

$$\rho_2' = \frac{1}{\lambda_2^2} \log \lambda_2 - \rho_{02}, \quad (6.12)$$

and

$$\rho_{02} = \frac{(\lambda_2^2 - 1)^{1/2}}{\lambda_2^2} \arctan(\lambda_2^2 - 1)^{1/2}$$

Equating the logarithmic derivatives of $u_1(\rho_1)$ and $u_2(\rho_2)$ at $\rho_1 = \rho_2 = 0$, we can calculate C_2 and hence the scattering matrix S_m . We have considered only relative $\ell = 0$ state.

6.3 Life time and decay width

To calculate the decay width or life time of a given system having some decay energy we have used the method presented in the ref.[Dav00]. In the present work the potential in the outer region $r > R_1$ has been considered as pure Coulombic potential and the solution $u_2(\rho_2)$ has been replaced by the Coulomb-distorted outgoing spherical wave $f_c(kr) = G_0(\eta, kr) + iF_0(\eta, kr)$ for the s wave. $k = \sqrt{2mQ/\hbar^2}$ is the wave number, m is the reduced mass and Q is the alpha decay energy. $G_0(\eta, kr)$ is irregular Coulomb wave function and $F_0(\eta, kr)$ is a regular Coulomb wave function. $\eta = mZ_p Z_t e^2 / \hbar^2 k$ is the Coulomb parameter. The probability rate per second at which particle goes through a surface element $dS = r^2 \sin \theta d\theta d\phi$ is given by

$$F = |u_2(\rho_2)|^2 v dS \quad (6.13)$$

where $v = \hbar k / m$ is the velocity of the particle. Since

$$\lim(r \rightarrow \infty) |f_c(kr)|^2 = |N_0|^2,$$

the decay probability per second, i.e. the inverse of the mean life τ , obtained by

$$\text{integrating eq. (6.13) over the angle is } \tau = \frac{\hbar}{\Gamma} = \frac{m}{\hbar k} \frac{1}{|N_0|^2} \quad (6.14)$$

where $|N_0|^2$ has a dimension of fm^{-1} . Thus at $r = R_1$, the normalized regular solution $u_1(r)$ of Schrödinger equation is matched with the distorted outgoing Coulomb wave.

$$u_1(R_1) = N_0[G_0(\eta, kR_1) + iF_0(\eta, kR_1)] \quad (6.15)$$

where R_1 , is outside the range of the nuclear field.

Thus eq.(6.14) represents the mean life time or decay width in terms of normalization constant. The normalization constant in turn can be calculated by using eq. (6.15).

The wave function $u_1(r)$, which decreases rapidly with radius outside the nucleus, can be normalized by the condition

$$\int_0^{R_1} |u_1(r)|^2 = 1 \quad (6.16)$$

This normalization is confined to the inner domain $r \leq R_1$. Normalized $u_1(r)$ gives the normalization constant as

$$N_0 = \frac{u_1(R_1)}{G_0(\eta, kR_1) + iF_0(\eta, kR_1)} \quad (6.17)$$

In the present analysis $u_1(r) = A_1 \bar{u}_1(r)$ calculated at $r = R_1$ gives $u_1(R_1)$. Thus $\bar{u}_1(r)$ at $r = R_1$ is given by

$$\bar{u}_1(R_1) = \lambda_1^{1/2} F\left(a_1, b_1, c_1, \frac{1}{2}\right) - C_1 \lambda_1^{1/2} F\left(a_1', b_1', c_1', \frac{1}{2}\right) \quad (6.18)$$

$$F\left(a_1, b_1, c_1, \frac{1}{2}\right) = \pi^{1/2} \frac{\Gamma(1 - ik_1)}{\Gamma\left(\frac{\bar{v}_1}{2} - \frac{ik_1}{2} + 1\right) \Gamma\left(-\frac{\bar{v}_1}{2} - \frac{ik_1}{2} + \frac{1}{2}\right)} \quad (6.19)$$

$$F\left(a_1', b_1', c_1', \frac{1}{2}\right) = \pi^{1/2} \frac{\Gamma(1 + ik_1)}{\Gamma\left(\frac{\bar{v}_1}{2} + \frac{ik_1}{2} + 1\right) \Gamma\left(-\frac{\bar{v}_1}{2} + \frac{ik_1}{2} + \frac{1}{2}\right)} \quad (6.20)$$

where $C_1 = (-A_2/A_1)$ is given by eq. (6.5) and $A_1 = \left(\int_0^{R_1} |u_1(r)|^2 \right)^{-1/2}$ has been obtained from the normalization of eq. (6.16). In the special case of Coulomb- nuclear problem, there are some specific values of η, k and R_1 for which $F_0(\eta, kR_1)$ and $G_0(\eta, kR_1)$ can have approximate value. If $2\eta > kR_1$ for $\ell = 0$ then [Abr65],

$$F_0(\eta, kR_1) \approx \frac{1}{2} \beta e^\gamma, \quad G_0(\eta, kR_1) \approx \beta e^{-\gamma}, \quad t = \frac{kR_1}{2\eta},$$

$$\gamma = 2\eta \left\{ [t(1-t)]^{1/2} + \sin^{-1} t^{1/2} - \frac{1}{2} \pi \right\} \quad (6.21)$$

$$\beta = \{t/(1-t)\}^{1/2}$$

Furthure in the case $2\eta > kR_1$, one finds $|G_0(\eta, kR_1)| \gg |F_0(\eta, kR_1)|$ by several order of magnitude. This condition is applied in alpha-nucleus systems of interaction at energies below the height of the Coulomb barrier. The equation (6.17) can then be reduced to

$$N_0 \cong \frac{u_1(R_1)}{G_0(\eta, kR_1)} \quad (6.22)$$

By using eq. (6.18) for $u_1(R_1)$ and eq.(6.21) for $G_0(\eta, kR_1)$ in eq.(6.22), N_0 has been calculated at a given energy and eq.(6.14) has been used to calculate half life.

6.4. Resonance energy

The potential form (3.13) described in chapter III has a pocket followed by repulsive Coulomb barrier. This kind of potential generates quasibound states with discrete positive energies called as resonance energy. One of these resonance energies is identified as decay energy or Q value of the decaying system with some life time of decay. Thus in the case of a potential with a pocket followed by a barrier as the case in alpha-daughter system, one can identify the following distinct feature for a resonance state. The resonance with energy less than the barrier energy whose wave function is predominantly localized in the pocket region can be termed as pocket resonance. Such a

state decays by tunneling across the barrier and if the effective barrier is large the decay possibility and hence the resonance width will be very small. Detection of such resonance requires energy resolution smaller than this width. Such states are almost like bound state and should manifest through the dominance of wave function in the pocket region [Sus 94]. This is called the confinement property of the wave. In this condition exactly at resonance energy the probability density ($I_1 = \int |u_1|^2 dr$) in the interior region ($0 < r < R_1$) is very large compared to the probability density in the outer region ($r > R_1$). However if the energy is different from the resonance energy then the characteristic of the wave will be reversed. For the calculation of Q value we see the behavior of the probability density in two regions:

From $r = 0$ to $r = R_1$, $I_1 = \int_0^{R_1} |u_1|^2 dr$ and from $r = 0$ to $r = R_2$, $I_2 = \int_0^{R_2} |u_1|^2 dr$, where

$R_2 > R_1$ and R_2 is a large distance close to the classical outer turning point.

6.5. Relative Probability Density

The analytically solvable potential used in the present work comprises of five parameters $r_0, a, B_0, b_1 = \sqrt{B_1} A_t^{-1/3}$ and λ_1 . The experimental Q value of a given system has been reproduced by variation of just a single parameter λ_1 , which describes the flatness of the barrier in the inner region while other parameters of the potential are fixed. To obtain the value of λ_1 corresponding to best fit to the experimental Q value we have plotted the graph between the ratio of two probability densities I_1/I_2 and λ_1 . At certain value of λ_1 plot gives $I_1/I_2 \cong 1$ as is shown in figure 6.1. This value of λ_1 , along with other parameters describes the potential with resonance energy equal to experimental Q -value. For the prediction of Q -value of unknown systems which experimental Q -value is not known we have fixed the value of parameter λ_1 by using the global formula described in section 6.6. Corresponding to this value of λ_1 along with other parameters we plot the ratio of two probability densities I_1/I_2 with respect to energy. The energy position of the peak gives the required Q -value for the system. Plot is shown in fig.6.2. This method of

finding Q -value is called relative probability density (RPD) method. At this value of λ_1 and Q -value half life can be calculated using the wave function method described in section 6.3.

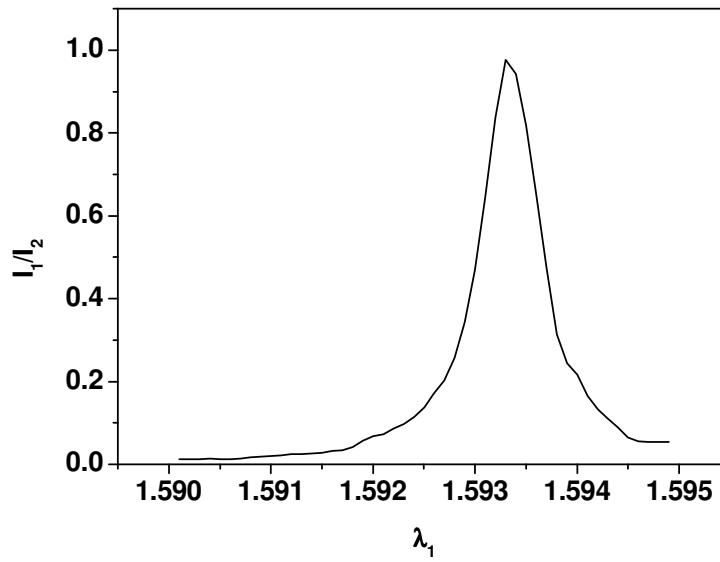


Figure 6.1: Plot of the ratio of two probability densities I_1 and I_2 as a function of λ_1 for $\alpha + {}^{289}_{115}$ system for $E_{c.m.}=11.03\text{MeV}$. The peak position corresponding to $I_1/I_2 \cong 1$ gives the value of λ_1 .

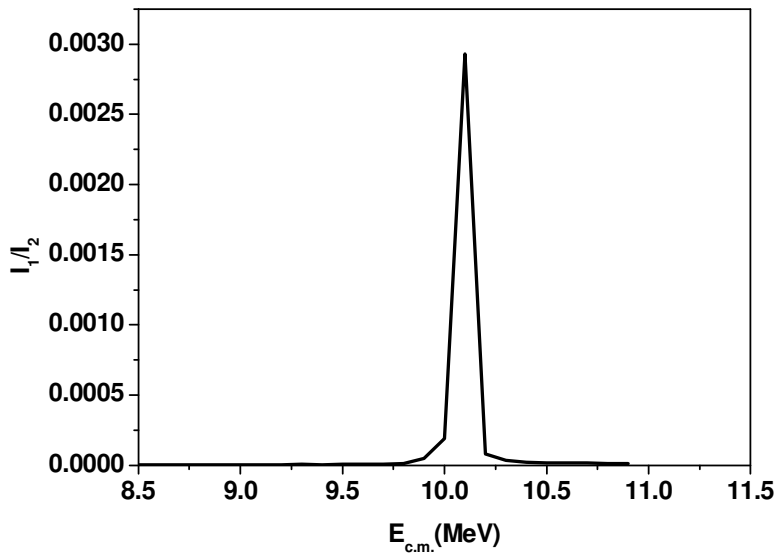


Figure 6.2: Plot of the ratio of two probability densities I_1 and I_2 as a function of energy for $\alpha + {}^{282}\text{111}$ system for $\lambda_1 = 1.623825$. The peak position ($E_{c.m.} = 10.22$ MeV) represents the Q value of the decay.

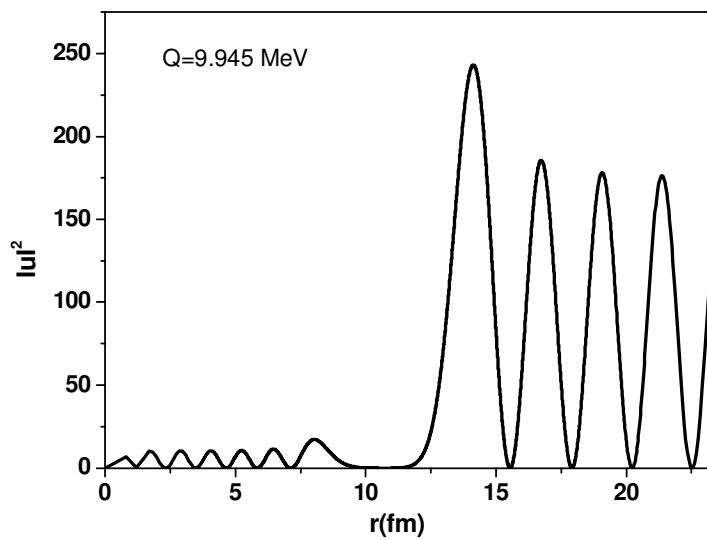


Figure 6.3: Plot of the square modules of the wave function as a function of radial distance r for the $\alpha + {}^{286}\text{113}$ system at the energy 0.005 MeV less than the exact resonance energy for $\lambda_1 = 1.46650$.

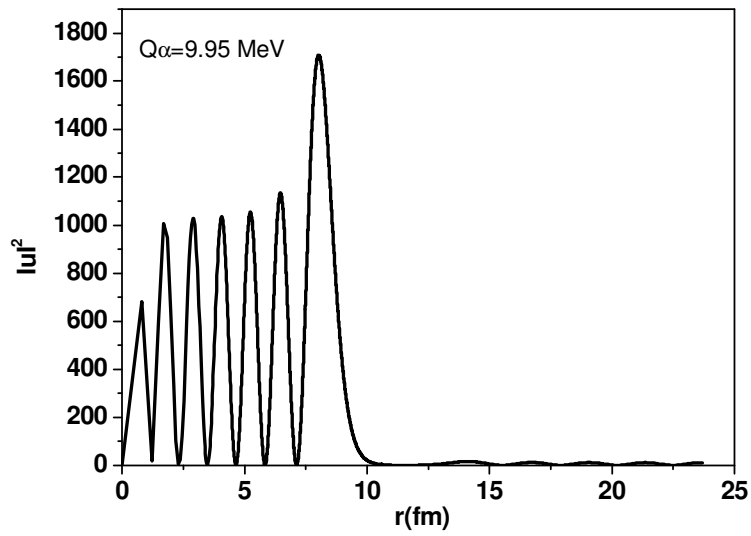


Figure 6.4: Same as fig.6.3 exactly at resonance energy $Q=9.95 \text{ MeV}$.

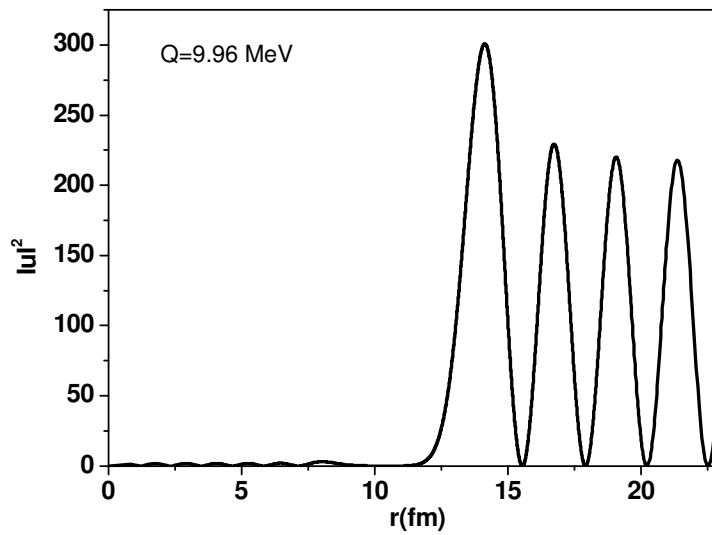


Figure 6.5: Same as fig. 6.3 at energy 0.01 MeV larger than the exact resonance energy.

6.6 Details of calculation

The potential used in the present work has five parameters for the estimate of resonance energy and half life $t_{1/2}$. In the present work only one parameter λ_1 has been varied within the range $1 < \lambda_1 < 2$, remaining four parameters are fixed at $r_0 = 0.97 \text{ fm}$, $b_1 = 0.82$, $a = 1.6 \text{ fm}$ and $B_0 = -78.75$ as in ref [Sah 08]. To maintain the consistency, parameters of the potential have been kept same for each system. First of all by using the confinement property of wave function and by using the relative probability density (RPD) method, we obtained exact experimental Q -value for certain specific value of λ_1 . Using this value of λ_1 and Q , half life has been calculated from equations (6.14) and (6.22).

For the unknown nuclei we have developed a global formula to fix the value of the parameter λ_1 . The formula has been developed in terms of λ_1 as a function of neutron number N of the target nucleus.

$$\lambda_1 = \begin{cases} \lambda_0(N_{t0}/N_t) & \text{if } N_t < N_{t1} \\ \lambda_0(N_{t0}/N_{t1}) \times (N_{t1}/N_t)^2 & \text{if } N_t > N_{t1} \end{cases} \quad (6.23)$$

where λ_0 is starting value for a given isotopic chain. N_{t0} is initial value of neutron number, N_{t1} is central value of neutron number.

Thus this formula gives the value of λ_1 for a given N of the isotopes, which has been kept fixed. With this value of the potential parameter along with other potential parameters, we calculate the Q -value using the relative probability density method. To develop a global formula, we have plotted a graph between neutron numbers of the target nuclei and λ_1 obtained corresponding to best fit value to the decay energy for the experimentally known Pb isotopes. Plot is shown in fig.6.6. From the plot it has been observed that the nature of λ_1 follows $1/N$ path up to some value of neutron number, after that it follows $1/N^2$ path. So the resultant nature of the graph can be expressed as eq. (6.23). It has been observed that the calculated λ_1 , obtained from the formula for any isotopic chain including mid, heavy and super heavy region follow the same graph as eq. (6.23).

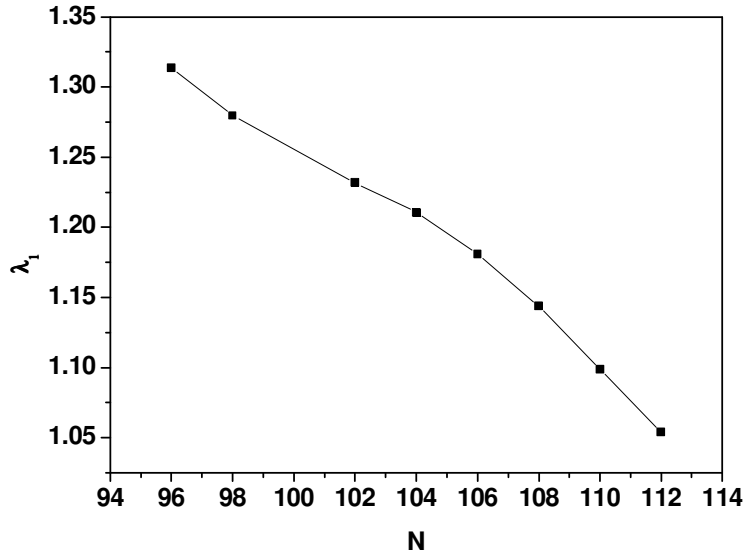


Figure 6.6: Plot of λ_1 versus neutron number of target nuclei. The dots indicate the values of λ_1 , which explain the respective experimental Q values. The solid curve represents the global formula given by equation (6.23), for λ_1 as a function of neutron number N , with $N_{i0} = 96$, $N_{i1} = 105$ and $\lambda_0 = 1.313$.

6.7. Result and discussion

Behavior of the square modules of the wave function at different energies has been shown in figure 6.3 to 6.5. In table 6.2 and 6.3 we have shown the calculated alpha decay half life for the decay chain of $^{294}117$ and $^{293}117$. From the tables it is clear that good agreement has been obtained between calculated and experimental data. From the table 6.2 it is seen that the calculated alpha decay half life of $^{282}111$ is 69.48 sec. However the experimental half life is 0.51sec. The calculated result can be improved to obtain closer agreement with the experimental result by small variation in the potential parameters. Thus in the case of $^{282}111$ we have obtained the calculated half life 0.58 sec. very close to the experimental half life by using $r_0 = 1.12 fm$ and $b_1 = 0.82$. Similarly for $^{290}115$ system

calculated alpha decay half life is 2.08 sec using $r_0 = 0.97 \text{ fm}$ and $b_1 = 0.82$, however experimental half life is 0.016 sec. If we fix $r_0 = 1.1 \text{ fm}$ and start increasing the value of b_1 , then calculated result becomes closer and closer with experimental result. Results are shown in table 6.1. Thus we can conclude that the increase in the value of the parameter b_1 , which in turn means lesser the diffuseness of the potential results in longer half life.

For the prediction of decay energy (Q -values) and half life of unknown nuclei we have used a global formula. To test the validity of global formula we have applied it to calculate the alpha decay energy and half lives of three isotopic chain $Z=74$, 102 and 113 in the mid and heavy mass region of the nuclear chart. Chowdhary et al have carried out theoretical studies of the isotopic chain of $Z=102$ and $Z=113$ by using DDM3Y model [Cho 08b] and VSS formula [Cho 08b]. These authors have calculated Q_α -values from Muntian (M) and Myres-Swiatecki (MS) mass estimate. The results of the present calculations have been compared with those of ref. [Cho 08b]. In table 6.4 we have presented predicted Q -values and corresponding half life for the isotopic chain of $Z=102$; $A=248$ -264. The reliability of the global formula can be understood as: in table 6.4 we have observed that there is one nucleus $^{258}102$, for which our predicted alpha decay energy $Q^{(cal.)} = 8.0076 \text{ MeV}$ and predicted alpha decay half life $t_{1/2}^{(cal.)} = 1.002 \times 10^2 \text{ sec}$ are very close to the experimental values ($Q^{(exp)} = 8.151 \text{ MeV}$ and $t_{1/2}^{(exp.)} = 1.2 \times 10^2 \text{ sec}$). In table 6.5 we have presented predicted Q values and half life for the isotopic chain of $Z=74$, $A=158$ -168. Our predicted Q values are very close to the experimental Q values. However in some cases calculated half lives are not very close to experimental data, but more importantly, the explanation of the measured results of long lives in the cases with large mass numbers is remarkable in this analysis. The discrepancy in the calculated half lives from experimental data can be further improved by small change in the value of the potential parameter. In table 6.6 we have shown the predicted Q values and alpha decay half life for the isotopic chain of $Z=113$. For the first three parent nuclei $^{282}113$ $Q^{(cal.)} = 10.62 \text{ MeV}$, $t_{1/2}^{(cal.)} = 7.3 \times 10^{-2} \text{ sec}$. and $Q^{(exp.)} = 10.63 \text{ MeV}$, $t_{1/2}^{(exp.)} = 7.3 \times 10^{-2} \text{ sec}$; for $^{283}113$, $Q^{(cal.)} = 10.52 \text{ MeV}$, $t_{1/2}^{(cal.)} = 1.8 \times 10^{-2} \text{ sec}$. and $Q^{(exp.)} = 10.26 \text{ MeV}$, $t_{1/2}^{(exp.)} = 10 \times 10^{-2}$

sec. and finally for $^{284}_{111}$
 $Q^{(cal.)} = 10.43$ MeV, $t_{1/2}^{(cal.)} = 3.12 \times 10^{-2}$ sec. and $Q^{(exp.)} = 10.15$ MeV, $t_{1/2}^{(exp.)} = 4.8 \times 10^{-1}$ sec.
 Experimental data has been taken from ref. [Roy 08]. Thus it is concluded that the results of the Q values and the half lives obtained by using the global formula of λ_1 as a function of neutron number give close agreement to the respective experimental data. Further, it is seen that the explanation of these data by our calculated results are found to be better than that obtained by other calculations [Cho 08b].

Table 6.1: Variation of b_1 and λ_1 to obtain experimental half life for $\alpha + ^{286}_{113}$ system, having $Q_{\alpha}^{exp} = 9.95$ and $t_{1/2}^{exp} = 0.016$ Sec. Potential parameters are $r_0 = 1.1 fm$, $a = 1.6 fm$ and $B_0 = -78.75$.

b_1	λ_1	$t_{1/2}^{cal}$ (sec.)
0.82	1.26400	0.0216
0.84	1.18359	0.0197
0.86	1.11280	0.0181
0.88	1.04990	0.017

Table 6.2: Calculated alpha decay half life for the decay chain of $^{294}_{117}$. Potential parameters are fixed at $r_0 = 0.97 \text{ fm}$, $b_1 = 0.82$, $a = 1.6 \text{ fm}$ and $B_0 = -78.75$. Experimental data have been taken from the ref. [Oga 10].

Parent Nucleus		$Q^{(\text{exp})}$ (MeV)	λ_1	$t_{1/2}^{(\text{cal.})}$ (sec.)	$t_{1/2}^{(\text{exp.})}$ (sec.)
Z	A				
117	294	10.81	1.59334	5.09×10^{-2}	7.76×10^{-2}
115	290	9.95	1.46650	2.08	0.015
113	286	9.63	1.47500	4.27	19.61
111	282	9.00	1.411570	69.48	0.51
109	278	9.55	1.62570	0.4117	7.62
107	274	8.80	1.52389	13.93	54

Table 6.3: Calculated alpha decay half life for the decay chain of $^{293}_{117}$. Potential parameters are fixed at $r_0 = 0.97 \text{ fm}$, $b_1 = 0.82$, $a = 1.6 \text{ fm}$ and $B_0 = -78.75$. Experimental data are taken from ref. [Oga 10].

Parent Nucleus		$Q^{(\text{exp})}$ (MeV)	λ_1	$t_{1/2}^{(\text{cal.})}$ (sec.)	$t_{1/2}^{(\text{exp.})}$ (sec.)
Z	A				
117	293	11.03	1.63539	1.55×10^{-2}	1.45×10^{-2}
115	289	10.31	1.53891	0.246	0.22
113	285	9.74	1.485739	2.03	5.47

Table 6.4: Predicted alpha decay half life and Q values for the isotopic chain of $Z=102$. Potential parameters are $r_0 = 0.97 \text{ fm}$, $b_1 = 0.82$, $a = 1.6 \text{ fm}$ and $B_0 = -78.75$. Parameters of the global formula are $\lambda_0 = 1.543$, $N_{i0} = 144$, and $N_{i1} = 157$.

Parent nucleus Mass no. (A)	λ_1	Q^{cal} (MeV) Present calculation	Q^{cal} (MeV) M Ref.[Cho08b]	$t_{1/2}^{(cal.)}$ (Sec.) present calculation	$t_{1/2}^{(cal.)}$ (Sec.) DDM3Y (M) Ref.[Cho08b]	$t_{1/2}^{(cal.)}$ (Sec.) VSS(M) Ref.[Cho08b]
248	1.54349	9.15	9.27	3.00×10^{-2}	1.87×10^{-2}	2.16×10^{-2}
249	1.53235	9.03	9.12	6.40×10^{-2}	1.21×10^{-1}	6.81×10^{-1}
250	1.52186	8.91	9.00	1.42×10^{-2}	1.07×10^{-1}	1.32×10^{-1}
251	1.51157	8.80	8.83	2.99×10^{-1}	8.11×10^{-1}	5.03
252	1.50129	8.68	8.53	6.60×10^{-1}	2.68	3.80
253	1.49122	8.57	8.19	0.15×10^1	8.92×10^1	6.00×10^2
254	1.48128	8.45	8.06	0.33×10^1	9.43×10^1	1.46×10^2
255	1.47147	8.34	8.32	0.75×10^1	3.05×10^1	2.17×10^2
256	1.46178	8.23	8.36	1.75×10^1	8.31	1.37×10^1
257	1.45223	8.11	8.19	4.20×10^1	7.80×10^1	6.00×10^2
258	1.44280	8.00	7.99	1.00×10^2	1.45×10^2	2.58×10^2
259	1.43349	7.89	7.71	2.46×10^2	3.75×10^3	3.18×10^4
260	1.42430	7.78	7.45	5.95×10^2	1.42×10^4	2.75×10^4
261	1.41523	7.67	7.1	1.53×10^3	9.80×10^5	8.75×10^6
262	1.3973	7.52	6.86	5.68×10^3	3.83×10^6	8.39×10^6
263	1.3798	7.36	6.45	2.18×10^4	8.94×10^8	8.19×10^9
264	1.17118	7.21	6.25	8.59×10^4	3.06×10^9	7.13×10^9

Table 6.5: Prediction of alpha decay half life and Q values for the isotopic chain of $Z=74$. Potential parameters are fixed at $r_0 = 0.97 fm$, $b_1 = 0.82$, $a = 1.6 fm$ and $B_0 = -78.75$. Parameters of the global formula are $\lambda_0 = 1.245$, $N_{i0} = 82$, and $N_{i1} = 87$. Experimental data has been taken from the ref.[Roy 00, Roy 08] and Q values of $A=159, 161, 165$ and 167 has been taken from ref.[nndc].

Parent Nucleus Mass no. (A)	λ_1	Q^{cal} (MeV) Present calculation	$Q^{(exp)}$ (MeV)	$t_{1/2}^{cal}$ (Sec.) Present calculation	$t_{1/2}^{(exp.)}$ (Sec.)
158	1.24520	6.61	6.61	1.7×10^{-4}	9.0×10^{-4}
159	1.230197	6.41	6.45	8.0130×10^{-4}	-
160	1.215552	6.22	6.06	3.8466×10^{-3}	1.0×10^{-1}
161	1.201251	6.03	5.92	1.9560×10^{-2}	-
162	1.187283	5.84	5.67	1.0915×10^{-1}	3.00
163	1.173636	5.65	5.52	6.444×10^{-1}	6.76
164	1.147114	5.37	5.28	1.103×10^1	2.5×10^2
165	1.12148	5.10	5.03	2.327×10^2	-
166	1.09669	4.82	4.86	6.2551×10^3	4.7×10^2
167	1.072727	4.54	4.77	2.446×10^5	-
168	1.049534	4.27	4.50	1.10×10^7	1.6×10^6

Table 6.6: Prediction of alpha decay half life and Q values for the isotopic chain of $Z=113$. Potential parameters are fixed at $r_0 = 0.97 \text{ fm}$, $b_1 = 0.82$, $a = 1.6 \text{ fm}$ and $B_0 = -78.75$. Parameters of the global formula are $\lambda_0 = 1.662$, $N_{i0} = 167$, and $N_{i1} = 173$.

Parent nucleus Mass no. (A)	λ_1	Q^{cal} (MeV) Present Calculation	Q^{cal} (MeV) MS [Cho08b]	$t_{1/2}^{cal}$ (sec.) Present Calculation	$t_{1/2}^{cal}$ (Sec.) DDM3Y [Cho08b]	$t_{1/2}^{cal}$ (Sec.) VSS [Cho08b]
282	1.66272	10.62	10.00	7.3×10^{-2}	4.51	1.12×10^1
283	1.652822	10.52	9.56	1.87×10^{-2}	2.05×10^1	9.99×10^1
284	1.643042	10.42	9.36	3.12×10^{-2}	3.41×10^2	9.08×10^2
285	1.633377	10.32	9.18	5.96×10^{-2}	2.96×10^2	1.54×10^3
286	1.623825	10.22	9.10	1.07×10^{-1}	2.15×10^3	6.17×10^3
287	1.614385	10.12	9.04	1.92×10^{-1}	7.87×10^2	4.42×10^3
288	1.605053	10.02	8.97	3.58×10^{-1}	5.40×10^3	1.66×10^4
289	1.586657	9.88	8.66	8.19×10^{-1}	1.46×10^4	8.71×10^4
290	1.568576	9.75	8.65	0.18×10^1	6.59×10^4	2.08×10^5
291	1.550802	9.62	8.11	0.44×10^1	1.40×10^6	9.41×10^6
292	1.533328	9.48	7.80	1.08×10^1	1.11×10^8	3.59×10^8
293	1.516148	9.35	8.21	2.64×10^1	5.49×10^5	3.88×10^6

6.8. Summary and Conclusion

In the present work phenomenon of alpha decay has been studied in the framework of quantum collision, considering alpha as projectile and daughter as target. For the systems like alpha plus daughter the resultant potential is the combined effect of short range attractive nuclear force and the long range electrostatic Coulomb force. Such type of potential have pocket near the origin and a barrier in the outside region. Sahu has simulated the composite potential by an analytically solvable potential, which is highly

versatile in nature. The parameters of the potential can be varied to generate different forms. This potential is able to generate discrete positive energy state called resonance state. We have used the analytically solvable potential to calculate the experimental half life values for the decay chain of $^{294}117$ and $^{293}117$ for the first time. The confinement property of the wave function and relative probability density method has been used for the calculation of exact resonance energy (Q -value). At this exact resonance energy (Q -value) half life has been calculated by using the exact expression obtained from the wave function method. We have also used the analytically solvable potential to predict Q -values and half life of unknown alpha decaying system. For the prediction we have developed a global formula in terms of λ_1 as a function of neutron number of target nuclei. In order to test the reliability of the global formula we have compared our calculated Q -values and half life of different nuclei with the corresponding experimental values. Good agreement has been found between experimental and calculated values indicating the reliability of the method used in the present work. The prediction has been made in the three region of nuclides for the isotopic chain of $Z=74, 102$ and 113 . Good agreement with the experimental data shows that the global formula can be applied in any mass region successfully.

Chapter VII

Summary and conclusion

The aim of the present work is to perform alpha decay study using two different approaches (i) Quantum tunneling in unified fission model and (ii) scattering theory as applied to decay of resonance states.

Using unified fission like approach alpha decay half lives have been calculated for proton rich Pb isotopes in the region $A=182-210$, Bi isotopes in the region $A=189-214$ and for super heavy nuclei in the region $Z=106-128$ and $A=258-320$. Also the half lives have been predicted for the nuclei in the mass region given above for those which experimental data are not available. In all the cases good agreement has been obtained with the experimental data where it is available. In the unified fission like approach alpha decay has been considered as asymmetric fragmentation of parent nucleus in to alpha and daughter nucleus. Our study is different than the earlier existing studies in literature adopting fission like approach in the following ways.

- (i) We have expressed the potential barrier by a highly versatile form developed by Sahu et al [Sah 02] which itself is based on the Ginnochio potential [Gin 84]. One expects that due to various renormalization effects, the shape of the barrier changes such that there is a sharp fall in the potential in the interior region. The effective barrier experienced by alpha gets modified from its simple Coulomb and centrifugal form due to various renormalization processes. This notion of modification of the fission barrier has been taken into account by choosing the appropriate values of the potential parameters, the barrier height V_B , top curvature λ and range ν . We have thus for the first time parameterized the full geometrical shape of the potential.
- (ii) In almost all the earlier theoretical studies the transmission probability has been calculated using WKB approximation method. We have used an exact expression of transmission coefficient given by Sahu et al [Sah 02]. To test the relative accuracy of the WKB approximation method we have compared the exact transmission probabilities calculated with those obtained by WKB

method for symmetric Eckart barrier of different ranges. It has been observed that when the de Broglie wavelength of the incident particle is larger than the size of the obstacle the tunneling becomes more and more quantal and hence the semiclassical approximation becomes poorer.

- (iii) The assault frequency P_0 has been obtained from the zero point vibration energy $E_v = \frac{1}{2}hP_0$. From a fit to the experimental data on cluster emitters a law is given by Poenaru et al [Poe 84] which relates E_v with Q values. The same law has been extended to alpha decay and is used to calculate vibration energies. The shell effect is implicitly contained in the zero point vibration energy due to its proportionality with the Q value. Our method of calculating the assault frequency from the zero point vibration energy is more appropriate than the method used by other authors. Tavers et [Tav 05] have used a constant value of assault frequency $2 \times 10^{21} \text{ s}^{-1}$. Shanmugam et al [Sha 00] have calculated it from the relative motion of the fragments in the range described by the sum of Susmann central radii of the parent and the daughter nuclei.

Using second line of approach the alpha decay half lives and decay energy have been calculated for recently discovered alpha decay chain of $^{294}117$ and $^{293}117$. We have also predicted the alpha decay energy and alpha decay half for the isotopic chain of $Z=74$, 102 and 113, for which experimental data are not known. In this approach the decaying state has been considered as the resonance state of the alpha-daughter nucleus system with in the frame work of quantum scattering theory. This approach is different from other theoretical approaches in the following way

- (i) For this study we have used an analytical expression of the alpha-daughter potential which simulates nuclear Wood-Saxon part in the interior of the barrier and repulsive Coulomb form in the outer region of the barrier.

- (ii) To estimate the resonance energy or Q value of the decaying state, confinement property and bound state like behavior of the wave function at resonance state has been taken into account.
- (iii) To calculate decay width or half life an analytical expression has been used. The expression has been obtained by matching the interior wave function with the outside Coulomb wave function.

The method used in the present work to calculate decay energy and half life is simple and free from any other difficulties experienced in other methods e.g S-matrix, Imaginary Phase shift method, Imaginary test potential method and quantum tunneling using WKB method. In the quantum tunneling method with WKB approximation, which has been used in almost all the earlier studies the decay constant has been calculated as the product of assault frequency and penetrability factor through the barrier. In the present approach there is no need of assault frequency only wave function method has been used to calculate decay constant. Also in the present work a global formula has been developed. The formula has been used in the prediction of half life and decay energy of experimentally unknown systems. To check the reliability of the formula predicted results has been compared with the experimental data, for the cases where experimental data is available. Results have been found in very good agreement with the experimental data. Thus the global formula can be used freely for the prediction of decay energy and decay half lives of unknown systems.

List of publication

Journals

- 1 Alpha decay study of Proton rich even Pb Isotopes.
Arati Devi, S. Prakash and I. Mehrotra, *Pramana J Physics*,72(2009)753.
- 2 Alpha decay study of Bi isotopes
Arati Devi and I. Mehrotra, *Physics of atomic nuclei* (under review).
- 3 Alpha decay study of super heavy elements
Arati Devi and I. Mehrotra, *Comm. Theo. Phy.* (under review).
- 4 Prediction for unknown Alpha decaying system
Arati Devi, B. Sahu and I.Mehrotra, to be communicated to *Int. J. Mod. Phy. E*.

Conferences

- 1 Alpha decay half life for proton rich even Pb Isotopes.
A. Devi, S.Prakash and I. Mehrotra, Proceedings of DAE-BRNS, symposium
Vol. 52(2007), 448.
- 2 Predictions of alpha decay half lives of super heavy elements
Arati Devi and I. Mehrotra
accepted for presentation in International Conference APSORC '09',
California, USA
- 3 The structure of ${}_{56}\text{Ba}^{136}$ using HI reaction.
Suresh Kumar, A. K Jain, A. Devi, I.Mehrotra, Proceedings of DAE-BRNS
symposium Vol.52(2007), 292
- 4 Alpha decay half life of Bi isotopes
Arati Devi and I.Mehrotra
submitted to DAE-BRNS symposium-2010
- 5 Prediction of alpha decay energy and alpha decay half-life of unknown
alpha decaying system.
Arati Devi, B. Sahu and I. Mehrotra, submitted to DAE-BRNS symposium-2010.

Bibliography

- [Abr 65] M. Abramowitz and I. A. Stegun, *Handbook of Mathematical Functions*, (Dover, New York, 1965), p. 542.
- [Ahm93] Z Ahmed, *Phys. Rev. A* **47** (1993) 4761.
- [And00] A N Andreyev *et al*, *Nature (London)* **405** (2000) 430.
- [And97] A N Andreyev *et al*, *Z. Phys. A* **358** (1997)63.
- [And 99] A N Andreyev *et al*, *J. Phys. G: Nucl. Part. Phys.* **25** (1999) 835.
- [Arm 03,85] P Armbruster, *Acta Phys. Pol. B*, **34** (2003)1825; P. Armbruster, *Annu. Rev. Nucl. Part. Sci.* **35**(1985)135.
- [Aud03] G. Audi *et al*, *Nuclear Physics A* **729** (2003) 337.
- [Bas 04] D N Basu *et al*, *J. Phys. G: Nucl. Part. Phys.* **30**, (2004) B 35.
- [Ben 00] R. Bennet *et al.*, *Radioactive Nuclear Beam Facilities*, NUPECC Report, April 2000.
- [Ben 99] M Bender *et al*, *Phy. Rev. C*, **60** (1999)034304.
- [Boh 39] N Bohr *et al*, *J A Phys. Reu.* **56** (1939) 426.
- [Bro 92] B A Brown, *Phys. Rev. C* **46** (1992) 811.
- [Buc89] B Buck *et al*, *J. Phys. G: Nucl. Part. Phys.* **15** (1989) 615.
- [Buc 91] B Buck *et al*, *J. Phys. G: Nucl. Part. Phys.* **17** (1991)1223.
- [Buc 75] B Buck *et al*, *Phys. Rev. C* **11** (1975)1803.
- [Buc 89] B Buck *et al*, *J. Phys. G: Nucl. Part. Phys.* **15** (1989) 615.
- [Cho 07] P R Chowdhury *et al*, *Phys. Rev. C* **75**, (2007) 047306.
- [Cho 08] P Roy chowdhury *et al*, *Phy.Rev.C*, 77 (2008) 044603.
- [Cho 08b] P Roy chowdhury *et al*, *Atomic Data and Nuclear Data Tables*, **94**, (2008) 781.
- [Cho 07] P Roy Chowdhury *et al*, *Phy. Rev. C*, **75**(2007)047306.
- [Cho 06] P R Chowdhury *et al*, *Phys. Rev. C* **73** (2006)014612.
- [Con 28] E U Condon *et al*, *Nature* **122** (1928) 439.
- [Dav 00] C N Davids *et al*, *Phys. Rev. C* **61**(2000)054302.
- [Dec 94] J Decharge *et al*, *Rapport CEA-R-5672* (1994).
- [Dil 82] F A Dilmanian *et al*, *Phys. Rev. Lett.* **49** (1982)1909.

- [Don 08] Dong Jian-Min *et al*, Chin. Phy. Lett, **12**(2008)4230.
- [Dua 04] S B Duarte *et al*, J. Phys. G: Nucl. Part. Phys.**30** (2004) 1487.
- [Dua 96] S B Duarte *et al*, Phys. Rev. C **53** (1996) 2309.
- [Dua 04] S B Duarte *et al*, J. Phys. G: Nucl. Part. Phys, **30** (2004) 1487.
- [Dua 97] S B Duarte *et al*, Phy. Rev. C, **56**(1997)3414.
- [Dvo 06] J Dvorak *et al*, Phys. Rev. Lett. **97** (2006) 242501.
- [Eur 02] Europhysics News (2002) Vol. 33 No. 1.
- [Fle 81] G N Flerov *et al*, Pure Appl. Chem. **53**(1981) 909.
- [Fre 39] Frenkel, J Phys. Rev. **55** (1939) 987.
- [Fro 57] P O Froman *et al*, Mat. Fys. Skr. Dan. Vid. Selsk. 1, no. 3 (1957).
- [Gam 28] G Gamow, Z. Phys. **51** (1928) 204.
- [Gam 03] Y K Gambhir *et al*, Phy. Rev. C, 68(2003)044316.
- [Gar 00] F Garcia *et al*, J. Phys. G: Nucl. Part. Phys. **26** (2000) 755.
- [Gei 11] H Geiger *et al*, Phil. Mag. **22** (1911) 613.
- [Gei 95] H Geissel *et al*, Ann. Rev. Nucl. Part. Sci. 45 (1995) 163.
- [Ghi 74] A Ghiorso *et al*, Phys. Rev. Lett. **33** (1974) 1490.
- [Gin 03] T N Ginter, *et al*. Confirmation of production of element 110 by the $^{208}\text{Pb} \quad ({}^{64}\text{Ni},n)$ reaction. Phys. Rev.C **67** (2003) 064609; erratum C **68**(2003) 029901.
- [Gin 84] J N Ginocchio, Ann. of Phys, **152** (1984) 203.
- [Gon 93] M.Goncalves *et al*, Phy.Rev.C, **48**(1993)2409.
- [Han 61] S H Hanauer *et al*, Phys. Rev.**124** (1961)1512.
- [Hat 90] Y Hatsukawa *et al*, Phys. Rev. C **42**(1990)674.
- [Hof07,00, 98] S Hofmann *et al*, Euro. Phys. Jour. A, **32** (2007)251, S. Hofmann *et al*, Rev. Mod. Phys. **72** (2000) 733; S. Hofmann, Rep. Prog. Phys. 61 (1998) 639; G. Munzenberg, Rep. Prog. Phys. 51(1988) 57.
- [Hon 05] Hongfei Zhang *et al*, Phy. Rev. C, **71**(2005)054312.
- [Hon 06] Hongfei Zhang *et al*, Phy. Rev. C, **74** (2006) 017304.
- [Hor 04] M Horoi *et al*, J. Phys. G: Nucl. Part. Phys. **30** (2004) 945.
- [Hor 74] P Hornsh *et al*, Nucl. Phys. A **230**(1974)365.
- [Hof 81] S Hofman *et al*. Z. Phys.A **299**(1981)281.

- [Kel 72] K A Keller *et al*, Z. Phys. 255, 419 (1972).
- [Kle 82] O. Klepper et al., Z. Phys. A **305** (1982) 111.
- [Kou 02] H.Koura, Journal of Nuclear and Radiochemical Sciences, **3** (2002) 201.
- [Kou 05] H Koura *et al*, Prog. Theor. Phys. **113** (2005) 305.
- [Kor 97] A A Korshennikov et al, Nucl. Phys. A, **617** (1997) 45.
- [Mac 65] R D Macfarlane *et al*, Phy. Rev. Lett. **14** (1965) 114.
- [Mah 06] S. Mahadevan *et al*, Phys. Rev. C **74**, (2006) 57601.
- [Mal 89] S.S.Malik *et al*, Phy.rev.C, **39**(1989) 1992.
- [Med 06] E L Medeiros et al, J. Phys. G: Nucl. Part. Phys. **32** (2006) B23.
- [Meh 08] I Mehrotra et al, Pramana J. Phy, **70**(2008)101. [Mor 04a] K. Morita, *et al*. Status of heavy element research using GARIS at RIKEN. Nucl. Phys. A **734**(2004) 101.
- [Min 92] T Minamisono *et al*, Phy. Rev. Lett. **64** (1992) 2058.
- [Moe95,97] P. Moeller *et al.*, At. Data Nucl. Data Tables **59**, 185 (1995); Tables **66**, 131 (1997).
- [Mol 95] P Mollar *et al*, At. Data Nucl. Data Tables **59** (1995)185.
- [Mor 04a] K. Morita *et al*, Status of heavy element research using GARIS at RIKEN. Nucl. Phys. A **734** (2004) 101.
- [Mor 04b] K. Morita *et al*, J. Phys. Soc. Jpn.**73**(2004)1738.
- [Mou 01] R Moustabchir *et al*, Nucl. Phys. A **683** (2001) 266.
- [Mun 81a] Munzenberg G *et al*, Z. Phys. A **300** (1981a) 107.
- [Mye 65] W.D. Myers *et al*, Report UCRL (1965) 11980.
- [Myr 77] W D Myres 1977 Droplet Model of Atomic Nuclei (New York:Plenum).
- [Nav 62] Q O Navarro, *Phys. Lett.* **2** (1962) 353.
- [Nil 69] S G Nilsson *et al*, Nucl. Phys. A **131** (1969) 1.
- [Nix 67] J RNix, Ann.Phy.**41**(1967)52.
- [nndc] See webpage of National Nuclear Data Centre: WWW.nndc.bnl.gov.
- [Oga 74] Yu Ts Oganessian *et al*, Zh. Eksp. Teor. Fir. Pis. **20** (1974) 580.
- [Oga 76] Yu Ts Oganessian *et al*, Nucl. Phys. A **273** (1976) 505.

- [Oga 88] Yu Ts Oganessian *et al*, in *Treatise on Heavy-Ion Science*, Ed. by D.A. Bromley (Plenum Press, New York, 1985), p. 3; Yu. Ts. Oganessian, Nucl. Phys. A **488**(1988)65.
- [Oza 94] A Ozawa *et al*, Phys. Lett. B, **18** (1994) 534.
- [Oga 04] Yu Ts Oganessian *et al*. Heavy element research at Dubna. Nucl. Phys. **734** (2004) 109.
- [Oga 04, 05, 06] Yu.Ts. Oganessian, *et al.*, Phys. Rev. C 70 (2004) 064609; Phys. Rev. C 71 (2005)029902(E); Phys. Rev. C 74 (2006) 044602.
- [Oga 04a] Yu Ts Oganessian, *et al*. Measurements of cross sections for the fusion-evaporation reactions $^{244}\text{Pu}(^{48}\text{Ca},\text{xn})^{292-x}114$ and $^{245}\text{Cm}(^{48}\text{Ca},\text{xn})^{293-x}116$. Phys.Rev. C **69**(2004)054607.
- [Oga 10] Yu Ts Oganessian *et al.*, Phy. Rev. Lett. **104** (2010) 142502.
- [Pag 96] R D Page *et al*, Phys. Rev. C **53** (1996) 660.
- [Par 05] A Parkhomenko *et al*, Acta Phys. Pol. B **36** (2005) 3095.
- [Pei 07] J C Pei *et al*, Phys. Rev. C **76** (2007) 044326.
- [Pik 86] G A Pik Pichak Yad.Fiz.**44**(1986)1421, Sov. J. Nucl. Phys. **44**(1986)923.
- [Poe 79] D N Poenaru *et al*, J.Phys.G: Nucl. Part. Phys.**5** (1979) L169.
- [Poe 80] D N Poenaru *et al*, J. Phys. Lett., Paris **41** (1980) L589.
- [Poe 83] D N Poenaru *et al*, J. Phys. **44**(1983)791.
- [Poe 85] D N Poenaru *et al*, Phys. Rev. C **32** (1985)572.
- [Poe 86] D N Poenaru *et al*, Z. Phy.A-Atomic Nuclei **325**, 435(1986).
- [Poe 06] D N Poenaru *et al*, Phys. Rev. C **74** (2006)014312.
- [Poe 06b] D N Poenaru *et al*, J. Phys. G: Nucl. Part. Phys. **32** (2006)122.
- [Pre 08] P Prema *et al*, Int. J. of Mod. Phy. E, **17**(2008)611.
- [Rav 89] H R Ravn *et al*, "On-Line Mass Separators",in *Treatise on Heavy-Ion Science*, Edt. D. A. Bromley,Plenum Press, New York, 1989, ISBN 0-306- 42949-7.
- [Ren 96] Z Ren *et al*, Phy. Rev. C, **53** (1996) 572.
- [Ren 05] Z Ren *et al*, Nucl. Phys. A **759**(2005)64.
- [Ren 07] Z. Z. Ren *et al*, J. Radioanalytical and Nuclear Chemistry, **272** (2007)

209.

- [Roe 78] E Roeckl *et al*, Phys. Lett. B **78**(1978)393.
- [Ros 84] H J Rose *et al*, Nature (London), **307**(1984)245.
- [Roy 00] G Royer, J. Phys. G **26** (2000)1149.
- [Roy 02] G. Royer *et al*, Nucl.Phys. A, **699**(2002) 479.
- [Roy 04] G. Royer *et al*, Nucl.Phys. A, **730**(2004)355.
- [Roy08] G. Royer *et al*, Phys. Rev. C **77** (2008) 037602.
- [Rut 97] K.Rutz *et al*, Phy.Rev.C, **56**(1997)238.
- [Rut 08, 09] E Rutherford *et al*, Proc. R. Soc. A **81** (1908)141, 162, Rutherford *et al*, *Phil. Mag.* **17** (1909) 281.
- [Sah 91] B Sahu *et al*, Phys. Rev. C, **44**(1991)2729.
- [Sah 99] B Sahu *et al*, Pramana J Physics **53** (1999) 545.
- [Sah 02] B Sahu *et al*, J. Phy. A. Maths. Gen. **35** (2002) 4349.
- [Sah 02a] B. Sahu *et al*, Phys. Lett. **A303**(2002)105.
- [Sah 03] B Sahu *et al*, Nucl. Phys. **A727**(2003)299.
- [Sah 08] B Sahu, Phy. Rev.C, **78**(2008) 044608.
- [Sam07] C. Samanta *et al*, Nuclear Physics A **789** (2007) 142.
- [Sam07a] C. Samanta, Romanian Reports in Physics, **59**(2007)667.
- [Sam 07b] C Samanta, Nucl. Phys. A, **789** (2007) 142.
- [Sam 09] C.Samanta, Progress in Particle and Nuclear Physics, **62**(2009)344.
- [San 00] K P Santhosh *et al*, Proc. Int. Nat. Symp. Nucl. Phys., India **43B** (2000)296.
- [San 02] K P Santhosh *et al*, Pramana J. Phys.**58** (2002) 611.
- [San 08] K P Santhosh *et al*, J. Phys.G: Nucl. Part. Phys. **35** (2008) 085102.
- [San 09] K.P Santosh *et al*, J.Phy.G:Nucl.Part.Phy., **36**(2009)115101.
- [Sat 79] G R Satchler *et al*, Phys. Rep. **55** (1979) 183, see references therein.
- [Sch 79] D Schardt *et al*, Nucl. Phys. A, 326(1979).
- [Sch 96] P Schuurmans *et al*, Phys. Rev. Lett. **77** (1996) 4720.
- [Sch 99] C Scheidenberger, European Organization of nuclear rsearchCERN-EP/99-165,19 November 1999.
- [Sha88] G Shanmugam *et al*, Phys. Rev.C **38** (1988) 1377.

- [Sha 86] G. Shanmugam *et al*, in proceeding of nuclear physics symposium, Waltair, India, 29B(1986)255.
- [Sha 90a] G. Shanmugam *et al*, *Phy. Rev. C*, **41**(1990)1184.
- [Sha 90b] G. Shanmugam *et al*, *Phy. Rev. C*, **41**(1990)1742.
- [Sha 95] G Shanmugan *et al*, *Phys. Rev. C*, 51 (1995) 2616.
- [Sha 05] M. M. Sharma *et al*, *Phys. Rev. C* **71** (2005) 054310.
- [Shi 85] Yi-Jin Shi *et al*, *Nucl. Phys. A*, **438**(1985)450.
- [Shw 95] W Shwab *et al*, *Z. Phys. A*, **350**(1995)283.
- [Sic 76] I Sick *et al*, *Phys. Lett. B* **64** (1976)33.
- [Sil 01] I Silisteanu *et al*, *Nuclear Physics A* **679** (2001) 317.
- [Sob66] A. Sobiczewski *et al*, *Phys. Lett. B* 22 (1966) 500.
- [Sob89] A Sobiczewski *et al*, *Phys. Lett. B* **224**(1989)1.
- [Soi 70] A J Soinski *et al*, *Phys. Rev. C*, **2**(1970)2379.
- [Soi 74] A J Soinski *et al*, *Phys. Rev. C*, **10** (1974) 1488.
- [Sto 06] M.A. Stoyer, *Nature* **442** (2006) 876, see references therein.
- [Stu 54] M H Studier *et al*, *Phys. Rev.* 96 (1954) 545.
- [Taa 61] R Taagepera *et al*, *Ann. Acad. Sci. Fenn., Ser. A*, VI, **1** (1961)no. 78.
- [Tan 96] I Tanihata, *J. Phys. G*. **22** (1996) 157.
- [Tav 98] O A P Tavares *et al*, *J. Phys. G: Nucl. Part. Phys.* **24** (1998) 1757.
- [Tav 05] O A P Tavares *et al*, *J. Phys. G: Nucl. Part. Phys.* **31**(2005) 129.
- [Tot84] K. Toth, *et al.*, *Phys. Rev. Lett.* **53** (1984) 1623.
- [Van 94] L Van Wormer *et al*, *Astrophys J*. **432**(1994) 326.
- [Vio 66] V E Viola *et al*, *J. Inorg. Nucl. Chem.* **28** (1966)741.
- [Wau 94] J Wauters, *et al.*, *Phys. Rev. Lett.* **72** (1994) 1329.
- [Wou 86] J Wouters *et al*, *Phys. Rev. Lett.* **56** (1986)1901.
- [Xu 97] Xu Xj *et al*, *Phy. Rev. C*, **55**(1997) R553.
- [Zha 06] H F Zhang *et al*, *Phys. Rev. C* **74**, (2006) 017304.
- [Zha 07] H F Zhang *et al*, *Phys. Rev. C* **76**, (2007) 047304.